PATHWAY OF HISTONE mRNA DEGRADATION: OLIGOURIDYLATION FOLLOWED BY BIDIRECTIONAL DECAY

Thomas Edward Mullen, Jr.

A dissertation submitted to the faculty of the University of North Carolina at Chapel Hill in partial fulfillment of the requirements of Doctor of Philosophy in the Department of Biochemistry and Biophysics

Chapel Hill
2008

Approved by:

Advisor: Dr. William F. Marzluff

Reader: Dr. Jean G. Cook

Reader: Dr. Howard M. Fried

Reader: Dr. Robert Duronio

Reader: Dr. Scott Hammond

Reader: Dr. Mariano Garcia-Blanco

ABSTRACT

THOMAS EDWARD MULLEN, JR.: Pathway of Histone mRNA Degradation: Oligouridylation Followed by Bidirectional Decay
(Under the direction of Dr. William F. Marzluff)

Histone mRNAs are rapidly degraded at the end of S phase or when DNA replication is inhibited. Histone mRNAs end in a conserved stemloop rather than a poly(A) tail. Degradation of histone mRNAs requires the stemloop sequence, which binds the stemloop binding protein (SLBP), active translation of the histone mRNA, and the location of the stemloop close to the termination codon. In this thesis I present evidence that the initial step in histone mRNA degradation is the addition of uridines to the 3' end of the histone mRNA, both after inhibition of DNA replication and at the end of S-phase. Lsm1 is required for histone mRNA degradation and is present in a complex containing SLBP on the 3' end of histone mRNA after inhibition of DNA replication. I cloned degradation intermediates that had been partially degraded from both the 5' and the 3' end. RNA interference (RNAi) experiments demonstrate that both the exosome (3'-5') and 5' to 3' decay pathway components are functionally required for degradation. cRT-PCR experiments corroborate the findings from the functional RNAi experiments by providing direct evidence that individual histone mRNAs are degraded simultaneously 5' to 3' and 3' to 5' when DNA synthesis is inhibited. Finally, I present evidence that SLBP protein expression is required for proper regulation of histone mRNA degradation when

DNA synthesis is inhibited, but that the underlying mechanism is due to nuclear retention of properly processed histone mRNA. The latter suggests that one of the critical functions of SLBP in human cells is the proper export of histone mRNA to the cytoplasm.

ACKNOWLEDGEMENTS

I would first like to acknowledge and thank my parents, Thomas and Erlinda. Their unconditional love and support is infinite and without them none of the work I present in this dissertation is possible. I would also like to acknowledge the rest of my family, particularly my sister Christine and my brother Ronel for their everlasting support.

The key ingredient that has made all this work a reality has been my mentor Bill Marzluff. Bill's constant enthusiasm towards science permeates to others around him and I am honored to have been one of those people. His scientific brilliance is inspiring and I hope my scientific career reaches a fraction of his success. His selfless contribution to my science, the science of his lab, and to the entire basic medical research that takes place at the University of North Carolina School of Medicine is unmatched. I am most sincerely grateful to him for giving me the opportunity to conduct my doctoral dissertation under his wing and for providing me with an environment that has provided me with experiences that will surely last me a lifetime.

I would like to acknowledge my dissertation committee members: Bob Duronio, Mariano Garcia-Blanco, Jean Cook, Scott Hammond, and Howard Fried. Their continued support and scientific guidance have improved the quality of my research.

I would also like to thank the present and former Marzluff lab members that I have had the privilege to work with over the years. I would like to especially acknowledge Eric Wagner, whose expertise in molecular biology has improved the technical abilities of those that have had the opportunity to work with him, including myself. Special thanks go to Kelly Sullivan, who I've had countless opportunities to discuss science and who shares as much enthusiasm for science as myself. I would also like to acknowledge Handan Kaygun. It was almost 20 years since Bill had published a landmark paper describing the role of translation in histone mRNA degradation. Handan was the first graduate student during that time to successfully forge new roads towards a better understanding of this fascinating molecular mechanism. In the absence of her work, my work does not progress to the level it has reached.

Finally, I would like to thank all the friends and scientific colleagues that I have made while in Chapel Hill. Their quality friendship does not go unnoticed. The last four years of this dissertation coincided with the presence of Lydia Morrison in my life. I want to especially thank her for her love and support during some of the hard times, but particularly during the good times. Her companionship is truly something special and I sincerely thank her for it.

TABLE OF CONTENTS

LIST OF TABLES

Table

LIST OF FIGURES

Figure

ABBREVIATIONS

mRNA	messenger RNA
SL	stemloop
SLBP	stemloop binding protein
RNAi	RNA interference
snRNA	small nuclear RNA
mRNP	messenger ribonucleoprotein
TUTase	terminal uridylyltransferase
PAP	poly(A) polymerase
HU	hydroxyurea
cRT-PCR	circularization RT-PCR
bp	basepairs
nts	nucleotides

CHAPTER 1

INTRODUCTION

THE EUKARYOTIC CELL DIVISION CYCLE

The eukaryotic cell faithfully replicates itself in a well characterized set of events termed the cell division cycle. A cell that is not dividing is termed to exist in a resting, G0 state. Once the proper stimuli prompt the cell to divide and duplicate itself, it enters the cell division cycle (or cell cycle). The cell cycle is separated into four major phases: the first growth phase (G1), the DNA synthesis phase (S), the second growth phase (G2), and finally mitosis (M) where the newly replicated chromosomes are segregated into two daughter cells.

The cell cycle is a highly ordered process of events that ensures proper completion of each phase prior to beginning the subsequent phase. Much of this regulation is accomplished by cyclin-dependent kinases (CDKs). Their regulated enzymatic activity functions to control cell signaling events that dictate the passage from each phase to the next. The dividing cell encounters a variety of endogenous (e.g. oxidative stress) and exogenous (e.g. ultraviolet and ionizing radiation) stresses that challenge the fidelity of the cell division cycle. The impact of the stress is most deleterious at the DNA level since this fundamental nucleic acid encodes the essential information of life and damage or alteration to it will affect, likely in the negative direction, the encoded information present within the subsequent

generations. Fortunately eukaryotes have evolved a complex molecular surveillance system known as DNA damage checkpoints (or cell cycle checkpoints) that exists to protect the integrity of DNA.

HISTONES ARE THE ARCHITECTURAL UNITS OF CHROMATIN

During each cell division a eukaryotic cell undertakes the arduous task of faithfully replicating its DNA during S phase for later segregation into two daughter cells. Not only must the cell replicate the entire genome but it must also appropriately package the newly replicated DNA into chromatin. The cell accomplishes this by coordinating the metabolism of histone proteins with chromatin assembly and DNA synthesis.

Histone proteins play an essential architectural role in compacting DNA molecules into structures we have come to know as chromosomes. Nuclear DNA exists in various compacted states through the function of the various histone proteins that exist in the cell. The more extended form of DNA exists as nucleosomes where approximately 146 bp of DNA is wrapped twice around an octamer containining two copies of each of the four core histone proteins H2A, H2B, H3 and H4. A linker histone protein, histone H1, associates with each nucleosome as well as a variable length of linker DNA. Nucleosomes can then be compacted into the higher order of condensation termed chromatin.

Two major classes of histone proteins exist. The first class encompasses the replication-dependent histone genes (H2A, H2B, H3, H4 and H1), which are encoded by over 75 genes and expressed strictly during the DNA replication phase

of the eukaryotic cell cycle (Marzluff et al., 2002). Two copies of each heterodimer consisting of both H2A:H2B and H3:H4 underlie the composition of the nucleosome. These heterodimers are deposited during the process of DNA replication in order to fill in the nucleosomal gaps that exist as a consequence of the progressing replication fork. The replication-dependent histone genes are coordinately expressed and are clustered in close proximity to one another in the genome of metazoans (Wang et al., 1996a; Wang et al., 1996b). Two major clusters encompass these genes and are present on chromosomes 1 and 6 in humans. The major cluster on the short arm of chromosome 6 (HIST1) includes the majority of the H2A, H2B, H3 and H4 genes as well as all the H1 genes. There are actually two smaller clusters of replication-dependent histone genes on chromosome 1 (HIST2 and HIST3) that together encompass another several copies each of H2A, H2B, H3 and H4.

The second class of histone genes encodes the variant (or replacement) histone genes where, in general, their expression is not restricted to S phase. These genes do not occur in clusters within the genome as do the replication-dependent histone genes. Examples of some histone variants include H2A.X, H2A.Z, H2ABbd, macroH2A, H3.3, and centromeric H3 (cenH3) (Malik and Henikoff, 2003). The variant histone H2A.X varies from H2A at the C-terminus and is the target of post-translational phosphorylation in response to DNA damage (e.g. DNA double strand breaks, ionizing radiation) (Rogakou et al., 1998). Studies on H2A.Z have revealed that this histone variant plays an important role in maintaining a transcriptionally active state of chromatin (euchromatin) (Li et al., 2007). MacroH2A

is enriched in the chromatin of the X-inactivated chromosome in female mammals (Costanzi and Pehrson, 1998). Histone variant H2ABbd (Barr body deficient) is deposited within transcriptionally active chromatin and seems to be mutually exclusive to that of macroH2A (Gautier et al., 2004). Histone H3.3 is unusual in that it differs from the canonical H3 by only four amino acid positions. The precise function of these changes is still unclear but appear to affect the ability of H3.3 to be deposited into transcriptionally active sites of chromatin (Malik and Henikoff, 2003). Centromeric H3 (cenH3) is, as its name suggests, strictly localized to the centromeres of eukaryotic chromosomes and functions in packaging chromatin at these sites. Additionally, tissue specific histones exist such as the testis specific histone H1t which is thought to play a role in meiotic events during spermatogenesis (Lin et al., 2004). Finally, it is interesting to point out that histone variants exist only in H2A and H3, while both H2B and H4 are invariant. Evolutionary and structural determinants certainly underlie the existence of H2A and H3 variants but such a discussion is out of the scope of this introduction.

The S phase-restricted synthesis of the core histones is the main, gross difference distinguishing the expression of the replication-dependent histone genes from the variant histone genes. The replication-dependent histone genes encode the only eukaryotic messenger RNAs (mRNAs) that are not polyadenylated. Instead, the mRNAs encoding the core histone genes end in a conserved stem-loop structure on their 3' end (see below and Figure 1). The 3' end unique to the replication-dependent histone mRNAs serves important roles in the post-transcriptional regulation of these genes, including processing and mRNA stability.

Variant histone genes are, like all other mRNAs, polyadenylated at the 3' end and their post-transcriptional regulation is for all intents and purposes identical to other polyadenylated mRNAs.

CHROMATIN ASSEMBLY

Chromosome replication is a rapid, error-prone process involving the coordination of the DNA synthesis machinery (e.g. DNA polymerases, helicases, etc.) with the molecules involved in the various types of DNA repair. The DNA polymerases (DNA polymerase α/primase, δ, and ε) at the replication fork also require that a delicate balance of histone proteins as well as chromatin assembly activity is present in order to ensure proper assembly of the newly replicated DNA into chromatin. During the process of DNA replication, a major chromatin assembly pathway exists that includes the heterotrimeric chromatin assembly factor 1 (CAF-1) complex. CAF-1 is comprised of the p150, p60, and p48 subunits and together are present at replication foci within the nucleus of eukaryotic cells (Verreault et al., 1996). CAF-1 activity is restricted to DNA replication and CAF-1 associates with proliferating cell nuclear antigen (PCNA), which acts as the processivity factor for the DNA polymerase at the replication fork (Groth et al., 2007). It performs the initial step in chromatin assembly, deposition of the H3-H4 tetramer.

HIRA is a second chromatin assembly complex that also functions to deposit H3-H4 tetramers, but it largely functions to assemble chromatin outside of S phase, or in a replication-independent manner. HIRA contains seven WD repeat motifs as well as a domain distinct to itself (HIRA domain) (Tagami et al., 2004). The WD

repeats allow HIRA to interact with other proteins, particularly the histone variant H3.3. Chromatin assembly outside of S phase largely encompasses incorporation of histone variants as a consequence of local changes in chromatin due to transcription or normal histone protein turnover (Gunjan et al., 2005). It is clear that HIRA prefers to interact with H3.3 which is often associated with active chromatin domains. The reason for this specificity is not clear but recent evidence suggests that H3.3-H4 histone dimers act as important intermediates in the replication-independent assembly of chromatin (Tagami et al., 2004).

REPLICATION-DEPENDENT HISTONE mRNA METABOLISM

In this dissertation I examine specifically the molecular mechanisms controlling the stability of replication-dependent histone mRNAs and therefore an overview of histone mRNA metabolism as well as general mechanisms of histone mRNA stability are in order. Additionally, general mechanisms of mRNA degradation will also be discussed. The following sections examine these subjects in detail.

Transcription

The levels of histone mRNA are tightly coupled to DNA synthesis. When cells enter S-phase, the transcription of histone genes increase 3-5 fold (Figure 2) due to the phosphorylation of the positive transcription factor $p220^{NPAT}$ (NPAT) by cyclin E/cdk2 (Ye et al., 2003b). Cyclin E/cdk2 is an essential cyclin-dependent kinase that regulates multiple aspects of the transition from G1 to S phase of the cell cycle. These aspects include E2F1-dependent transcription of genes involved in DNA

replication. NPAT is located within subnuclear structures termed Cajal bodies that a foundation of literature suggests is the primary site of histone gene transcription and pre-mRNA processing (Handwerger and Gall, 2006). In support of its suggested role in histone gene transcription, NPAT and its subsequent phosphorylation at the G1/S transition, is required for proper accumulation of coilin (p80) foci, a major structural component of Cajal bodies (Ma et al., 2000). Although the transcriptional contribution is significant to increasing histone mRNA levels, there are a number of post-transcriptional mechanisms that ultimately result in the 35-fold increase in histone mRNA seen during S phase. These mechanisms include increased pre-mRNA processing and changes in mRNA half-life. As I will subsequently discuss, histone mRNA stability and translation are intimately connected.

Pre-mRNA Processing

There are two *cis*-acting elements in histone mRNA that contribute to the processing of the pre-mRNA. One is the 26 nucleotide (nt) stem-loop (SL) sequence that is present on the 3' end of histone mRNA. The second is a purine-rich downstream sequence termed the histone downstream element (HDE) (Figure 1). The HDE is recognized through the complementary base pairing with the 5' end of U7 snRNA, which is contained within the U7 snRNP. The U7 snRNP is composed of the U7 snRNA as well as a heteroheptameric set of Sm proteins (Marzluff and Duronio, 2002). Typical splicesomal snRNPs contain SmD1, SmD2, SmB/B', SmD3, SmE, SmF and SmG. In contrast, the U7 snRNP contains Lsm10 and Lsm11 in place of SmD1 and SmD2 (Pillai et al., 2001). The SL is recognized by a second *trans* acting factor, the stem-loop binding protein (SLBP). This protein is required for

histone pre-mRNA processing in *Drosophila* and human cells (Dominski et al., 1999; Sullivan et al., 2001) and additionally functions in histone mRNA metabolism including translation.

The two *cis* elements allow for an endonucleolytic cleavage of the pre-mRNA between the SL and HDE that results in the formation of the mature 3' end of the message. Importantly, replication-dependent histone genes do not contain introns, therefore processing of histone pre-mRNA does not require the elaborate mechanisms of splicing. Instead, the final step in processing of the message is the endonucleolytic cleavage which occurs at the end of a conserved ACCCA sequence following the SL. The endonuclease responsible for cleavage of the pre-mRNA has recently been identified through UV cross-linking studies as CPSF-73 (Dominski et al., 2005a). CPSF-73 and the heat-labile factor Symplekin are core components of the histone pre-mRNA processing apparatus (Kolev and Steitz, 2005). Recent evidence from the Steitz lab suggests protein components of the splicesomal U2 snRNP plays a non-splicing role in stimulating U7-dependent histone pre-mRNA processing (Friend et al., 2007).

The SL, HDE, SLBP and U7 snRNP have an inter-dependent function in histone pre-mRNA processing. This relationship and the data supporting it are described in more detail in the Introduction of Chapter 5. A more relevant topic to this discussion, is how histone pre-mRNA processing contributes to the increase in histone mRNA levels when cells enter S phase. That is, if transcription contributes a 3-5 fold increase in histone mRNA levels, where does the additional 10 fold increase to give the final increase of 35-fold originate?

Harris et al. conducted a convincing study where they set out to separate the contributions of transcription and pre-mRNA processing to the dramatic increase of histone mRNA levels at the beginning of S phase (Harris et al., 1991). They constructed a transgene containing a constitutive U1 snRNA promoter, followed by the complete U1 coding region, and a normal histone 3' sequence (U_5H transgene). Using CHO cells synchronized by mitotic shake-off, they determined that the transgene was regulated normally in a cell cycle regulated manner and responded to inhibition to DNA synthesis. More interestingly, they observed that the U_5H transgene increased 10-fold as cells entered S phase compared to the 35-fold of a normal cloned H2A gene. Therefore, it was clear the 3.5-fold difference was due to transcription while the 10-fold effect was likely post-transcriptional. Indeed this was the case since using a different transgene construct that had two processing sites: a normal histone processing site and a downstream polyadenylation site. Therefore, the accumulation of each transcript reflected the efficiency of 3' end formation. The larger transcript (polyadenylated) predominated in G1 while the smaller, histone 3' end-containing transcript was restricted to S phase. The levels of the histone 3' end transcript present between G1 and S phase was approximately an 8-fold difference supporting the notion that as cells transit from G1 to S phase, histone pre-mRNA processing efficiency increases from 8-10 fold. Taken together, the processing efficiency of histone pre-mRNAs, like other pre-mRNAs, contributes a significant component in determining the abundance of the mature mRNA found in the cytoplasm. As we will soon discover below, in contrast to the contribution of

transcription and processing, there is a remarkable decrease in the half-life of histone mRNA that is specific to the end of S and throughout G2 phase.

SLBP as the Post-Transcriptional Regulator of Histone mRNA

SLBP plays a major role in all aspects of histone mRNA metabolism. The level of SLBP mRNA does not significantly change throughout the cell cycle but at the beginning of S phase, translation is stimulated by an unknown mechanism resulting in a 20-fold increase in SLBP protein (Figure 2) (Whitfield et al., 2000). The increased levels of SLBP are thought to be the driving factor that stimulates histone pre-mRNA processing efficiency 8-10 fold. Following pre-mRNA processing, SLBP remains bound to the SL as the mature message is exported to the cytoplasm for translation (Figure 3).

SLBP does not contain a nuclear export signal but instead is exported while being bound to the RNA. The details of histone mRNA export have been investigated in both *Xenopus* oocytes and *Drosophila* S2 cells and it is clear that the mRNA export receptor TAP is important for translocating the histone mRNP through the nuclear pore complex (Erkmann et al., 2005a). Once exported, SLBP is required for translation of the message (Sanchez and Marzluff, 2002). When histone mRNAs are degraded, SLBP is recycled back to the nucleus through interactions with the import receptors Importinα/Importinβ (Erkmann et al., 2005b). SLBP contains a nuclear localization (import) signal and amino acid mutations within the C-terminus of SLBP abrogate binding to Impα/Impβ.

The role of SLBP in histone mRNA translation has been studied in detail using the *Xenopus* oocyte system where transcription is inactive but the translational

machinery is fully competent. Unlike humans, frogs have two forms of SLBP: xSLBP1 and xSLBP2. The latter is oocyte-specific and involved in translational repression of maternally stored histone mRNAs in frogs (Sanchez and Marzluff, 2002, 2004). xSLBP1 functions analogously to human SLBP and its role in translation has been conclusively defined using an MS2 fusion protein tethering system. Recruitment of an MS2-xSLBP1 to the 3' end of an injected histone mRNA containing an MS2 stem-loop sequence (also on the 3' end) is sufficient for robust stimulation of translation compared to a reporter control RNA (Gorgoni et al., 2005; Sanchez and Marzluff, 2002). Recently the lab has discovered a protein, termed SLIP1 (SLBP Interacting Protein 1), which interacts with both SLBP and the 5' cap binding protein eIF4G. SLIP1 is involved in histone mRNA translation and likely bridges between SLBP and the 5' end of the mRNA (Cakmakci et al., 2008). In summary, SLBP plays an integral role in histone mRNA metabolism. Many of the functions of SLBP mirror that possessed by poly(A) binding protein (PABP), multiple molecules of which binds stoichiometrically to the approximately 200 nt polyadenylated 3' end that is formed during the cleavage and polyadenylation of mRNAs. PABP is important in regulating translation initiation and is a major determinant of mRNA degradation.

Degradation of Histone mRNA

The final step in metabolism of an mRNA is degradation of the mRNA. Regulation of the half-life of an mRNA can be a critical regulatory step in gene expression. It provides the best mechanism for irreversibly inactivating the translation of an mRNA, and hence halting synthesis of a particular protein until

more mRNA is synthesized. The half-life of the mRNA is a critical contributor to the steady-state level of an mRNA, and hence potentially as important as the rate of transcription of the gene in determining mRNA levels. The information for the half-life of an mRNA, and regulation of that half-life, is encoded in the mRNA, often in the 3' untranslated region (3' UTR), and is often mediated by proteins that interact with the 3' UTR. Degradation of histone mRNA plays a critical role in regulation of histone protein biosynthesis, helping to maintain the balance between DNA and histone biosynthesis (Sariban et al., 1985). Replication-dependent histone mRNAs are present in large amounts only in S-phase cells; they are rapidly synthesized just prior to entry into S-phase and rapidly degraded at the end of S-phase or when DNA synthesis is inhibited. A more detailed discussion of the known mechanisms controlling histone mRNA stability and general mechanisms of mRNA decay are detailed in subsequent sections (see below).

SIGNIFICANCE OF MAINTAINING PROPER HISTONE PROTEIN LEVELS

The various post-transcriptional mechanisms discussed above contribute to the increased levels of histone mRNA at the beginning and continuing throughout S phase. Maintaining the appropriate levels of histone biosynthesis is critical for proper chromatin formation. This was first shown in the budding yeast *Saccharomyces cerevisiae* where Meeks-Wagner and Hartwell showed that overexpression of histone H2A-H2B and H3-H4 dimers results in significant chromosome loss (Meeks-Wagner and Hartwell, 1986). Additional data in budding yeast demonstrate that Rad53 is required for the degradation of excess histone

proteins in the nucleus (Gunjan and Verreault, 2003). Rad53 is a kinase that is required for efficient DNA replication and recovery from DNA damage. Mutants in Rad53 have a loss of viability phenotype that is exacerbated by increasing histone gene expression. Decreasing histone gene expression attenuates this phenotype. In addition, the highly net positive charge of histone proteins combined with the overall negative charge of nucleic acid, particularly double-stranded DNA, has been shown to result in chromatin aggregates when excess histone proteins are present (Steger and Workman, 1999). The result of such chromatin aggregates is a blockage in transcription.

In flies, null mutants of SLBP are embryonic lethal and accumulate misprocessed, polyadenylated histone mRNAs that are not cell cycle regulated (Lanzotti et al., 2002; Sullivan et al., 2001). Moreover, hypomorphic SLBP mutant flies have decreased levels of properly processed histone mRNA and examination of mitotic cells in developing embryos reveal dramatic malformations of the mitotic spindle due to improperly formed chromatin that results as a consequence of low maternal levels of histone proteins present in the developing embryo. Together these data suggest an important role for maintaining a fine balance of histone biosynthesis with the changing demands of DNA synthesis. A major mechanism that allows the eukaryotic cell to rapidly regulate histone biosynthesis with DNA synthesis is through post-transcriptional mechanisms that rely on rapidly altering the half-life of histone mRNA.

HISTONE mRNA DEGRADATION IS A REGULATED PROCESS

It has been appreciated for over 30 years that mRNAs encoding various gene transcripts have different half-lives (Perry and Kelley, 1973; Singer and Penman, 1973), but only recently have we come to appreciate the significance. We have learned from the preceding section the contributions of transcription, pre-mRNA processing and stability imparts to the levels that a particular mRNA accumulates in the cytoplasm. Early studies on housekeeping genes that are constitutively expressed observed that the mRNA of the different housekeeping genes accumulated at variable levels (Berger and Cooper, 1975). Detailed kinetic measurements of polyadenylated mRNAs revealed dramatic differences in the half-lives of rare and abundant mRNAs in the developing sea urchin (Cabrera et al., 1984). Moreover, molecular studies examining the 3' UTR of the cytokine granulocyte-macrophase colony-stimulating factor (GM-CSF) revealed the presence of specific AU-rich sequence elements (AREs) that rendered this mRNA inherently unstable (Shaw and Kamen, 1986). Histone mRNAs are an excellent example of a class of mRNAs that are coordinately regulated by a common *cis*-element, the stemloop.

Histone mRNA half-life is normally regulated during the cell cycle, but the regulation of degradation is most easily studied by inhibiting DNA replication, which triggers a rapid degradation of histone mRNA. By all the parameters studied, degradation of histone mRNA under these conditions is similar to histone mRNA degradation at the end of S-phase (Kaygun and Marzluff, 2005a, b; Mullen and

Marzluff, 2008). After inhibition of deoxynucleotide synthesis, there is a short lag (5-10 min) before histone mRNA degradation is initiated, likely as a result of depletion of the deoxynucleotide pool (Graves and Marzluff, 1984), and then degradation proceeds rapidly with a half-life of the mRNA of about 10 min., compared to the half-life of about an hour in S-phase cells (Heintz et al., 1983).

A number of different studies have clearly demonstrated the cell cycle regulated expression of histone genes (Harris et al., 1991; Morris et al., 1991). Using double thymidine synchronized HeLa cells (Morris et al., 1991) or mitotic shake-offs of CHO cells (Harris et al., 1991), the restriction of histone mRNA expression to S-phase has been well documented. In addition, pulse-chase studies using ^{3}H-precursors performed over 30 years have shown in double thymidine synchronized HeLa cells and logarithmically growing mouse L cells, that histone mRNA levels rapidly disappeared from polyribosomes when DNA synthesis was inhibited using either hydroxyurea or cytosine arabinoside (Gallwitz, 1975; Perry and Kelley, 1973). It was clear from these early mRNA stability studies that changes in histone mRNA levels was not a stochastic process, but instead regulated, molecular events were underlying the rapid changes observed in histone mRNA stability. These early data in combination with work by others (Graves et al., 1987) pointed to a translational component of this process since pre-treatment of synchronized HeLa cells with cycloheximide (inhibitor of translation elongation) followed by treatment with hydroxyurea rendered histone mRNAs stable (Gallwitz, 1975). Moreover, studies using the transcription initiation inhibitor actinomycin D clearly demonstrated

that inhibition of transcription had only a minor effect in the levels of histone mRNA during S-phase (Gallwitz, 1975; Perry and Kelley, 1973).

A landmark study in 1987 provided overdue insight into how the mRNA itself as well as translation contributed to the regulated degradation of histone mRNA (Graves et al., 1987). Using altered transgenes of histones H2A and H3 transfected into mouse L cells, the investigators made two major findings. The first was that an intact 3' end (i.e. the stem-loop sequence) was necessary for efficient degradation of histone mRNA. In support of this data, replacement of the poly(A) tail on a globin mRNA with the stem-loop resulted in an mRNA that was rapidly degraded when DNA replication was inhibited (Pandey and Marzluff, 1987). The second was that the mRNA needed to be translated to within 300 nt of the 3' end. The latter suggested some of the early evidence for what we now understand to be an intimate link between translation termination at the stop codon and mRNA degradation (Akimitsu, 2008).

Although the above literature provided early clues into the role of translation and the importance of the 3' stem-loop of histone mRNA, the actual enzymes responsible for degrading histone mRNA remained elusive. Ross and colleagues sought to solve this problem by developing an in vitro histone mRNA degradation system (Ross and Kobs, 1986). By isolating polysomes from human K562 erythroleukemia cells, they were able to study some of the early steps involved in histone mRNA degradation. Using S1 nuclease mapping using probes to the 5' and 3' end of histone H4 mRNA, they were able to demonstrate that degradation intermediates accumulated that were trimmed from the 3' end but not the 5' end

(Ross and Kobs, 1986). This data suggested the involvement of a 3'-5' exoribonuclease that was present in their polysome fractions. Moreover, they could identify intermediates that appeared to stall early in the degradation process, presumably due to the presence of the structured 3' stem-loop sequence found on replication-dependent histone mRNAs. Despite extensive efforts to characterize the biochemical properties of this 3'-5' exonuclease activity using this *in vitro* degradation, Ross and colleagues were never able to identify the suggestive enzyme.

In 2003, Dominski and colleagues identified a 3'-5' exonuclease (3'hExo) as a protein that was purified using a biotinylated stemloop RNA as an affinity ligand (Dominski et al., 2003). 3'hExo forms a ternary complex with the 3' stem-loop RNA substrate and SLBP *in vitro*. It could degrade efficiently 2-3 nucleotides from the 3' end of the SL RNA and could degrade as far as 13 nucleotides into the stem of the 30 nt RNA substrate. In the presence of SLBP it only removed 2-3 nts from the 3' end of the mRNA. Although the 3'hExo *in vitro* data was suggestive of being the elusive 3'-5' exonuclease Ross and coworkers were hunting, the function of 3'hExo on histone mRNA degradation *in vivo* remained to be determined. Kupsco et al. attempted to use a genetic approach in *Drosophila* to address the biological role of 3'hExo in histone mRNA degradation (Kupsco et al., 2006). Following the identification of a 3'hExo (Snipper in flies) mutant, they were able to test if Snipper functioned in degrading histone mRNAs in the imaginal eye disc and developing embryo. Snipper mutants were indistinguishable from wild-type flies suggesting the closest 3'hExo ortholog in flies did not play a role in controlling histone mRNA

degradation. Despite the efforts from a number of different groups, the enzymes responsible for degrading histone mRNA upon inhibition of DNA synthesis and normally at the end of S phase remain to be determined.

However, recent data from our lab provide more direct evidence that indeed translation is required for rapid destabilization of the mRNA. By putting the translation of histone mRNAs under the regulation of the iron response element (IRE) (Hentze et al., 1987), Handan Kaygun showed that active translation is required for efficient degradation (Hentze et al., 1987; Kaygun and Marzluff, 2005b). The translation of a number of cellular mRNAs have an IRE located in their 5' untranslated region (UTR), and the translation of these mRNAs is regulated by both iron response element binding protein (IRP) and intracellular iron levels (Klausner et al., 1993). Handan's study also carefully mapped specific distance effects of the SL in relation to the termination codon and found moving the SL only 30 nucleotides from the termination codon was sufficient for destabilizing the mRNA. A mutant form of SLBP (SAVEE-SLBP) that is defective in efficiently translating histone mRNAs was also shown to impair histone mRNA decay.

Handan Kaygun also demonstrated that the RNA helicase Upf1, which is involved in a specialized form of mRNA quality control termed nonsense-mediated decay (NMD, see below), was required for efficient decay of histone mRNA both in response to inhibition of DNA synthesis and normally at the end of S phase (Kaygun and Marzluff, 2005a). This was shown by transfection of mutant forms of Upf1 and RNAi-mediated downregulation of Upf1 protein. Surprisingly, a stable cell line expressing hemagglutinin (HA)-tagged SLBP could immunoprecipitate Upf1 protein

in a hydroxyurea-dependent manner. This interaction was independent of binding to Upf2 and Upf3, two proteins normally found in complex with Upf1. These data suggest that Upf1 specifically associates with SLBP when DNA synthesis is inhibited or upon completion of S phase to promote rapid degradation of histone mRNA. These data provided the first insights into the possibility that the eukaryotic cell uses the NMD surveillance machinery, once specifically thought to target only aberrant mRNAs, to control mRNA levels of normal intronless mRNAs.

NONSENSE-MEDIATED DECAY

Nonsense mediated decay (NMD) was originally identified in yeast (Leeds et al., 1991) and was subsequently shown to be conserved in humans (Belgrader et al., 1994). NMD functions as a molecular surveillance system in eukaryotes to eliminate aberrantly spliced mRNAs containing premature termination codons (PTCs), since the expression of truncated forms of any mRNA might lead to aberrant proteins which might have activities that could be detrimental to the cell. In fact, this is the case in yeast where Upf1 mutant strains accumulate PTC-containing transcripts that lead to cytotoxicity (He et al., 1993). In mammals this pathway affects only mRNAs encoded by spliced transcripts (Maquat, 2004; Maquat and Li, 2001), and hence does not affect histone mRNAs (Maquat and Li, 2001), since these lack introns. During pre-mRNA splicing a complex of proteins, termed the exon-junction complex (EJC), is deposited on the mRNA to mark the removal of each intron (Le Hir et al., 2000). In the case that there is a termination codon greater than 50-55 nt upstream of an exon-exon junction, these mRNAs are rapidly degraded once the ribosome has

terminated (Lykke-Andersen et al., 2000), suggesting that an EJC in the 3' UTR destabilizes mRNAs. Indeed there are approximately 12-16 proteins contained within the exon junction complex of which Upf1, Upf2 and Upf3 are included (Schell et al., 2003).

Nonsense mediated decay results from recognition of an inefficient translation termination codon by Upf1. Recent biochemical studies have revealed that Upf1 stably exists in a complex of proteins that include SMG-1, eRF1, and eRF3 (SURF complex) (Kashima et al., 2006). SMG-1 (also known as ATX) is a phosphoinositide-3-kinase-like kinase (PI3K-like) that plays a critical role in regulating Upf1 activity via phosphorylation of 16 SQ/TQ substrate sites present in the C-terminus of this protein. The eukaryotic translation termination factor eRF1 recognizes any of the three stop codons and has a multidomain structure that allows it to interact with the stop codon, the peptidyl transferase center of the ribosome, and the other release factor eRF3. eRF3 is a small GTPase that enhances stop codon recognition by eRF1 and release of the growing polypeptide chain from the ribosome. Upf2 binds to Upf3 in the EJC and Upf2 then binds to Upf1. This in turn results in the activation of mRNA decay as a result of the activity of the SURF complex to the premature termination codon.

Additional mRNA surveillance systems exist to monitor aberrant mRNAs such as non-stop decay and no-go decay. Non-stop decay functions to target mRNAs that lack a stop codon while no-go decay functions to eliminate mRNAs that have stalled ribosomes on them (Doma and Parker, 2006; Frischmeyer et al., 2002). The details of these pathways are not well understood.

As we have learned from the aforementioned sections, an intimate link between mRNA degradation and translation has been observed for many years but only recently (Ivanov et al., 2008; Keeling et al., 2006) have we begun to understand the detailed molecular mechanisms that coordinate translation termination and mRNA degradation. Histone mRNAs are the only known example of degradation of a normal cellular mRNA, likely regulated through the efficiency of translation termination (Kaygun and Marzluff, 2005a, b), requiring Upf1 for its degradation.

GENERAL MECHANISMS OF mRNA DEGRADATION

During the past decade our understanding of mRNA degradation has increased dramatically (Decker and Parker, 1994; van Hoof and Parker, 1999). Most of this information is from work done in yeast, but studies in higher eukaryotes are providing significant insight into the shared pathways between these organisms. The mechanisms in yeast are for the most part conserved in metazoans, but certainly exceptions exist (Gatfield and Izaurralde, 2004; Moore, 2005). Additionally, recent genome-wide studies in human cells have highlighted the importance of mRNA stability in regulating gene expression in response to various types of cellular stress (UV, heat shock, and prostaglandins) or cellular signals that direct T cell activation (Cheadle et al., 2005; Fan et al., 2002). These microarray-based studies have revealed that 40-50% of the changes in gene expression that occur in response to various cellular signals result due to changes in mRNA stability. Additionally, the impact that small RNA pathways (see below) have on mRNA stability and gene expression has certainly been a major scientific discovery that

underscores the importance of mRNA degradation. The purpose of this section is to provide an overview of the various mechanisms that exist to regulate mRNA degradation. The reader should come away with an understanding that mRNA degradation does not simply serve as a garbage disposal for tired, unwanted mRNAs but that nature has evolved several mRNA degradation pathways that serve integral functions in regulating gene expression through mRNA stability.

Two Major mRNA Degradation Pathways Exist in Eukaryotes

Eukaryotic mRNAs have structural elements on their 5' and 3' ends that impart a certain level of stability to any particular mRNA. The first is the 5' hypermethylated 7-methylguanosine cap structure that is added to the mRNA cotranscriptionally. The second is the 3' poly(A) tail which is also added contranscriptionally. The 5' cap structure and poly(A) tail interact with the translation machinery via eIF4E and PABP, respectively. Most, but certainly not all, mRNA degradation pathways begin with deadenylating the mRNA (Tucker and Parker, 2000). The removal of the poly(A) tail breaks the assocation of PABP with the scaffolding translation factor eIF4G, thereby effectively breaking the circular structure of translating mRNAs. Following this the mRNA is deadenylated probably by CCR4/Not1/Pop2 (Goldstrohm et al., 2006; Yamashita et al., 2005), although other deadenylases exist such as PARN and PAN2-PAN3 (Brown et al., 1996; Funakoshi et al., 2007). The deadenylation of the poly(A) tail may serve as a molecular clock dictating the exit of the mRNA from translational competency. The 5' hypermethylated m^7-GTP cap can then be removed by decapping enzymes, namely the Dcp1/Dcp2 complex of which Dcp2 is the catalytic subunit. In higher

eukaryotes there exists an additional decapping cofactor know as hedls, or Ge-1, that has been shown to be an enhancer of decapping (Fenger-Gron et al., 2005). Once decapping has occurred the mRNA can be degraded by Xrn1, the major cytoplasmic 5'-3' exonuclease. The 5' cap structure that has been removed is eventually degraded by a scavenger pyrophosphatase known as DcpS (Liu et al., 2002). A schematic of the mechanism of 5'-3' degradation is outlined in Figure 5 and Table 1 lists a number of the major enzymes involved in RNA degradation.

Decapping is a tightly regulated process since the 5' cap structure serves an important role in specifying stability as well as participating in translation of a particular mRNA. A number of accessory factors therefore exist that are known enhancers of decapping, and these are recruited to mRNA after deadenylation. The decapping enzymes are recruited to the 5' end by a heteroheptameric complex of Sm-like proteins, Lsm1-7 (Bouveret et al., 2000). In budding yeast, Lsm1 mutant strains accumulate deadenylated, capped mRNAs (Tharun et al., 2000; Tharun et al., 2005). Similarly, decapping enzyme mutant strains of budding yeast also accumulate deadenylated mRNAs, providing compelling genetic evidence for the Lsm1-7 complex functioning as a positive regulator of decapping activity (Tharun et al., 2000). Lsm1-7 is similar to another Sm-like complex, Lsm2-8, which share identical subunits with the exception of course being Lsm1. Lsm2-8 however functions in stabilizing U6 snRNA as well as processing of pre-tRNAs, pre-snoRNAs, and pre-rRNAs (Kufel et al., 2002). Sm and Sm-like proteins are RNA binding protein complexes that recognize U-rich sequence elements (Schumacher et al., 2002). They form a ring structure that crystallographic studies have shown bind

RNA on one face of the complex, although it is also possible the complex assembles around the RNA molecule. Lsm1-7 is similar to the *Escherichia coli* Sm-like protein Hfq, which is an important regulator of mRNA degradation in bacteria.

Other Lsm proteins have also been implicated in having roles in mRNA degradation such as Lsm14 (PABP-binding protein-1, Pbp1) and Lsm16 (enhancer of decapping-3, EDC3) (Kshirsagar and Parker, 2004; Morrissey et al., 1999). Additionally, other decapping accessory proteins exist such as the DEAD/H-box RNA helicase Dhh1 and Pat1, which are also recruited by Lsm1-7. Dhh1 (or RCK/p54) has been well characterized in budding yeast and through elaborate polysome profiling by Coller and Parker has been shown to be involved in translational repression and mRNA degradation (Coller and Parker, 2005; Coller et al., 2001). Genetic evidence of Pat1 also suggests Dhh1 and Pat1 function to cooperatively regulate translational repression and/or mRNA degradation.

The 5'-3' degradation pathway described above represents the first of two predominant mRNA decay pathways in eukaryotes. The second pathway involves 3'-5' mRNA degradation by a complex of proteins termed the exosome. The eukaryotic exosome contains 10-11 proteins that either have 3'-5' exoribonuclease activity or possess RNA recognition and binding properties. Figure 6 depicts a generalized 3'-5' pathway and Table 1 lists a number of the protein components involved. There are 6 predicted exonucleases in the exosome, both phosphorlytic and hydrolytic enzymes. These are Rrp41, 42, 43 (OIP2 in humans), Rrp45 (PM/Scl-75 in humans), Rrp46, and Mtr3 (Liu et al., 2006). These six proteins share close sequence homology to *E. coli* RNase PH and the polynucleotide

phosphorylase (PNPase) PH domain (Houseley et al., 2006). Both enzymes are processive, hydrolytic 3'-5' exoribonucleases. I should point out that the exonuclease activity sounds contradictory to the naming of polynucleotide phosphorylase. This is because PNPase was originally described as an RNA polymerase and indeed Severo Ochoa received the Nobel Prize for its discovery. However, as an exonuclease it produces diphosphates as a product in a reaction that is readily reversible. Thus in high nucleotide diphosphate concentrations, PNPase can catalyze the polymerization of nucleotides where phosphate is released. It was this latter activity that PNPase is best known for since this enzyme plays an important role for priming bacterial mRNA degradation by adding A's to the 3' ends of transcripts for subsequent degradation by the degradosome (Garneau et al., 2007; Wilusz and Wilusz, 2005). The yeast exosome contains an additional component Rrp44 which is another 3'-5' exoribonuclease which is similar to bacterial RNase R and RNase II (Schneider et al., 2007). Rrp44 (Dis3 in humans) has not been identified in human exosome preparations.

There are three additional components of the exosome that possess S1 or KH RNA binding domains that are presumed to perform the substrate recognition function of the complex. These include Rrp4, Rrp40 and Csl4 (Liu et al., 2006). The final component for the yeast and human exosome is Rrp6 (PM/Scl-100 in humans), which is a distributive hydrolytic exoribonuclease. There still exists some contention surrounding whether or not PM/Scl-100 is restricted to the nuclear exosome or present in both the nuclear and cytoplasmic exosome. Biochemical purification experiments suggest restriction of Rrp6 to the nucleus while subcellular localization

studies combined with functional experiments provide more compelling evidence that indeed Rrp6 (PM/Scl-100) is present, at least in mammals, in both cellular compartments (Graham et al., 2006; Lejeune et al., 2003).

The exosome was originally described in budding yeast (Mitchell et al., 1997). The nuclear exosome complex plays an important role in eliminating aberrant precursors of various RNAs including pre-mRNAs, pre-tRNAs and pre-rRNAs (Allmang et al., 1999). Although the nuclear exosome has defined roles in processing and quality control, it also has a clear role in cytoplasmic mRNA decay where the only known substrate in the cytoplasm is mRNA. Like the cytoplasmic 5'-3' degradation pathway, the exosome relies on the deadenylation of the poly(A) tail to render the transcript translationally inactive. At this point the exosome's numerous 3'-5' exonucleases can function to rapidly degrade the mRNA, although the precise mechanisms that are responsible for this recruitment are not well understood. As mentioned earlier, Rrp4, Rrp40 and Csl4 certainly impart some of the substrate recognition properties of the exosome but several studies implicate 3' end processing complexes (TRAMP complex) and translation regulation complexes (Ski7, Ski2/Ski3/Ski8, EF1A, and eRF3) in specifically directing exosome activity to particular mRNAs (Houseley et al., 2006; LaCava et al., 2005). The TRAMP complex and its components will be discussed in more detail in Chapters 3 and 6.

I have described the 5'-3' and 3'-5' pathways as separate pathways but they do not appear to be mutually exclusive. Although there is evidence that the 5'-3' decay pathway performs the bulk of mRNA degradation under normal laboratory growth conditions in budding yeast, there does not appear to be a significant effect

on the yeast mRNA population when either the 5'-3' or 3'-5' decay machinery is knocked out (He et al., 2003; Houalla et al., 2006). The latter suggests some redundancy in the pathways. Whether or not the two pathways cooperate to degrade a single mRNA molecule is a subject of debate and although some evidence in humans (Lejeune et al., 2003) is suggestive of cooperation, no direct evidence exists.

Other Decay Pathways

In addition to the 5'-3' and 3'-5' RNA decay pathways, there exist other mRNA degradation pathways. These include deadenylation-independent mechanisms and endonucleolytic decay. The two examples of deadenylation-independent decapping and degradation in budding yeast involve an autoregulatory feedback for *EDC1* and *RPS28B* mRNAs (Badis et al., 2004; Muhlrad and Parker, 2005). Figures 7 and 8 provide schematic representations of these two mechanisms. Edc1 protein is an enhancer of decapping and binds an oligo(U) sequence in the 3' UTR of its own mRNA (Muhlrad and Parker, 2005). In contrast, Rps28B protein binds a stem-loop structure in the 3' UTR, but also within its own mRNA. Rps28B protein recruits another protein Edc3, which has been described previously as an enhancer of decapping (Badis et al., 2004). Thus, when there is excess Rps28B or Edc1 protein, the cell responds by degrading these mRNAs. These examples of deadenylation-independent decapping and 5'-3' degradation apply to specific mRNAs and it is generally thought to be an infrequent degradation pathway. As yet there are no examples of RNAs degraded by this pathway in metazoans.

Three enzymes PMR1, IRE1 and RNase MRP have been implicated as endoribonucleases involved in another deadenylation-independent mRNA degradation pathway (Stevens et al., 2002; Yang and Schoenberg, 2004). However, a very limited number of substrates have been identified for these enzymes. Although their substrates are limited, these enzymes are particularly potent since they can by-pass both the 5' cap structure and poly(A) tail that serve as structural mRNA stabilizing elements. In *Drosophila*, endoribonucleases appear to play a more integral part in RNA degradation than in other metazoans. For example, Gatfield and Izzauralde have demonstrated that the degradation of aberrant mRNAs harboring a premature termination codon (i.e. NMD substrates) is initiated by endonucleolytic cleavage (Gatfield and Izaurralde, 2004). The subsequent 5' and 3' cleavage products are then degraded in both the 3'-5' and 5'-3' directions, respectively.

Probably the most fascinating example of endonucleolytic mRNA degradation is that carried out by the RNA interference (RNAi) and microRNA (miRNA) machinery. The RNAi pathway functions to regulate gene expression at the post-transcriptional level by silencing the expression of mRNAs through a combination of translational repression and mRNA degradation. RNAi is essential in animal development and its significance is underlined by the presence of other small RNA pathways that function to regulate a variety of cellular processes (Zamore and Haley, 2005). The *trans* factors that mediate RNAi are small (approximately 19-22 nt long) non-coding, double-stranded RNAs. These small RNAs are processed from double-stranded RNA through an elaborate set of processing steps that requires the

RNase III type of endonuclease Dicer (Bernstein et al., 2001; Hammond, 2005). The processed miRNA (or siRNA) is delivered to the 3' UTR of target mRNA substrates through a ribonucleoprotein complex termed the RNA interference silencing complex (RISC). In the case of post-transcriptional gene silencing by mRNA degradation, the RISC complex delivers the complementary strand of the small RNA to the substrate mRNA and results in the endonucleolytic cleavage of the miRNA:mRNA hybrid. The subsequent 5' and 3' cleavage products are then degraded 3'-5' and 5'-3', presumably by the exosome and Xrn1, respectively. The RISC complex contains the small RNAs as well as a number of Argonaute family of proteins, particularly Argonaute 2 (Ago2). Ago2 is a PIWI domain-containing endonuclease V enzyme that is responsible for the catalytic 'slicer' activity possessed by the RISC complex (Hammond et al., 2001).

Whether miRNAs function to silence gene expression by mRNA degradation or translational repression was recently a subject of debate, but it is clear that both situations exist (Bagga et al., 2005; Pillai et al., 2005) and many miRNAs form imperfect double-stranded sequences with their targets which would preclude cleavage by Ago2. To complicate matters, Steitz and coworkers have recently shown that miRNAs can function to upregulate gene expression of target mRNAs in mammalian cells that are not undergoing cell division (Vasudevan and Steitz, 2007; Vasudevan et al., 2007). Regardless, the importance of small RNA pathways in regulating gene expression is clear and in time the details and mechanisms by which they function will be elucidated.

Processing Bodies

The final subject I will cover regarding the general mechanisms of RNA degradation is the presence of two major subcellular structures that function to remodel mRNA ribonucleoprotein (mRNP) complexes. In general, these structures sequester both translationally repressed mRNAs as well as the bulk of mRNAs that are being degraded. In the last section we discussed the potential of miRNAs to translationally repress target mRNAs. Translational repression is a common mechanism to inactive gene expression and a good developmental example of this is the repression of maternal mRNAs of flies, frogs, and worms, where localization factors (e.g. Me31b and Exuperantia in flies) sequester translationally repressed mRNAs to discrete granular foci (Nakamura et al., 2001), where they are stored for use during early development.

Processing bodies (P bodies or GW bodies) are punctate foci found in the cytoplasm of eukaryotic cells that contain protein components of the 5'-3' mRNA degradation pathway. Evidence suggests that the GW182 protein (identified as an autoantigen) functions as an essential scaffolding protein in their formation (Yang et al., 2004). P bodies though are not found in all cells and are most apparent under conditions of stress; although they do occur, albeit to a much lesser degree, in conditions where stress is absent. They were first identified in *S. cerevisiae* under conditions of arsenic exposure (Sheth and Parker, 2003). Green-fluorescent protein (GFP)-tagged proteins involved in translational repression and 5'-3' degradation factors were examined by immunofluorescence and found to colocalize to discrete foci with mRNA (Sheth and Parker, 2003). The number and size of the P bodies

changed upon deletion of particular components of the mRNA decay machinery. For example, Pat1 mutants (which affect initiation of mRNA degradation) had smaller P bodies while mutants of the 5'-3' degradation pathway (e.g. Xrn1, Dcp2, Lsm1), which would interfere with later steps in mRNA degradation had more P bodies and these were larger than wild-type yeast. These and other data suggest that large amounts of cytoplasmic mRNA degradation occur in P bodies.

It is clear however that not all mRNA targeted to P bodies are destined for degradation. For example, Pillai et al. demonstrated in an elegant study that the let-7 miRNP inhibits cap-dependent but not cap-independent translation, suggesting that this miRNP might function to repress translation through recognition of the cap (Pillai et al., 2005). Moreover, this repression occurred in foci that overlapped or were directly adjacent to P bodies and Ago2 protein. In conjunction with other data, it seems clear that miRNAs function first at an early step to inhibit translation initiation by targeting the cap-binding complex eIF4F, and can then either remain repressed (and potentially be reactivated) or undergo degradation 5' to 3'.

In mammalian cells, P bodies also show cell cycle regulation. Chen and coworkers have shown using synchronized HeLa cells that P body components were small in size in G1, but increase in number during S phase and this pattern changed when cells entered G2 phase. Then, the P bodies were remarkably, larger in size but fewer in number. P body size and number decreased as cells progressed through mitosis (Yang et al., 2004). Based on a decreased electrophoretic mobility of GW182 protein as cells progressed through the cell cycle, they hypothesized that post-translational modification(s) of GW182 play a role in regulating P body

accumulation. Regardless of the precise mechanism, the data are suggestive of the notion that dividing human cells require bulk mRNA degradation at the end of S phase and that this demand is sustained throughout G2 phase. Intriguingly, Whitfield and coworkers found that the greatest changes in mRNAs occurred not as cells progressed from G1 to S phase but as cells entered G2 (Whitfield et al., 2000).

Together, the literature on P bodies clearly implicates these punctate granules in mRNA turnover. However, it is also clear that P body components (e.g. Lsm1, Dcp2, and Xrn1) occur outside of P body foci. A working model of P body formation points to P body formation as a cellular state that reflects the quantity of degradation and/or repression that is occurring in the cytoplasm; that is, larger P bodies reflect P body aggregation or polymerization. The model also incorporates the notion that degradation can occur outside of P body aggregates in so-called P body monomers. In summary, P bodies appear to be the eukaryotic cell's way of compartmentalizing mRNAs that are destined to be degraded, likely by preventing their reassociation with the translation machinery.

In summary, a number of mechanisms have evolved to regulate gene expression by altering mRNA stability using multiple mechanisms of mRNA degradation and translational repression. In this dissertation I will describe a novel method of degrading histone mRNAs, which expands the known pathways of mRNA degradation.

CONNECTION BETWEEN HISTONE METABOLISM AND THE CELL CYCLE CHECKPOINTS

Eukaryotic cells have evolved a number of molecular surveillance mechanisms to monitor the complex processes it carries out. We have discussed NMD as a molecular surveillance system to monitor the quality of mRNAs being exported from the nucleus. Another molecular surveillance system known as cell cycle checkpoints exist to preserve the integrity of the genome. Cell cycle checkpoints are complex signal transduction pathways that monitor DNA damage that is the consequence of external sources such as UV light, ionizing radiation, endogenous sources such as free-radical oxidation, or the results of the error-prone process of DNA replication. Slowing progression through the cell cycle or arresting the cell cycle provides time for the cell to coordinate DNA repair activity to repair the damage or, if the damage is too severe, results in cell fate decisions such as apoptosis. Collectively, the checkpoint machinery slows or arrests the progression of the cell cycle in order to provide time for repair and prevent any subsequent generations from inheriting genetic abnormalities such as mutations and chromosome loss or gain.

Checkpoints are present in all phases of the cell cycle. The PI-3K-like kinases (PI3K-like) ATM (ataxia telangiectasia-mutated), ATR (ATM and Rad3-related), DNA-PK (DNA protein-activated kinase), and most recently hSMG-1 serve as apical sensors in the signal transduction cascade. ATM and ATR cooperate with mediator proteins sometimes referred to as adaptor proteins that modulate their activities (no known mediators of hSMG-1 have been identified). Together the apical kinases

ATM and ATR and their mediator proteins signal downstream to the transducer kinases Chk1 and Chk2 which leads to further downstream signaling to effector proteins that ultimately target cyclin-dependent kinases or regulatory phosphatases responsible for preventing entry into the next cell cycle phase. Heightened interest in the ATM and ATR kinases has led to an ever-growing mechanistic understanding of their participation in cell cycle checkpoints (Kastan and Bartek, 2004). DNA-PK function is required for repair of double-stranded breaks as well as in maintaining telomere length.

The least characterized member of this family is the ATM-like PI3K-like kinase, hSMG-1 (formally known as ATX). SMG-1 metazoans is an mRNA surveillance protein that regulates the NMD pathway through its function in the SURF complex (Grimson et al., 2004) and it was first described in *C. elegans* (CeSMG-1) (Pulak and Anderson, 1993). A recent report showed hSMG-1 kinase activity is increased in response to ionizing radiation and ultraviolet light and that hSMG-1 can also phosphorylate p53 and Upf1 *in vivo* (Brumbaugh et al., 2004). Additionally, NMD is suppressed in hSMG-1 null cells but not in ATM null cells. Upf1 is a target of SMG-1 likely explaining its function in NMD. These data provide evidence for a role of hSMG-1 in regulating both genotoxic stress response with mRNA quality control.

DNA synthesis is a tightly regulated process that requires precisely regulated temporal and spatial firing of replication origins in order to efficiently replicate the genome. Active origins of replication can proceed only as quickly as there are sufficient levels of histone proteins. In this way histone proteins levels, which we

have seen are regulated post-transcriptionally at the mRNA level, can limit the rate of DNA replication. Between these two levels of regulation is chromatin assembly, which couples DNA synthesis with *de novo* histone deposition, which in turn requires a constant supply of histone proteins. Recent evidence from the Stillman and Kaufman labs have shown that using either siRNA-mediated knockdown of CAF-1 (Hoek and Stillman, 2003) or a dominant-negative form of CAF-1 (Ye et al., 2003a) results in S phase arrest, causes DNA damage, and activates a Chk1-dependent checkpoint response. These data provide a link between efficient replication fork progression and the S phase checkpoint machinery that monitors appropriate chromatin assembly. In agreement with this data, Handan Kaygun in our lab recently showed using an inducible kinase-inactive ATR cell line that overexpression of the kinase-inactive ATR attenuated efficient histone mRNA degradation (Kaygun and Marzluff, 2005a).

Most recently, Müller et al. provide evidence that DNA-PK may also play an important role in maintaining proper histone mRNA abundance with DNA replication (Muller et al., 2007). Much work in the DNA replication field have shown that when human cells undergo replication stress, such as when cells are treated with inhibitors of DNA synthesis, replication fork collapse can occur following slowing and stalling of the replication machinery. This can result in double-stranded breaks in the DNA that can be repaired by ATM or DNA-PK through homologous recombination or non-homologous end-joining, respectively. Using a variety of inhibitors of cell cycle checkpoint function, their data suggest that DNA-PK is the LY294002-sensitive PI3K-like kinase responsible for regulating histone mRNA levels in response to

inhibition to DNA synthesis (Muller et al., 2007). Considering the above data and more by others (Gunjan and Verreault, 2003; Sullivan et al., 2001) it is clear that the eukaryotic cell requires a fine balance between histone levels and the rate of DNA synthesis in order to preserve the integrity of their genomes. Cell cycle checkpoints function in helping coordinate these needs and likely impact directly on histone mRNA metabolism.

SUMMARY

The eukaryotic cell coordinately regulates histone biosynthesis with the demands of DNA replication. This tight regulation is necessary to ensure proper chromatin formation. Regulation of histone protein synthesis occurs post-transcriptionally at the mRNA level, where inhibition of DNA synthesis results in rapid decay of histone mRNA levels. Therefore, altering the half-life of the mRNA serves as a major mechanism in regulating histone mRNA levels. Much is known about the initial steps in the metabolism of histone mRNA, such as pre-mRNA processing and translation. Only recently has much insight been achieved into the mechanisms of how the cells coordinate histone synthesis with DNA replication. These data suggest an exciting cooperation between two molecular surveillance systems that monitor mRNA quality control (NMD) and preserve the integrity of the genome (cell cycle checkpoints). What remains unknown regarding histone mRNA degradation are the actual enzymes responsible for regulating the rapid changes in histone mRNA stability *in vivo* both in response to inhibition of DNA synthesis as well as normally at the end of the DNA synthesis phase of the cell cycle. In addition, the

precise molecular mechanism(s) that target histone mRNAs specifically for degradation remain undefined.

The subsequent chapter (Chapter 2) of this thesis describes experimental data that point to a bidirectional degradation mechanism for rapidly altering histone mRNA levels. In addition, I present data in Chapter 3 that identify the initial step in histone mRNA degradation is addition of oligouridine residues to the 3' end of histone mRNA. Following is a chapter (Chapter 4) that outlines detailed methodologies I have developed to detect these oligouridylated histone mRNA degradation intermediates. In Chapter 5, I describe the critical functions of SLBP in regulating histone mRNA metabolism, including histone mRNA degradation. Finally, the last chapter (Chapter 6) summarizes the observations I have made regarding histone mRNA degradation and provides insight into a exciting field of RNA biology that involves a family of eukaryotic enzymes known as terminal uridyltransferases (TUTases) or poly(U) polymerases (PUPases).

Figure 1. The 3' end of replication-dependent histone mRNAs end in an evolutionarily conserved stemloop. The mammalian stemloop sequence and the histone downstream element (HDE), which is recognized by the U7 snRNA, are depicted. A single processing reaction is required to form the mature histone mRNA 3' end. Replication dependent histone mRNAs have short UTRs and do not contain any introns.

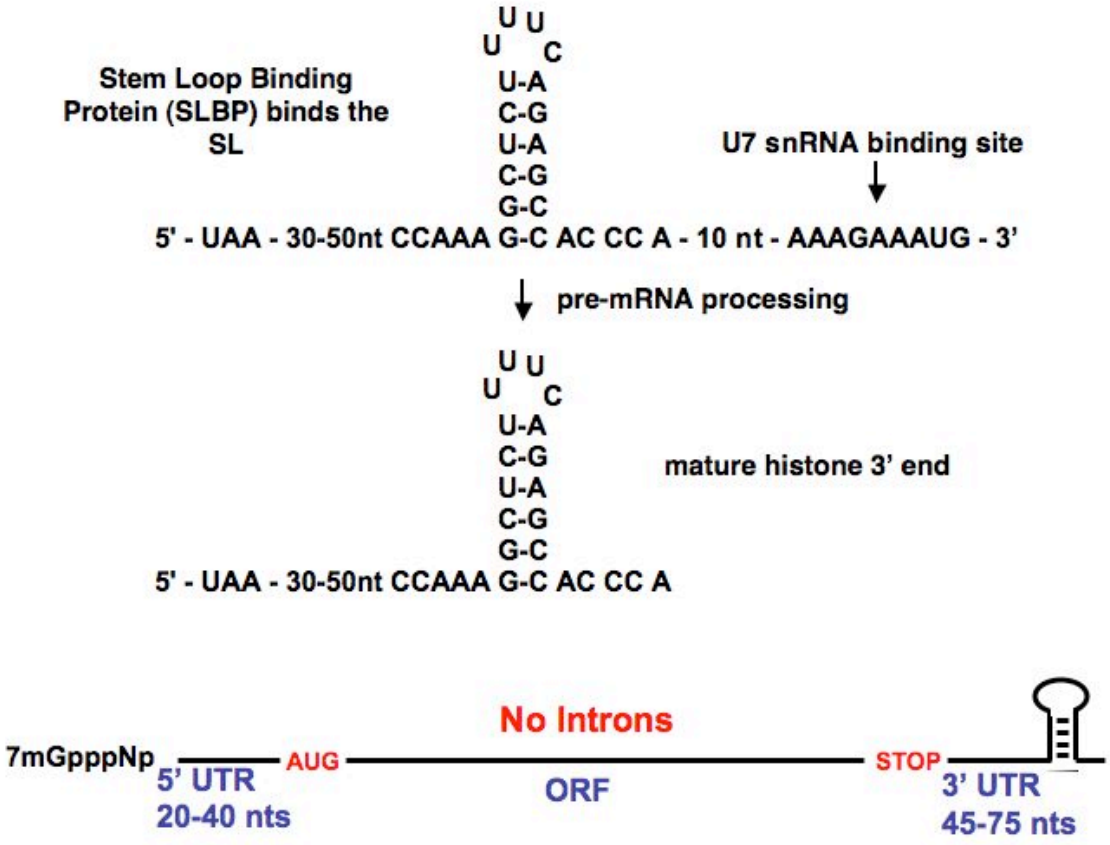
Stem Loop Binding Protein (SLBP) binds the SL
U U
U C
U-A
C-G
U-A
C-G
G-C
U7 snRNA binding site
5' - UAA - 30-50nt CCAAA G-C AC CC A - 10 nt - AAAGAAAUG - 3'
pre-mRNA processing
mature histone 3' end
5' - UAA - 30-50nt CCAAA G-C AC CC A

No Introns
7mGpppNp
AUG
STOP
5' UTR
20-40 nts
ORF
3' UTR
45-75 nts

Figure 2. Cell cycle regulation of histone mRNA, SLBP mRNA and SLBP protein. The different events responsible for the cell cycle regulation of histone mRNA are depicted.

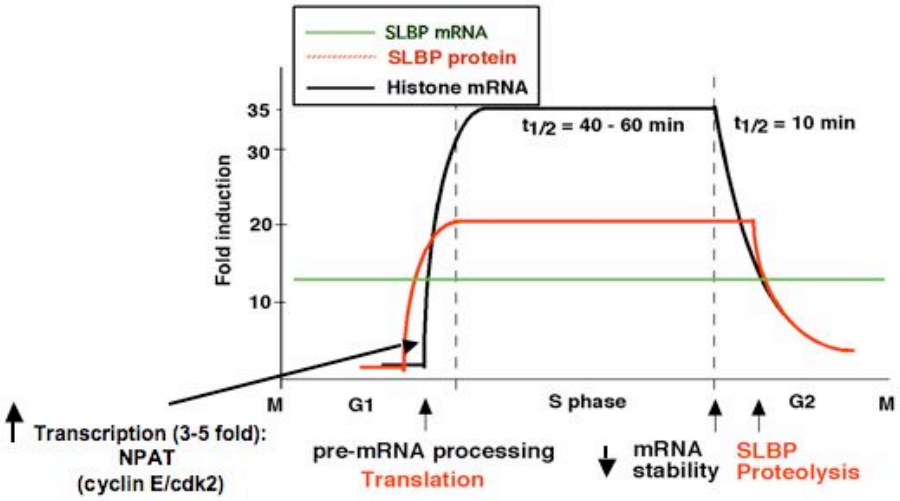
SLBP mRNA
SLBP protein
Histone mRNA
Fold induction
35
30
20
10
t1/2 = 40 - 60 min
t1/2 = 10 min
M
G1
S phase
G2
M
Transcription (3-5 fold):
NPAT
(cyclin E/cdk2)
pre-mRNA processing
Translation
mRNA
stability
SLBP
Proteolysis

Figure 3. Model of histone mRNA metabolism. (CB) Cajal body. Figure from: (Marzluff and Duronio, 2002).

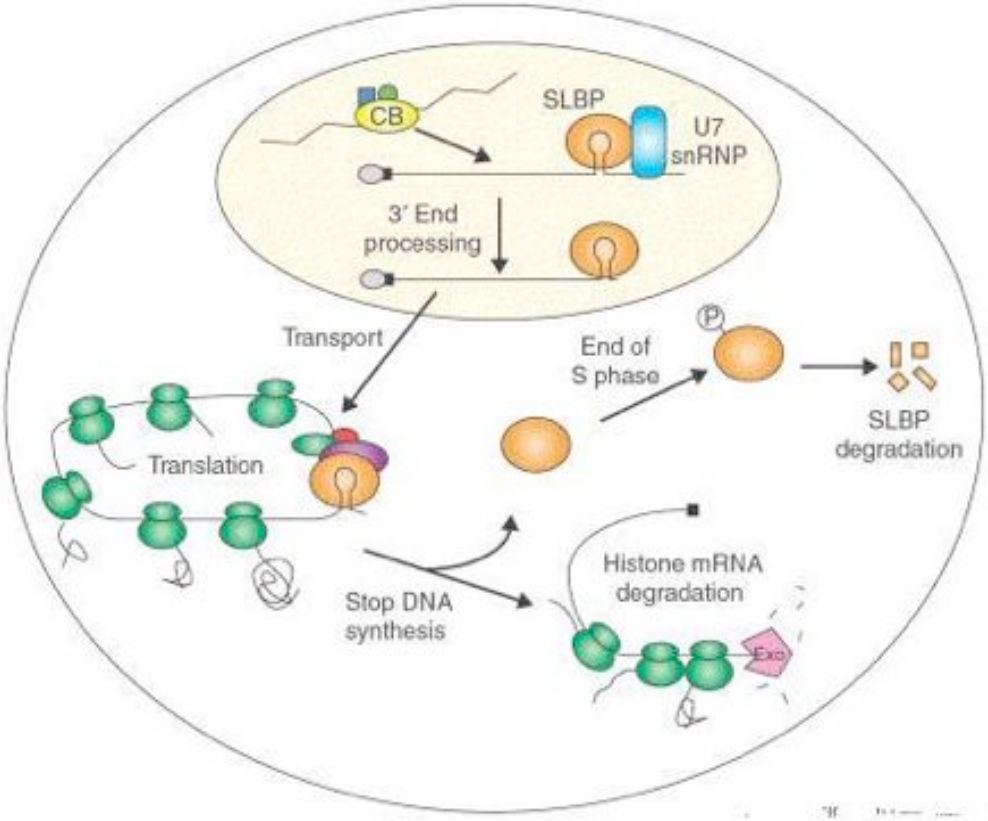
CB
SLBP
U7
snRNP
3′ End
processing
Transport
End of
S phase
P
SLBP
degradation
Translation
Histone mRNA
degradation
Stop DNA
synthesis
Exo

Figure 4. Model of histone mRNA degradation (2004). Depicted is the model of histone mRNA degradation at the time I began my dissertation work.

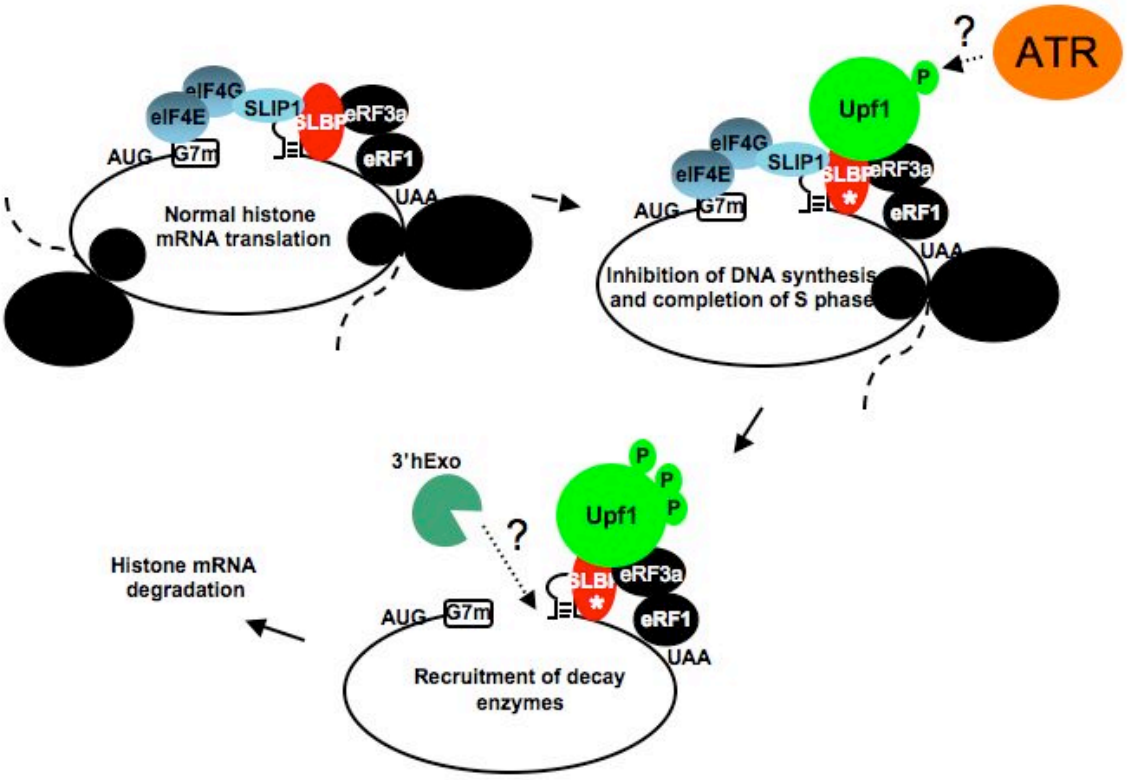
eIF4G
eIF4E
SLIP1
SLBP
eRF3a
eRF1
AUG
G7m
UAA
Normal histone
mRNA translation
?
ATR
P
Upf1
Inhibition of DNA synthesis
and completion of S phase
3'hExo
Histone mRNA
degradation
Recruitment of decay
enzymes

Table 1. mRNA decay factors. Listed are the major proteins involved in general mechanisms of mRNA degradation including deadenylation, 5'-3' degradation, and 3'-5' degradation.

Decay Complex	Protein	Known Protein Domain, Function
DEADENYLATION		
CCR4-NOT	Ccr4	3'-5' exonuclease, main deadenylase complex
	Pop2/Caf1	3'-5' exonuclease, main deadenylase complex
	Not1	Unknown
PAN2-PAN3	PAN2	WD40 repeat, involved in an initiating deadenylase activity
	PAN3	3'-5' exonuclease, involved in an initiating deadenylase activity
PARN	PARN	3'-5'exonuclease, 5' cap-dependent activity
5'-3' DECAY		
Decapping	Dcp1	EVH1
	Dcp2	MutT, catalytic component that produces hypermethylated GDP
	Hedls (Ge-1)	WD40 repeat
Dhh1	Dhh1 (RCK/p54, Me31B)	DExD/H box RNA helicase, involved in decapping
Pat1	Pat1	Unknown, translational repression
Edc complex	Edc1	Unknown, decapping enhancer
	Edc2	Unknown, decapping enhancer
	Edc3	Sm-like, decapping enhancer
Lsm 1-7	Lsm1-7	Sm-like, required for decapping
Xrn1	Xrn1	5'-3' exonuclease
3'-5' DECAY		
Exosome (cytoplasmic)	Rrp41, Rrp42, PM/Scl-75, Rrp46, Mtr3, OIP2	RNase PH, 3'-5' exonuclease, form the core ring structure of exosome,
	Csl4, Rrp4, Rrp40	S1 and KH, substrate RNA binding
	Rrp6 (PM/Scl-100)	RNase D, 3'-5' exonuclease
	Ski2	DEVH RNA helicase
	Ski3	TTP repeat
	Ski7	EF1α-like GTPase
	Ski8	WD40 repeat

Figure 5. Eukaryotic 5'-3' mRNA degradation pathway. A schematic representation of the major regulatory steps in eukaryotic 5'-3' degradation of mRNA.

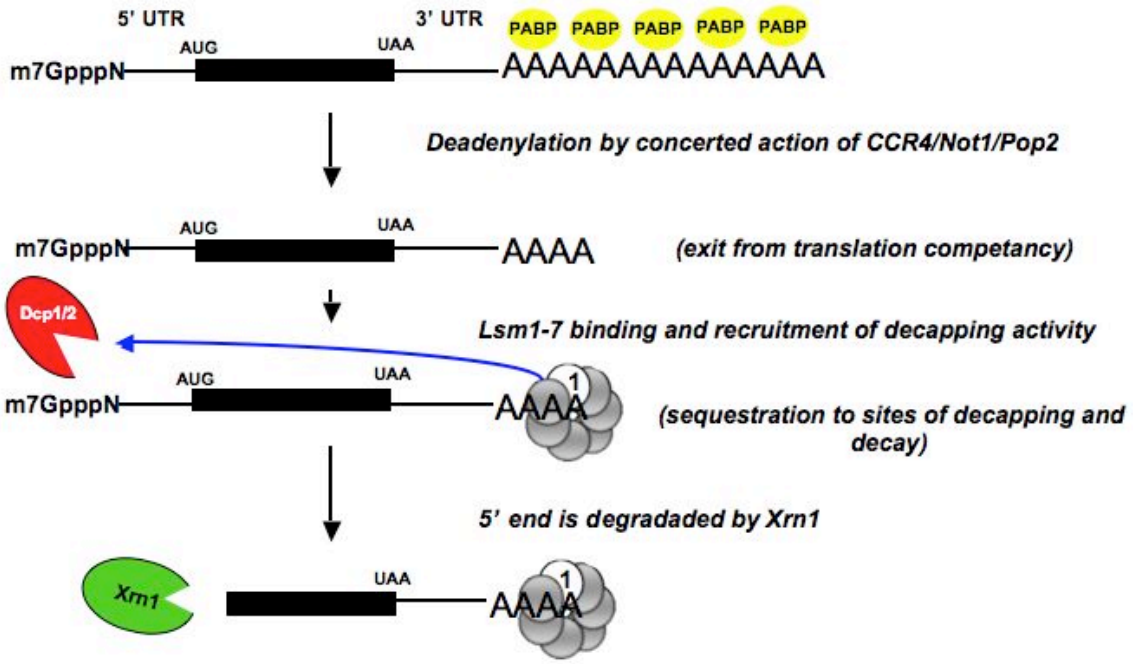
5' UTR
3' UTR
PABP
PABP
PABP
PABP
PABP
AUG
UAA
m7GpppN
AAAAAAAAAAAAAAA
Deadenylation by concerted action of CCR4/Not1/Pop2
AUG
UAA
m7GpppN
AAAA
(exit from translation competancy)
Dcp1/2
Lsm1-7 binding and recruitment of decapping activity
AUG
UAA
m7GpppN
1
AAAA
(sequestration to sites of decapping and decay)
5' end is degradaded by Xrn1
Xrn1
UAA
1
AAAA

Figure 6. Eukaryotic 3'-5' mRNA degradation pathway by the exosome. A schematic representation of the major regulatory steps in mRNA degradation by the cytoplasmic exosome is shown.

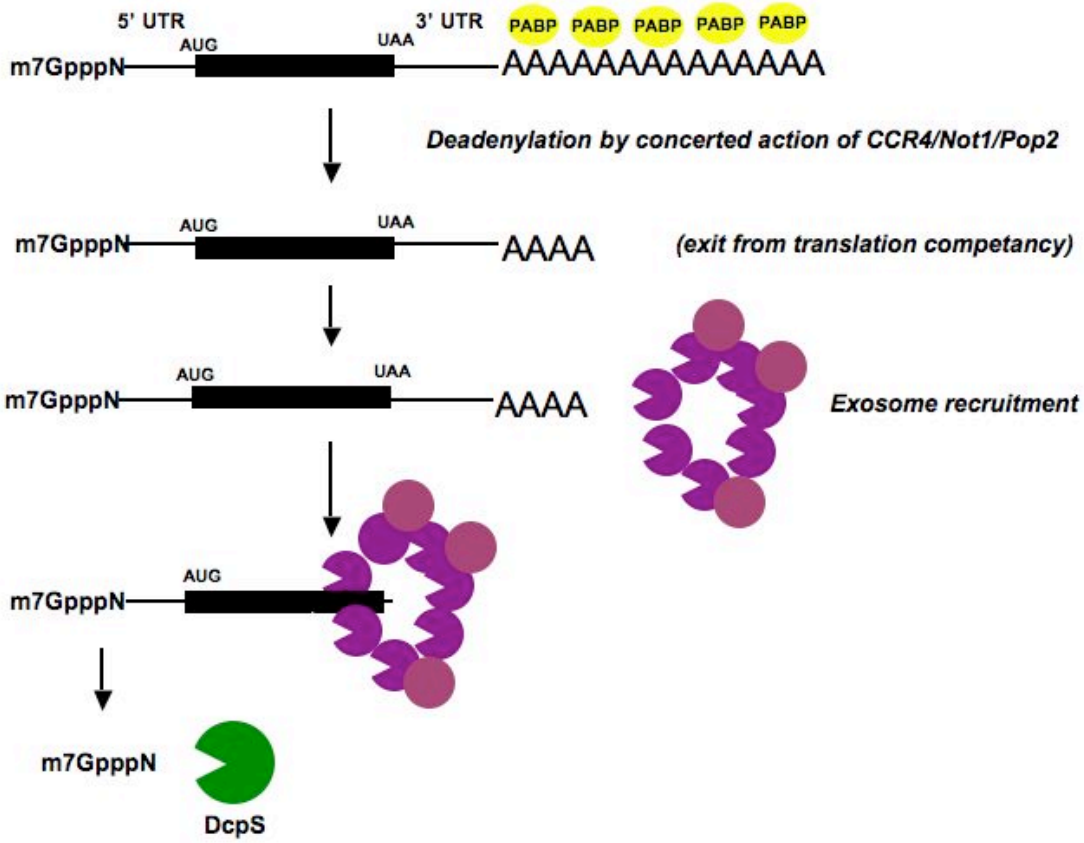
5' UTR
AUG
UAA
3' UTR
PABP
PABP
PABP
PABP
PABP
m7GpppN
AAAAAAAAAAAAAAA
Deadenylation by concerted action of CCR4/Not1/Pop2
m7GpppN
AUG
UAA
AAAA
(exit from translation competancy)
m7GpppN
AUG
UAA
AAAA
Exosome recruitment
m7GpppN
AUG
m7GpppN
DcpS

Figure 7. Deadenylation-independent decapping and 5'-3' mRNA degradation.

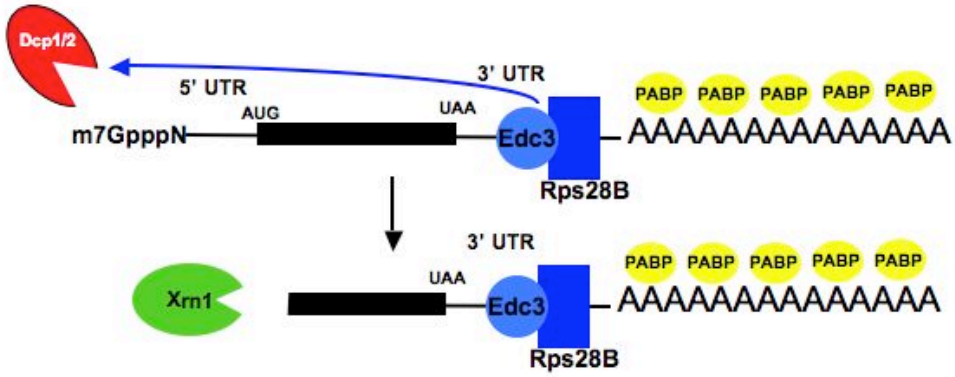
Dcp1/2
3' UTR
5' UTR
AUG
UAA
m7GpppN
Edc3
Rps28B
PABP PABP PABP PABP PABP
AAAAAAAAAAAAAA
3' UTR
Xrn1
UAA
Edc3
Rps28B
PABP PABP PABP PABP PABP
AAAAAAAAAAAAAA

Figure 8. General mechanisms of endonucleolytic mRNA degradation. (A) Endonucleolytic mRNA degradation by PMR1, IRE1, and RNase MRP. Following endonucleolytic cleavage, the 5' and 3' fragments are degraded by the exosome and Xrn1, respectively. (B) miRNA-mediated endonucleolytic degradation by Ago1.

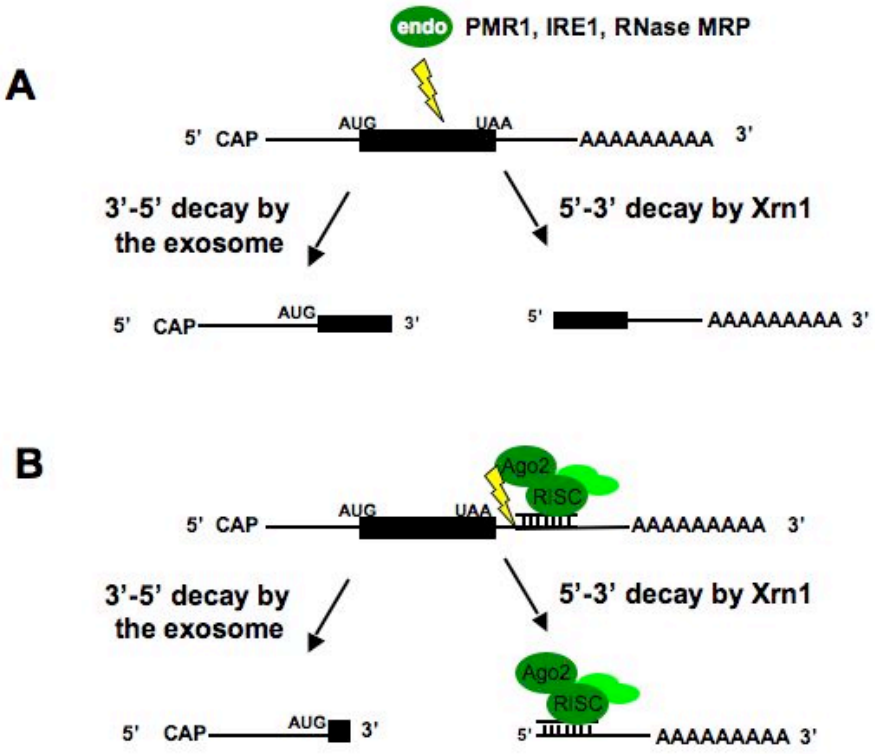
A
endo
PMR1, IRE1, RNase MRP
5' CAP
AUG
UAA
AAAAAAAAA 3'
3'-5' decay by the exosome
5'-3' decay by Xrn1
5' CAP
AUG
3'
5'
AAAAAAAAA 3'
B
Ago2
RISC
5' CAP
AUG
UAA
AAAAAAAAA 3'
3'-5' decay by the exosome
5'-3' decay by Xrn1
Ago2
RISC
5' CAP
AUG
3'
5'
AAAAAAAAA 3'

CHAPTER 2

HISTONE mRNA IS SIMULTANEOUSLY DEGRADED FROM BOTH THE 5' AND 3' ENDS

INTRODUCTION

Replication dependent histone mRNA levels are tightly coupled to DNA replication. Proper control of histone protein synthesis is essential to ensure proper chromatin formation. A major step in regulation of mammalian histone mRNA is a rapid alteration in the half-life of histone mRNA in response to changes in the rate of DNA synthesis, allowing the cell to rapidly adjust the rate of histone protein synthesis to maintain balanced synthesis of DNA and histone protein. The regulation of the half-life of histone mRNA is mediated by the unique 3' end of histone mRNA (Kaygun and Marzluff, 2005b; Pandey and Marzluff, 1987). The metazoan replication-dependent histone mRNAs are the only eukaryotic mRNAs that are not polyadenylated (Marzluff, 2005). The Stem Loop Binding Protein (SLBP) binds the conserved stemloop (SL) present at the 3' end of all 5 classes of histone mRNAs (Martin et al., 1997; Wang et al., 1996c). SLBP is required for histone pre-mRNA processing (Marzluff, 2005) and accompanies the histone mRNA to the cytoplasm (Erkmann et al., 2005a) where it is required for histone mRNA translation (Sanchez and Marzluff, 2002). SLBP plays a direct role in histone mRNA stability through an interaction with Upf1 (Kaygun and Marzluff, 2005a).

Inhibition of DNA replication using pharmacologic agents results in a rapid degradation of histone mRNA. Degradation requires active translation of the mRNA and the SL at the 3' end. The location of the SL relative to the stop codon, 45-80 nts, is also essential as increasing this distance results in a loss of regulated degradation and persistent expression (Graves et al., 1987; Kaygun and Marzluff, 2005b). These characteristics suggest that a terminating ribosome must be in close approximation to the SL and likely SLBP. Supporting this model, Handan Kaygun recently found that Upf1, a factor involved in translation termination and nonsense mediated decay (NMD) is required for histone mRNA degradation (Kaygun and Marzluff, 2005a).

The initial step in degradation of most polyadenylated mRNAs in eukaryotes is shortening of the poly(A) tail by a deadenylase complex (Parker and Song, 2004). Deadenylated mRNAs can subsequently return to a translationally active state on polysomes likely by the enzymatic action of cytoplasmic poly(A) polymerases (Coller and Parker, 2005) or can be degraded from either terminus using a distinct set of nucleases (see Chapter 1). Upon poly(A) shortening, the Lsm1-7 complex is thought to recruit a decapping complex (Dcp1/Dcp2) to remove the 5' cap of the mRNA (Coller et al., 2001). The decapped mRNA can then be degraded 5'-3' by the Xrn1 exoribonuclease or can be exposed to a large complex of 3'-5' exonucleases known as the exosome (Mitchell et al., 1997). A number of the proteins involved in catalyzing 5'-3' degradation are localized to discrete cytoplasmic loci termed P bodies or GW bodies (Eystathioy et al., 2003; Sheth and Parker, 2003). Whether 5'-3' degradation is restricted to P bodies is not known. Exosome components are located in both the nucleus and cytoplasm (Lejeune et al., 2003). Whether both the

5’-3’ and 3’-5’ pathways can contribute to the degradation of a single mRNA molecule is not clear.

The detailed biochemical pathway of regulated histone mRNA degradation is not understood. In this chapter I identify the enzymes and 3’ UTR binding proteins that regulate histone mRNA degradation using a combination of functional RNAi and biochemical approaches. The RNA interference experiments suggest a role for both the exosome and the decapping enzymes in degradation. In agreement with this result, I find decapped intermediates of histone mRNA degradation that have been decapped and the fragments of histone RNAs have been degraded from both the 5’ and 3’ end. Additionally, I find 14% of the decapped intermediates examined are nearly full-length and contain 8-15 nonencoded uridines on the 3’ end. Moreover, biochemical studies show the Lsm1-7 complex associates with SLBP but that this association is likely mediated by histone mRNA itself. Together, these data provide the first direct evidence for human bidirectional mRNA degradation as a regulatory mechanism responsible for altering the half-life of a physiologically important mRNA. These data also provide preliminary evidence for the addition of nonencoded uridine residues to the 3’ end of histone mRNA as the initiating event that targets histone mRNA specifically for rapid, bidirection degradation.

MATERIALS AND METHODS

RNA interference

HeLa cells were transfected with Lipofectamine 2000 (Invitrogen) using a two-hit RNAi method (Wagner and Garcia-Blanco, 2002). 48 hours following the second RNAi transfection, cells were treated with 5 mM HU for 0, 20 or 45 minutes. Histone mRNA level was measured by Northern blotting or S1 nuclease assays. siRNAs were synthesized by Dharmacon and the targeted sequences for the genes are listed in Table 2.

Western Blot Analysis

Total cell lysates were prepared as described (Kaygun and Marzluff, 2005a). Detection of endogenous proteins was made possible by generous gifts of antibodies to Lsm1/CaSm, Dcp2, Xrn1, Upf1, PM/Scl-100, Rrp41 and PTB. The generous gifts of antibodies used in this study were kindly provided by: Dennis Watson (Medical University of South Carolina) for chicken anti-Lsm1/CaSm; Mike Kiledjian (Rutgers University) for rabbit anti-Dcp2; Jens Lykke-Andersen (University of Colorado, Boulder) for rabbit anti-Xrn1; Chris Smith (Cambridge University) for rabbit anti-Upf1 antibody; Ger Pruijn (University of Nijmegen) for rabbit anti-PM/Scl-100 and Rrp41 antibodies; and Mariano Garcia-Blanco (Duke University) for rabbit anti-PTB antibody.

Northern Blot and S1 Nuclease Protection Assays

Total RNA was isolated using Trizol reagent (Invitrogen). For Northern blot assays, 2 μg of total RNA was separated on 6% acrylamide 7 M urea gels and transferred to Hybond N+ nitrocellulose membranes (Amersham). S1 nuclease protection assays to simultaneously measure the variant H3.3 and replication-dependent H2a mRNA were performed as described (Kaygun and Marzluff, 2005a). Gels were dried and exposed to phosphorimager cassettes, quantified using ImageQuant, and normalized to the amount of 7SK RNA.

Synchronization of HeLa cells

Determination of the 5' and 3' ends of histone mRNA is best done in a pure population of S-phase cells. Since histone mRNAs are present at high levels only in S-phase cells, some histone mRNAs will be rapidly degraded in a subset of cells in a population of exponentially growing cells. Thus to guarantee that I had a population of cells which have stable histone mRNA, cells were synchronized. HeLa cells synchronized by double thymidine block (DTB). This method ensures that 100% of the cells are synchronously progressing through S phase and therefore the entire population of cells will be expressing histone mRNA.

In a 10 cm^2 tissue culture dish, 2.5 – 3.5 x 10^5 HeLa cells were plated in a total of 9.8 ml 10% FBS containing Dulbecco's Modified Eagle's media (DMEM, Gibco). The following day (typically at 2 p.m.) I added 200 μl of 100 mM thymidine (Sigma) for a final concentration of 2 mM thymidine. Plates were washed twice with warm PBS 18 hours following addition of thymidine (8 a.m.) and 9.8 ml warm, fresh

media added. The cells blocked in S phase now resumed DNA replication. Cells arrested at the G1/S border are allowed to complete DNA replication, and the cells arrested at other points in S-phase complete S-phase but do not progress to the next S-phase. Once the cells have all completed S-phase (9 hrs after release), but none have re-entered S-phase, I added 200 μl of 100 mM thymidine (at 5 p.m.) after release from the first thymidine block. Fifteen (15) hours following the second thymidine block all the cells were at the G1/S border. I washed cells with warm PBS twice, making sure to remove as much of the thymidine-containing PBS as possible and added fresh, warm media. All of the cells are entering S phase at this point and I typically harvested cells in the middle of S phase (e.g. 3 hours following release). The length of S-phase varies slightly from experiment to experiment, but the entire population typically completes S-phase synchronously in each experiment (with the length of S-phase being 5-7 hours).

To promote rapid degradation of histone mRNA, I added warm, fresh media containing 5 mM hydroxyurea (HU, Sigma) to parallel synchronized cultures 3 hrs after release. For cRT-PCR (see below) I harvested cells 20 minutes following addition of HU-containing media. Since histone mRNA degradation is initiated about 5 minutes after addition of HU (Graves and Marzluff, 1984), cells harvested 15-20 min after HU treatment had initiated degradation of histone mRNA, and contained the largest amount of any degradation intermediates.

Circularization RT-PCR

A schematic diagram depicting the circularization RT-PCR (cRT-PCR) approach for determining the 5' and 3' end of an mRNA is diagrammed in Figure 15.

This requires only that the 5' end have a 5' monophosphate and the 3' end has a free 3' hydroxyl group. If the mRNA is capped it can be decapped prior to circularization. Detailed methods for the various steps are described below and are identical to or adapted from those previously described (Couttet et al., 1997; Fromont-Racine et al., 1993).

RNA preparation for cRT-PCR

Total RNA was harvested according to the Chomczynski and Sacchi method (Chomczynski and Sacchi, 1987, 2006). I resuspended precipitated RNA pellets in sterile water.

DNase treat total cell RNA.

Residual DNA does come through in the above RNA preparation and DNase treatment will eliminate any traces of genomic DNA. I used RQ1 DNase (Promega) to treat 20-50 μg of total RNA by adding 20 U of HPRI (New England BioLabs), 25 U of RNase-free DNase (1 U/μl for Promega RQ1 DNase), and 10 μl of 10X RQ1 buffer (40 mM Tris-HCl pH 7.9, 10 mM NaCl, 6 mM MgCl2, and 10 mM CaCl2) for a total volume of 100 ml. Reactions were incubated at 37° C for 30 minutes. The reaction was stopped by adding 10 μl STOP buffer supplied by Promega and and incubated at 65° C for another 10 minutes. After letting the reaction cool, I added 100 μl of phenol:chloroform:isoamyl alcohol (25:24:1 v/v, Invitrogen). Samples were briefly vortexed and spun in a microcentrifuge at room temperature for 5 minutes at 14,000 rpm. The top layer was removed and a chloroform extraction performed with an equal volume and spun as above. I ethanol precipitated the RNA by adding 1/10th of the volume of 3 M sodium acetate to the RNA followed by 2-2.5 volumes of

cold 100% ethanol. Precipitations were vortexed and put at -20° C overnight or -80° C for an hour. The tubes were then spun down at 4° C in a microcentrifuge for 30 minutes at 14,000 rpm. Visible pellets were washed with cold 80% ethanol by washing at full speed for 5 minutes at 4° C. RNA pellets were air-dried and resuspended in 15 μl of water.

Decapping

To remove the cap from the mRNAs, I used 10-15 μg DNase-treated total cell RNA in a 20 μl total volume and treated with tobacco acid pyrophosphatase (TAP, Epicentre). To obtain RNAs that have been already been decapped previously in the cell, I set up parallel reactions that do not contain TAP but are subjected to the same conditions. To decap RNA, I added the DNase-treated total cell RNA to 2.5 U of TAP (dilute Epicentre stock 1:4), 20 U of HPRI (Human placental ribonuclease inhibitor, NEB), and 2 μl of 10X TAP buffer (0.5 M sodium acetate pH 6.0, 10 mM EDTA, 1% β-mercaptoethanol, and 0.1% Triton X-100). Decapping reactions were carried out at 37° C for 1 hour. Following the 1 hour incubation I brought the total volume up to 100 μl and added 10 μl of 3 M sodium acetate and 250 μl of cold 100% ethanol. RNA was precipitated, washed, and air-dried as above. Decapped RNA was resuspended in10 μl of sterile water.

RNA circularization using T4 RNA ligase

RNA ligation was carried out at 16° C. In order prevent the possibility of intermolecular ligations the volume I used for the ligations needed to be quite large. At high concentrations of RNA I could potentially obtain intermolecular ligations, but

to prevent this, I carried out the ligation in a total volume of 400 μl where 4-6 μg of RNA from the decapping step was added to 20 U T4 RNA ligase (New England BioLabs), 20 U of HPRI (New England BioLabs), and 40 μl of 10X T4 RNA ligase buffer to make it 1X (50 mM Tris-HCl, 10 mM $MgCl_2$, 1 mM ATP, and 10 mM DTT). I performed the ligation for 16 hours and ligated RNA was subjected to a phenol:chloroform:isoamyl alcohol (25:24:1) purification followed by a chloroform wash as above, but using volumes appropriate for the ligation reaction (e.g. 400 μl). I precipitated the final top phase from the chloroform wash by adding $1/10^{th}$ the final volume of 3 M sodium acetate and 2.5 volumes of cold, 100% ethanol. The ligated RNA was precipitated at -20° C for at least 2 hours or overnight. Precipitated RNA was washed twice with cold 80% ethanol, air-dried, and the RNA pellet resuspended in 12 μl.

RT-PCR of circularized RNA.

For these experiments I used reverse transcriptase (RT) from MMLV (Invitrogen). Histone mRNAs are quite short (approximately 500 bp) and I designed the primers to obtain ligated fragments around 200 bp. I used 6 μl of the ligation (2 μg) and subjected it to reverse transcription using MMLV-RT (Invitrogen) and a human histone H3 oligo termed 'H3 Oligo 1' (5'-CTTCTGGTAGCGCCGGATCTC-3') targeting the open reading frame (ORF) of the *HIST2H3A*, *HIST2H3C, and HIST2H3D* genes (Marzluff *et al.*, 2002). This oligo primes synthesis toward the 5' end of the histone mRNA and will proceed through the 3' end if the mRNA has been circularized. I performed a 20 μl RT reaction according to the manufacturer's instructions and used 2 μl for the subsequent PCR.

To PCR the ligated 5' and 3' ends of histone H3 genes, I used 2 μl of the RT reaction above and performed a 100 μl PCR reaction using 2 μl of 10 mM dNTPs (Amersham), 1 μl each of 10 mM 'H3 Oligo 2' (5'-GACTTGCGAGCAGTCTGCTTAG-3') and 'H3 Oligo 3' (5'-GCTGTTCGAAGACACGAACCTG-3), 10 μl of 10X Taq buffer (100 mM Tris-HCl pH 8.3, 500 mM KCl, and 20 mM $MgCl_2$), 83 μl of water, and 1 μl recombinant Taq. These oligos target the ORF and amplify towards either the 5' or 3' UTRs, and hence will only amplify ligated products. A total of 28-30 cycles is sufficient to observe amplicons in the TAP treated samples under the conditions of: 95°C for 30 seconds, 52° C for 30 seconds, and 72° C for 30 seconds. 20 μl of each reaction was analyzed on a 1.5-2.0% agarose gel.

Sample preparation for cloning the 3' end of *in vitro* processed histone pre-mRNA.

This experiment was carried out to demonstrate I could accurately detect properly processed histone mRNA by this approach. Determination of the 3' end of a histone pre-mRNA substrate requires an *in vitro* processing extract which efficiently processes histone pre-mRNA (Dominski et al., 1999). To ensure the efficacy of the processing extract, two parallel reactions were performed. Both reactions had the same concentration of substrate but in reactions the pre-mRNA was radiolabelled to allow monitoring of the processing efficiency and the other which is not. The reactions that contained the labeled pre-mRNA substrate was monitored by denaturing urea acrylamide gel electrophoresis and autoradiography by Zbig Dominski as described (Dominski et al., 1999). RNA was isolated from the

reaction that did not contain the radiolabelled substrate at both 0 time and after 2 hrs when more than 90% of the mRNA has been processed.

Cloning of cRT-PCR and degradation intermediates

I used 2 μl of fresh PCR product from each reaction and ligateed it into the pCR4®–TOPO® vector (Invitrogen) according to the manufacturer's instructions for ligation and transformation. For the ligation reaction, I ligated the reactions for an extended amount of time (30 minutes) in an attempt to recover as many of the variety of different PCR molecules that exist in the reaction as possible. Transformants were plated on to Kanamycin-containing LB plates overnight. Colonies were screened using overnight cultures and double restriction enzyme digests of mini-prepped plasmid DNA to screen for inserts (SpeI and NotI, New England BioLabs).

Cell cycle analysis

Cells were fixed in 70% ethanol, stained with propidium iodide, and DNA content analyzed by FACS using either a FACScan (Becton-Dickinson) or CyAn Scan (Dako). Populations of G1 (2N DNA content), S phase (2N < S < 4N DNA content), and G2/M (4N DNA content) were quantified using Summit software and are represented as a percentage of the total population.

RESULTS

Knockdown of 3'hExo does not affect histone mRNA degradation in vivo

Polyadenylated mRNAs are primarily degraded by a pathway that initiates deadenylation, removing most of the poly(A) tail, followed either by decapping and 5'

to 3’ degradation or degradation 3’ to 5’ by the exosome (Parker and Song, 2004). Although it is known that the stemloop at the 3’ end of histone mRNA is the *cis*-element that regulates histone mRNA degradation (Pandey and Marzluff, 1987), the biochemical details of histone mRNA degradation are not known. Early studies by Ross and coworkers suggested that degradation of histone mRNA proceeded 3’ to 5’ (Ross and Kobs, 1986; Ross et al., 1986). Since Zbig Dominski and coworkers recently identified an exonuclease, 3’hExo, that can specifically degrade histone mRNA from the 3’ end *in vitro* (Dominski et al., 2003), and which can form a ternary complex with the stemloop of histone mRNA and SLBP, I tested whether the 3’ hExo might play a role in initiating histone mRNA degradation. Since the critical *cis* element for histone mRNA degradation is also at the 3’ end of the mRNA, I tested known factors in decay of polyadenylated mRNAs to see if they might also be involved in histone mRNA degradation.

For all RNA interference experiments, I knocked down the targeted proteins using two sequential treatments with siRNA (Wagner and Garcia-Blanco, 2002), and used two different siRNAs for each protein. Cells were treated with a control siRNA (C2) which did not knock down any of the proteins. We also used siRNAs that targeted the splicing factor polypyrimidine tract binding (PTB) protein, as a control. The cells were treated with 5 mM HU and the amount of histone mRNA degradation was measured over a 45 minute timecourse.

The transfected siRNA reduced 3’hExo protein levels by 80-90% as estimated by Western Blot analysis of a dilution series of control treated lysates (Figure 9A). Total RNA from these cells was subjected to Northern blot analysis simultaneously

probing for both histone H2A mRNA and 7SK RNA as a loading control. Knockdown of 3'hExo has no effect on histone H2A mRNA degradation in HeLa cells (Figure 9B and 9C). There was also no change in the cell cycle distribution as determined by FACS (Figure 9C). The steady state levels of histone mRNA in the exponentially growing cells (0 time point) was similar in both the C2 (control) and 3'hExo knockdowns (Fig. 9B, compare lanes 1 and 4). Thus, knockdown of 3' hExo had no discernable effect on histone mRNA metabolism or cell growth (Figure 9D). Knocking down PTB also had no effect on histone mRNA regulation or cell growth (Figure 3 and 2, respectively) and serves as a negative control for potential off-target effects for these studies. I could knock down PTB protein to 90% of the control as determined from a dilution series Western blot (Figure 10A).

Lsm1 plays an integral role in replication-dependent histone mRNA degradation

I tested a number of decay factors and enzymes involved in regulating poly(A) mRNA stability by RNA interference to see if any of these factors affected histone mRNA degradation. The Lsm1-7 complex is a heteroheptameric set of polypeptides that is a positive regulator of decapping in *S.cerevisiae* (Tharun et al., 2000; Tharun and Parker, 2001) and has also been shown to be important in regulating the stability of mRNAs containing AU-rich elements (ARE) (Mukherjee et al., 2002; Stoecklin et al., 2006). I carried out a series of RNAi experiments assessing the role of various factors using C2 siRNA as a negative control and Upf1 as a positive control for a factor that reduces histone mRNA degradation. Each experiment shown represents an example of a panel of experiments done on parallel cultures.

The downregulation of Lsm1 protein varied from 75-95% among different experiments as estimated from the protein dilution series of the control (C2) sample (Fig. 10D). Each siRNA had a similar degree of knockdown and Symplekin, a scaffold protein involved in mRNA 3' end formation (Kolev and Steitz, 2005; Takagaki and Manley, 2000), served as a loading control in this experiment. As mentioned previously, Handan Kaygun has shown that the NMD factor hUpf1 is important in regulating the rapid decay of histone mRNA (Kaygun and Marzluff, 2005a) and I used this as a positive control. Transfection of either of two siRNAs targeting Lsm1 resulted in stabilization of histone mRNA at the 20 minute time point (Figure 10E; compare lanes 2, 5 and 8) and over a 2.5 fold stabilization at the 45 minute time point (Figure 10E; compare lanes 3, 6, and 9, Figure 14) relative to C2 siRNA transfected cells. Figure 10F summarizes three independent RNAi experiments. The cell cycle distributions of the cells were not significantly changed by the Lsm1 knockdown (Figure 11).

Given the apparent role of Lsm1 in histone mRNA decay, I asked whether I could detect Lsm1 in SLBP immunoprecipitates when histone mRNAs were being rapidly degraded. Lysates were prepared 15 min after HU treatment from S-phase cells stably expressing HA-tagged SLBP (Erkmann et al., 2005b) and immunoprecipitated with anti-HA antibody. I then probed for Lsm1. Detectable amounts of Lsm1 were co-immunoprecipitated with HA-SLBP. When I treated the cell lysates with RNase A prior to immunoprecipitation the amount of Lsm1 coimmunoprecipitated was greatly reduced (Figure 10G, top, lanes 3 and 4). This result suggests that both SLBP and Lsm1 can be bound to histone mRNA but that

they do not stably interact with each other, in contrast to the interaction of SLBP and Upf1 which is resistant to RNase digestion (Kaygun and Marzluff, 2005a). In a separate experiment, I did not detect association of Lsm1 with SLBP in S-phase cells prior to HU treatment, although it was readily detected 15 min after HU treatment (Fig. 10G, bottom, lanes 5 and 6). Another RNA binding protein, PTB, was not present in any of the SLBP immunoprecipitates, demonstrating the specificity of the interaction. Thus Lsm1 only interacts with SLBP when histone mRNA is being rapidly degraded.

Downregulation of the decapping enzyme Dcp2 and the 5'-3' exonuclease Xrn1 reduce histone mRNA decay

Since the Lsm1-7 complex is a positive regulator of decapping and 5'-3 decay and had an effect on histone mRNA stability, I examined other components of the 5'-3' mRNA decay apparatus. I knocked down the catalytic subunit of the decapping complex Dcp2 (Wang et al., 2002) and the 5'-3' exonuclease Xrn1 (Long and McNally, 2003) using targeted siRNAs to these enzymes. Each protein was knocked down by an estimated 80-90% (Fig. 12A and 12E). As an alternative method to Northern blots, I used an S1 nuclease protection assay to monitor histone H2A mRNA levels (Kaygun and Marzluff, 2005a, b). HU treatment does not affect polyadenylated H3.3 mRNA levels and thus serves as a loading control. The degradation of histone mRNA was reduced by knocking down Dcp2 and Xrn1, and after 45 min of HU treatment there was twice as much histone mRNA remaining compared to control treated cells (Figure 12B,12C, 12F and 12G and Figure 14).

The downregulation of both Dcp2 and Xrn1 had minimal effects on the cell cycle distribution of the cells (Figure 12D and 12H). There was a small increase in the percentage of S phase cells of the Dcp2 knockdown compared to the control (Figure 12D). This likely accounts for the small increase in steady state histone H2a mRNA levels (Figure 12B, compare lane 1 and 3) in the Dcp2 knockdown cells. These data leads me to conclude that components of the 5' to 3' degradation pathway play a role in histone mRNA degradation.

Knocking down exosome components PM/Scl-100 and Rrp41 inhibits histone mRNA degradation

Polyadenylated mRNAs may also be degraded by the exosome following deadenylation, in addition to degradation 5' to 3' through the decapping pathway. It is possible the Lsm1-7 complex could also recruit the exosome. To determine whether the exosome may also play a role in histone mRNA degradation I knocked down two components of the exosome by RNA interference. I chose PM/Scl-100 and Rrp41, a core exosome component (Liu et al., 2006). PM/Scl-100 has been shown to be present in the cytoplasm of human cells (Lejeune et al., 2003), in contrast to initial reports (Allmang et al., 1999). PM/Scl-100 has substantial homology with *E.coli* RNase D, a 3'-5' exonuclease and Rrp41 has been shown to have 3'-5' exonuclease activity *in vitro* (Mitchell et al., 1997).

The RNAi treatment reduced PM/Scl-100 levels by about 80% (Figure 13A), and two different siRNAs against Rrp41 reduced its levels by at least 80% (Figure 3E). Knocking down either PM/Scl100 (Figure 13B) or Rrp41 (Figure 13F) had a significant effect on histone mRNA degradation, similar to that seen with knocking

down Lsm1. The average of 3 independent experiments is shown in Figures 13C and 13G. There was a 3-fold stabilization of histone mRNA 45 min after HU treatment when PM/Scl-100 is knocked down and a 2.3-fold stabilization when Rrp41 is knocked down (Figure 14). Knocking down the exosome components had no effect on cell growth or cell-cycle distribution (Figure 13D and 13H).

Determination of the 5' and 3' ends of individual histone mRNA molecules *in vivo*

To directly identify molecules which had been partially degraded, I utilized a circularization RT-PCR (cRT-PCR) strategy in which the 5' (containing a 5' phosphate) and 3' ends (with a 3' OH) are ligated to each other forming a circular RNA. One can then amplify the region containing the ligated 5' and 3' ends by RT-PCR. This method allows one to determine the 5' end and the 3' end of individual molecules. The ends of molecules that have 5' caps can be detected by first treating the RNA with tobacco acid pyrophosphatase (TAP). This method has been used to directly analyze deadenylated mRNAs in cells (Couttet et al., 1997; Fromont-Racine et al., 1993). A schematic of this RT-PCR strategy, adapted from Couttet and colleagues (Couttet et al., 1997) is depicted in Figure 15A. I designed primers to target histone H3 mRNA from two identical genes (*HIST2H3A* and *HIST2H3C*) of the 12 annotated histone H3 genes in the human genome (Marzluff et al., 2002).

As a control to demonstrate that I could isolate PCR products that result from ligating the authentic 3' ends of the mRNAs, and to eliminate the possibility of nuclease contamination in my cRT-PCR reagents, I analyzed the 3' end of histone H2A mRNA formed in an *in vitro* processing reaction. Since the *in vitro* transcribed

substrate histone pre-mRNA contains a 5' triphosphate, it is also necessary to treat these RNAs with TAP prior to ligation. At time 0 I cloned only products corresponding to the synthetic pre-mRNA substrate. After processing for 120 minutes, when most of the substrate has been cleaved, I recovered only histone RNA that ended with the conserved ACCCA nts following the base of the stemloop, precisely where the lab and others (Dominski et al., 2005b; Scharl and Steitz, 1994) have mapped the cleavage site *in vitro* (Figure 15C). These results demonstrate that I was able to recover RNA molecules that had their 3' and 5' ends intact and hence nuclease activity in my reagents was minimal.

Figure 15B shows the results from a cRT-PCR experiment using RNAs from control cells and cells treated with HU for 20 minutes, at which time about 40% of the histone mRNA has been degraded. Two amplicons were detected (about 190 and 235 nts) when TAP was used to decap the mRNA (Figure 15B, lanes 3 and 4) and these were more abundant in RNA from untreated cells compared to HU treated cells. No distinct, amplified products were detected by ethidium bromide staining when the RNA was not treated with TAP (Fig. 15B, lanes 1 and 2).

I cloned these two PCR products and sequenced multiple clones from each fragment. The 235 nt fragment was derived from the *HIST2H3A*, *HIST2H3C* genes I initially set out to amplify (Marzluff et al., 2002), while the 187 nt band was a previously unannotated histone H3 gene also found in the minor histone cluster on chromosome 1q21 (nts 276048-275157), which I have named *HIST2H3D* (Figure 16). Each of these genes is highly expressed in HeLa cells. Figure 15D and 15E show sequences for the 5' and 3' regions of these two genes. The top line

(*HIST2H3A/C* or *HIST2H3D*) gives the genomic sequence of these genes, extending from the region upstream of the TATA box into the ORF, and from the stop codon past the HDE. The 5' UTR of the *HIST2H3A/C* mRNAs is 47 nt, with the G at the start site located 27 nts from the TATAA box, the expected distance for a RNA polymerase II transcription initiation site. This G was ligated to an ACC sequence that follows the stemloop in 10 of the 11 circularized clones isolated. The cytoplasmic histone mRNA is thus 2 nts shorter than the mRNA formed by the *in vitro* processing reaction (Figure 15D, 15E, and 15F). In one clone the last 2 nts of the stem were missing and these were followed by several non-templated U's (Figure 15D, clone 2). As suggested below, I feel that this clone likely represents a degradation intermediate. This clone had two additional nts, a GT which could be part of the non-templated 3' UTR or result from slippage in the oligoT stretch in the 5' UTR.

Similar results were observed with the clones from the 187 nt fragment. These clones were also essentially identical, and correspond to the *HIST2H3D* gene. The 5' UTR of this mRNA is extremely short, only 11 nts from the A in the ATG codon in 23 of the 28 clones, which is located 27 nts from the TATAA box. The small amount of heterogeneity at the 5' end of the mRNA (one clone, Figure 15E, clone 2) starting at the C, one nt upstream and another (Figure 15E, clone 1) at an A 3 nts upstream from the major start site, likely represents the use of closely spaced transcription start sites, all of which were about 25 nts from the TATAA box. The 3' end of the mRNA in 23 of the 28 clones (Figure 15E, clones 2 and 3) is 3 nts after the stemloop, one ends 2 nts after the stemloop (Figure 15E, clone 4), and the other

4 clones (Figure 15E, clone 1) may have a single non-templated U (or the U may represent an alternative start site and may be the first nt of the transcript). Note that this gene has an unusual sequence after the stemloop ACTGC rather than the consensus ACCCA.

These results confirmed my ability to obtain full length 5' and 3' UTRs using the cRT-PCR procedure from total cellular RNA. Although the histone mRNA formed by cleavage of the histone pre-mRNA ends 5 nts after the stemloop, the cytoplasmic histone mRNAs end only 2-3 nts after the stem-loop. Thus there must be trimming of 2 nts from the processed mRNA at some point after the processing reaction, and this may be a function of the 3'hExo which has this activity *in vitro* in the presence of SLBP (Dominski et al., 2003; Yang et al., 2006).

cRT-PCR products of uncapped histone H3 mRNA identifies degradation intermediates containing oligouridine on the 3' end of the mRNA

If decapping occurs during histone mRNA degradation, as my data suggests, then I could potentially circularize decay intermediates of histone mRNAs, allowing me to clone single molecules of partially degraded histone mRNA. Because my primers are located near the end of each ORF, I will preferentially isolate intermediates from early in the degradation process. I cloned all the products of the circular RT-PCR reactions starting with the RNAs not treated with TAP, although I could not see any defined amplified products in these reactions. Unlike the clones obtained by TAP treatment these clones were heterogenous in size, accounting for the failure to see discrete bands. I sequenced these clones and all of them

represented fragments from either the *HIST2H3A/C* genes (Figure 17A) or *HIST2H3D* gene (Figure 17B).

Only 4 of the 37 clones I obtained were from full-length mRNAs (Figure 17A, clone 2; Figure 17B, clone 5). The remaining 33 clones encoded 28 shorter mRNAs (with nts removed from either the 5' end (Figure 17A, clone 5), 3' end (11 clones; Figure 17A, clones 3,4,7-9; Figure 17B, clones 6,9,10) or both (16 clones; Figure 17A, clones 6,11-20; Figure 17B, clones 7,8, 10-12), and 5 encoded mRNAs which had non-templated U's added to the 3' end (Figure 17A, clone 1 from *HIST2H3A/C* and Figure 17B, clones 1-4 *HIST2H3D*).

Most striking were the 5 mRNAs which contained 8-15 non-templated uridines added to the 3' end of the mRNA, starting 3 nts after the stemloop, the site where I mapped the 3' end of the cytoplasmic mRNA (Figure 15D, 15G, and 15F). Two of these clones contained a single A (Figure 17B, clone 1) or C (Figure 17B, clone 4) in the oligo U tract. One of these mRNAs from the *HIST2H3D* mRNA had lost 8 nts from the 5' end. The mRNA from the *HIST2H3A/C* genes (Figure 17A, clone 1) contains at least 8 non-templated U's at the 3' end. Since there is also a string of 5 U's in the 5' end just after the cap, it is also possible that this clone comes from a decapped mRNA that has lost a few nts from the 5' end. Figure 17C and 17D summarize the 3' ends of the *HIST2H3A/C* (Figure 17C) and the *HIST2H3D* (Figure 17D) showing the non-templated U's as well as partial degradation of the 3' side of the stem. An example of the sequence of a clone containing non-templated U's is shown in Figure 17E.

DISCUSSION

mRNA degradation is an important step in regulating gene expression, and destabilizing an mRNA is the only way to rapidly reduce mRNA levels when necessary. The pathway of mRNA degradation for most polyadenylated mRNAs has been determined over the past decade (Garneau et al., 2007). The initial step is the shortening of the poly(A) tail. Once the poly(A) tail is short enough that it can no longer bind PABP, Lsm1-7 can bind the 3' end and likely recruits Pat1, effectively inhibiting translation. The Lsm1-7 complex also stimulates decapping, allowing rapid degradation 5' to 3' by Xrn1, the cytoplasmic 5' to 3' exonuclease. Following deadenylation, the mRNA may also be degraded 3' to 5' by the exosome. In yeast, the 5' to 3' and the 3' to 5' degradation pathways are redundant, although the major pathway of mRNA degradation is 5' to 3' using the decapping machinery. Yeast mutant for members of either pathway are viable but debilitation of both pathways results in lethality. Thus it is likely the two pathways are redundant, and that most mRNAs in yeast can be degraded by either pathway (Caponigro and Parker, 1996).

A third pathway of mRNA degradation is endonucleolytic cleavage, followed by 5' to 3' degradation of the 3' fragment, and degradation of the 5' fragment either by the exosome or by decapping followed by 5' to 3' exonuclease. This pathway is used for degradation of mRNAs by siRNAs (Orban and Izaurralde, 2005), and some endonucleases involved in degradation of specific mRNAs (Yang and Schoenberg, 2004) or in NMD in *Drosophila* (Gatfield and Izaurralde, 2004).

Histone mRNAs are the only mRNAs that are not polyadenylated, ending instead in a conserved stemloop sequence. A major step in regulating histone

mRNA levels is rapid degradation of histone mRNA, mediated by the stemloop as the *cis* element that directs the degradation of histone mRNA. Despite the fact that the *cis* element that determines histone mRNA degradation has been known for 20 years (Pandey and Marzluff, 1987), the details of the biochemical pathway for degradation of histone mRNA are not known.

In this study I demonstrate three features of histone mRNA degradation: (1) both the 5' pathway and the 3' pathway are involved in histone mRNA degradation, and individual molecules of histone mRNA can be simultaneously degraded 5' to 3' and 3' to 5'1; (2) there appears to be oligouridylation of the 3' end of histone mRNA in response to inhibition of DNA synthesis; and (3) Lsm1 is essential for histone mRNA degradation suggesting that Lsm1-7 binds to the oligo(U) tail that is added to histone mRNA.

Both the 5' and 3' degradation pathways contribute to histone mRNA degradation

Previous work by Jeff Ross and coworkers had implicated 3' to 5' degradation as the major pathway of histone mRNA degradation, largely based on *in vitro* studies (Ross and Kobs, 1986; Ross et al., 1986). Despite the fact that the 3'hExo can potentially degrade the 3' end of histone mRNA, I find no evidence for a role of this enzyme in histone mRNA degradation in mammalian cells (Figure 9) or *Drosophila* (Kupsco et al., 2006). In contrast, knocking down components of both the 5' to 3' decay pathway or the exosome, resulted in a reduced rate of degradation of histone mRNA when DNA replication was inhibited (Figure 14). Strikingly, knocking down Lsm1 had a large impact on histone mRNA degradation. The cytoplasmic complex,

Lsm1-7, is essential for degradation of polyadenylated mRNAs and binds to short single-stranded RNAs, typically rich in U's and A's, at the 3' end of deadenylated mRNAs (Tharun and Parker, 2001). It functions both to block translation by recruitment of Pat1 (Coller and Parker, 2005), as well as to initiate degradation of the body on the mRNA by recruitment of the decapping complex (Tharun et al., 2005; Tharun and Parker, 2001), and possibly also the exosome (Lehner et al., 2004). Given that histone mRNAs lack an obvious binding site for Lsm1-7, the finding that Lsm1 was critical for histone mRNA degradation was surprising.

The cRT-PCR data from the decapped, HU-treated samples revealed direct evidence corroborating the functional RNAi experiments. The presence of almost half (43%) of the degradation intermediates sequenced with shortened 5' and 3' ends provide compelling evidence that indeed single histone mRNA molecules are degraded simultaneously from both ends (Figure 17F). The frequency of 3' end shortened (5' end intact) clones was 10 times more abundant than clones that had their 5' ends shortened (but 3' ends intact), (30% compared to 3%, respectively). Together these data suggest there is an initiating event(s) that recruit both pathways, possibly implicating Lsm1-7 as a participant in this event. How the two decay machineries cooperate to rapidly degrade histone mRNA in response to inhibition of DNA synthesis or normally at the end of S phase is not clear.

Histone mRNA in the cytoplasm has been trimmed

Although the product of the *in vitro* processing reaction of histone mRNAs ends in 5 nts, ACCCA, the 3' end of cytoplasmic histone mRNA ends 2-3 nts (usually AC or ACC) after the stemloop. Thus, following processing the 3' end must

be trimmed. The properties of the 3' hExo, which can remove 2-3 nts from the stemloop while SLBP is bound to the stemloop (Dominski et al., 2003; Yang et al., 2006), suggests that the 3'hExo carries out this final reaction in histone mRNA maturation. The oligo(U) stretches I detected were all added to the trimmed histone mRNA.

Preliminary evidence for oligouridylation of the 3' end of histone mRNA

The positive clones from the decapped, HU-treated samples revealed a high frequency (14%) of untemplated, uridines on the 3' end of histone mRNA (Figure 17F). For a number of reasons argued below, I feel that the presence of these uridine residues is of high significance in histone mRNA degradation.

Sequencing of positive clones generated by cRT-PCR revealed the precise 5' and 3' ends of each cDNA molecule recovered. Comparison of these ends to the genomic sequence revealed the orientation of the molecules and in the case of intact histone mRNA, there was a homogeneous population of inserts from the *in vitro* decapped (+TAP) reactions. I observed an obvious difference in clone number between the plus-TAP reactions compared to the reactions without TAP, regardless of whether the mRNA is undergoing rapid degradation *in vivo* (plus or minus HU). Defined amplicons were only observed in the RNA samples treated with TAP (although it could be possible that if there are discrete degradation intermediates these might be observed as a defined amplicon). For example, following a 15 minute treatment of cells with HU, approximately one-third of histone mRNA will have been degraded. For the uncapped reactions (-TAP) there will be recovery of cDNA molecules from the cell that had been previously decapped (and exposed to

HU) and these will yield heterogenous length fragments after restriction enzyme digestion. Only a small number of clones were obtained from cells that were not treated with HU from the minus TAP reactions. These resemble those seen from the HU treated cells, reflecting the slow degradation (i.e. increased stability) of histone mRNA during S-phase. In my hands the procedure is semi-quantitative in that I observed fewer clones from +TAP reactions using RNA from cells treated with HU (where the histone mRNA concentration is reduced).

An obvious concern in these experiments was whether there was a small amount of degradation that might occur during the decapping step and extensive handling of the RNA. Two results argue that this is not the case. First the clones obtained from the cellular RNAs treated with TAP were remarkably homogenous, and no full-length clones were observed from the RNAs not treated with TAP (although one RNA with an oligo(U) tail that was otherwise full-length was observed). Second, the four RNAs produced by *in vitro* processing had homogenous 3' ends that mapped precisely to the known cleavage site. Since these mRNAs had 5' triphosphate termini (as a result of *in vitro* synthesis) it was necessary to treat these with TAP prior to ligation. There was some heterogeneity at the 5' end that has been previously documented for some T7 RNA transcripts (Pleiss et al., 1998). Although the cRT-PCR data, particularly the sequenced clones from the decapped reactions (minus TAP, plus HU), are suggestive of the presence of oligo(U) tails playing a new and exciting role in histone mRNA degradation, the present data are insufficient to convincingly stand alone. Additional evidence is required to determine

the significance of the 3' oligouridylation of histone mRNA as well as to identify the enzyme(s) responsible for this activity.

Summary

A striking finding is that individual histone mRNA molecules are degraded both 5' to 3' and 3' to 5'. A recent report using the Invader RNA Assay to detect β-globin mRNA suggests that individual ARE-containing mRNAs are also degraded from both ends (Murray and Schoenberg, 2007), suggesting that this may be a common pathway for mRNA degradation in mammalian cells. Although we now know many of the requirements and the likely pathway for histone mRNA degradation (Figure 18), we still do not understand the molecular details of how the protein complex (including SLBP, Upf1, an enzyme with terminal uridylyltransferase activity, and Lsm1-7) is recruited to the 3' end of histone mRNA to activate degradation, or the signals that activate this pathway at the end of S-phase or when DNA replication is inhibited.

.

Table 2. siRNA sequences. The table below details the sequences targeting the open reading frames of the indicated target mRNA. All siRNAs were synthesized from Dharmacon with d(T)d(T) ends.

Target	Sequence	Reference
C2	5’-GGUCCGGCUCCCCCAAAUG-3’	(Wagner and Garcia-Blanco, 2002)
PTB	5’-GCCUCUUUAUUCUUCUCGG-3	(Wagner and Garcia-Blanco, 2002)
3’hExo	5’-UUACGAAUGGCUGUAUUAA-3	This paper
Lsm1-1	5’-CAAACUUAGUGCUACAUCA-3’	(Stoecklin et al., 2006)
Lsm1-2	5’-CCAGCAAGUAUCCAUUGAA-3’	(Stoecklin et al., 2006)
Upf1	5’-GAUGCAGUUCCGCUCCAUU-3’	(Kaygun and Marzluff, 2005)
Dcp2	5’-GUGGCAUGUAAUGGACAUUGC-3’	(Wang et al., 2002)
Xrn1	5’-UGAUGAUGUUCACUUUAGA-3’	(Stoecklin et al., 2006)
PM/Scl-100	5’-GCUGCAGCAGAACAGGCCA-‘3	(Lejeune et al., 2003)
Rrp41-1	5’-CUAUGCAGCUUGUGUGAAUUU-3’	This paper
Rrp41-2	5’-CGGACAGGGCCCUAGUGAAUU-3’	This paper

Figure 9. Knockdown of 3'hExo does not affect histone mRNA degradation. HeLa cells were treated with the 3'hExo (A-C) siRNAs as described in Materials and Methods, and then treated with 5 mM HU and total cell RNA prepared 0 and 20 or 45 min after HU treatment. (A) A dilution series of the control (C2) cell lysate together with a lysate from cells treated with the indicated siRNA was analyzed by Western blotting for 3'hExo and Upf1. The asterisk indicates a cross-reacting band. (B) 2 μg of total cell RNA was resolved by urea acrylamide gel electrophoresis and transferred to N+ nitrocellulose and probed with a mixture of histone H2a mRNA and 7SK snRNA probes. (C) The average of 3 independent experiments is shown. Panel C (◆, C2; ■, 3'hExo). Standard deviations are indicated by vertical bars. (D) Cell cycle analysis of knockdowns. HeLa cells were treated with siRNAs targeting the 3'hExo and C2 used as a control. Cells were fixed in 70% ethanol, stained with propidium iodide, and analyzed by FACS. Populations of G1 (2N DNA content), S phase (2N < S < 4N DNA content), and G2/M (4N DNA content) were quantified and are represented as a percentage of the total population. All experiments are paired samples that correspond to the protein and RNA samples analyzed by Western and Northern analysis in (A) and (B).

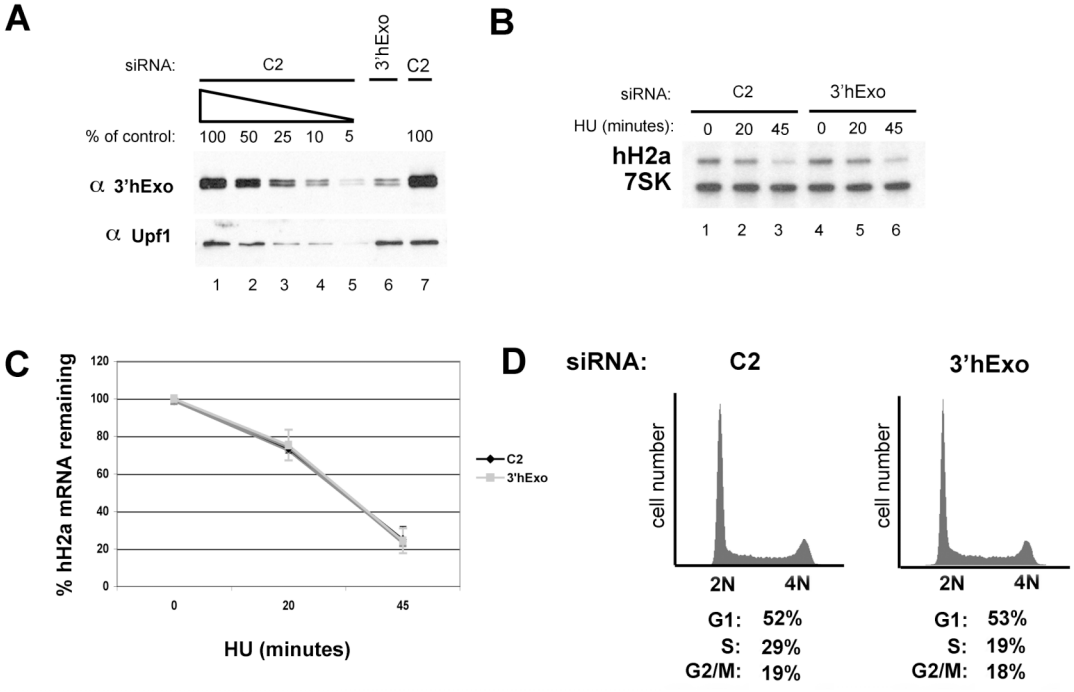
A
siRNA:
C2
3'hExo
C2
% of control:
100 50 25 10 5
100
α 3'hExo
α Upf1
1 2 3 4 5 6 7
B
siRNA:
C2
3'hExo
HU (minutes):
0 20 45 0 20 45
hH2a
7SK
1 2 3 4 5 6
C
% hH2a mRNA remaining
120
100
80
60
40
20
0
0
20
45
HU (minutes)
C2
3'hExo
D
siRNA:
C2
3'hExo
cell number
2N
4N
G1: 52%
S: 29%
G2/M: 19%
cell number
2N
4N
G1: 53%
S: 19%
G2/M: 18%

Figure 10. Effect of knocking down PTB and Lsm1. HeLa cells were treated with the PTB (A-C) or Lsm1 (D-F) siRNAs as described in Materials and Methods, and then treated with 5 mM HU and total cell RNA prepared 0 and 20 or 45 min after HU treatment. PTB is used as a negative control in these experiments. (A,D) A dilution series of the control (C2) cell lysate together with a lysate from cells treated with the indicated siRNA was analyzed by Western blotting for PTB and Upf1. The asterisk indicates a cross-reacting band. (B,E) 2 μg of total cell RNA was resolved by urea acrylamide gel electrophoresis and transferred to N+ nitrocellulose and probed with a mixture of histone H2a mRNA and 7SK snRNA probes. (C,F) The average of 3 independent experiments is shown. Panel C (◆, C2; ■, PTB); panel F (◆, C2; ■, Lsm1-1; ▲, Lsm1-2; ●, Upf1). Standard deviations are indicated by vertical bars. (G) Lysates were prepared from S-phase cells expressing HA-SLBP 15 min after treatment with HU as previously described (Kaygun and Marzluff, 2005a). (Top) A portion of the lysate was treated with RNase A (20 μg/ml; lane 3) for 15 minutes prior to immunoprecipitation with anti-HA antibody. The immunoprecipitates were analyzed for SLBP and Lsm1 by Western blotting. (Bottom) S-phase cells expressing HA-SLBP were treated with HU for 15 min, lysates prepared and subjected to immunoprecipitation with anti-myc (lanes 3 and 4) or anti-HA (lanes 5 and 6) antibodies. The immunoprecipitates were analyzed for SLBP, Lsm1 and PTB as a control by Western blotting. The input lanes (1 and 2) show 5% of the total lysate.

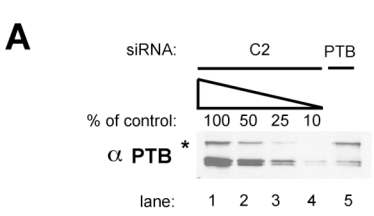
A
siRNA:
C2
PTB
% of control:
100 50 25 10
α PTB *
lane:
1 2 3 4 5

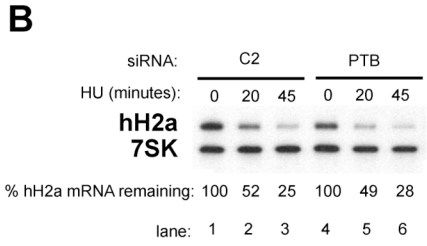
B
siRNA:
C2
PTB
HU (minutes):
0 20 45 0 20 45
hH2a
7SK
% hH2a mRNA remaining:
100 52 25 100 49 28
lane:
1 2 3 4 5 6

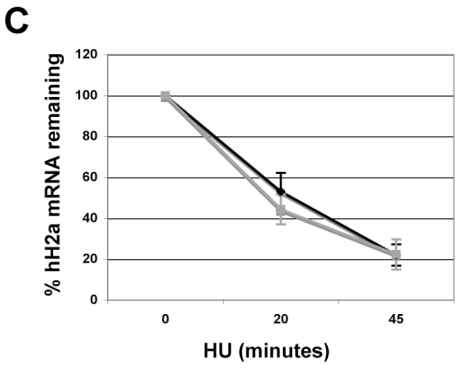
C
% hH2a mRNA remaining
120
100
80
60
40
20
0
0
20
45
HU (minutes)

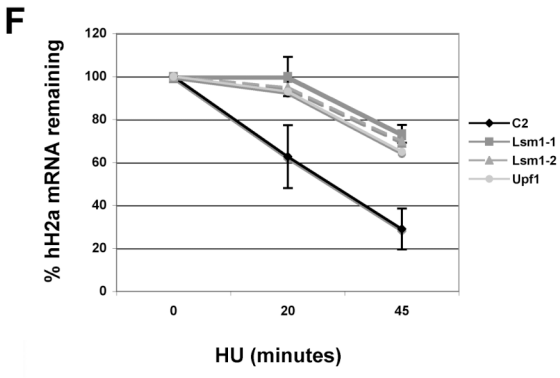
F
% hH2a mRNA remaining
120
100
80
60
40
20
0
0
20
45
HU (minutes)
C2
Lsm1-1
Lsm1-2
Upf1

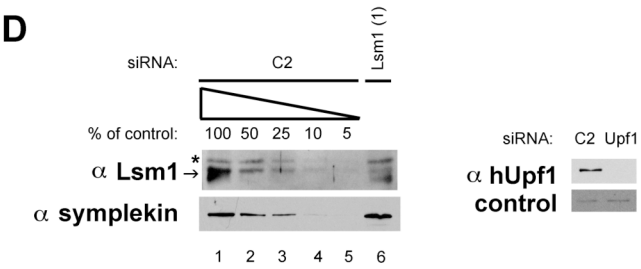
D
siRNA:
C2
Lsm1 (1)
% of control:
100 50 25 10 5
α Lsm1 →*
α symplekin
1 2 3 4 5 6
siRNA:
C2 Upf1
α hUpf1
control

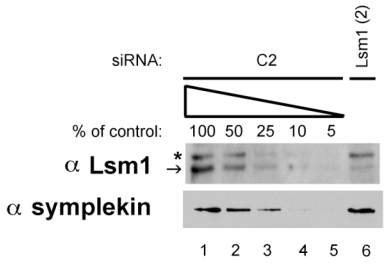
siRNA:
C2
Lsm1 (2)
% of control:
100 50 25 10 5
α Lsm1 →*
α symplekin
1 2 3 4 5 6

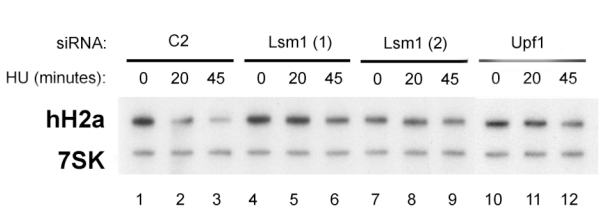
E
siRNA:
C2
Lsm1 (1)
Lsm1 (2)
Upf1
HU (minutes):
0 20 45 0 20 45 0 20 45 0 20 45
hH2a
7SK
1 2 3 4 5 6 7 8 9 10 11 12

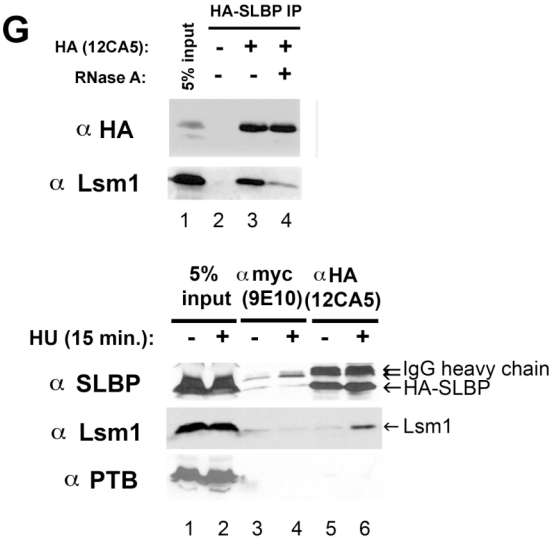
G
HA-SLBP IP
HA (12CA5):
RNase A:
5% input
- + +
- - +
α HA
α Lsm1
1 2 3 4
5% input
αmyc (9E10)
αHA (12CA5)
HU (15 min.):
- + - + - +
α SLBP
α Lsm1
α PTB
←IgG heavy chain
←HA-SLBP
←Lsm1
1 2 3 4 5 6

Figure 11. Cell cycle analysis of Lsm1 and Upf1 knockdowns. HeLa cells were treated with the indicated siRNAs (C2, Lsm1, and Upf1) and cell cycle analysis performed by FACS. The percent phase distribution is indicated below the histogram. The FACS analysis in this figure are paired samples from the experiments performed in Figure 10D-10E.

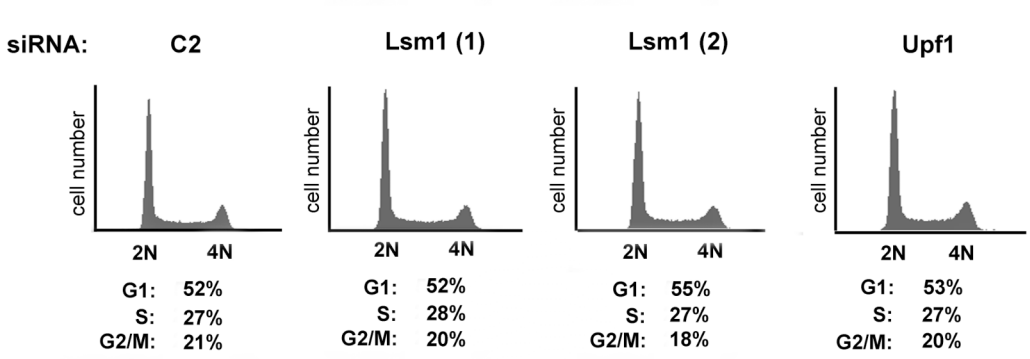
siRNA:
C2
Lsm1 (1)
Lsm1 (2)
Upf1
cell number
2N
4N
G1: 52%
S: 27%
G2/M: 21%
G1: 52%
S: 28%
G2/M: 20%
G1: 55%
S: 27%
G2/M: 18%
G1: 53%
S: 27%
G2/M: 20%

Figure 12. Effect of decapping complex and 5'-3' exonuclease knockdown on histone mRNA degradation. HeLa cells were treated with the indicated siRNAs to Dcp2 (A-C) or Xrn1 (E-G) and treated with 5 mM HU as described in Figure 1. (A and E) Protein levels of knockdowns were measured by Western blot using antibodies to Dcp2 (A) and Xrn1 (E). (B and F) S1 nuclease protection assays of 5 μg total RNA isolated from cells treated with 5 mM Hu for 0, 20 or 45 minutes from Dcp2 (B) or Xrn1 (F) knockdowns. Human H3.3 and H2a mRNAs were detected by mixing probes to detect the 3' and 5' ends of H3.3 and H2a mRNAs, respectively. (C and G) The average of 3 independent experiments from Dcp2 (C) and Xrn1 (F) knockdowns is shown. The vertical bars indicate the standard deviation. (D and H) Cell cycle analysis of Dcp2 (D) and Xrn1 (H).

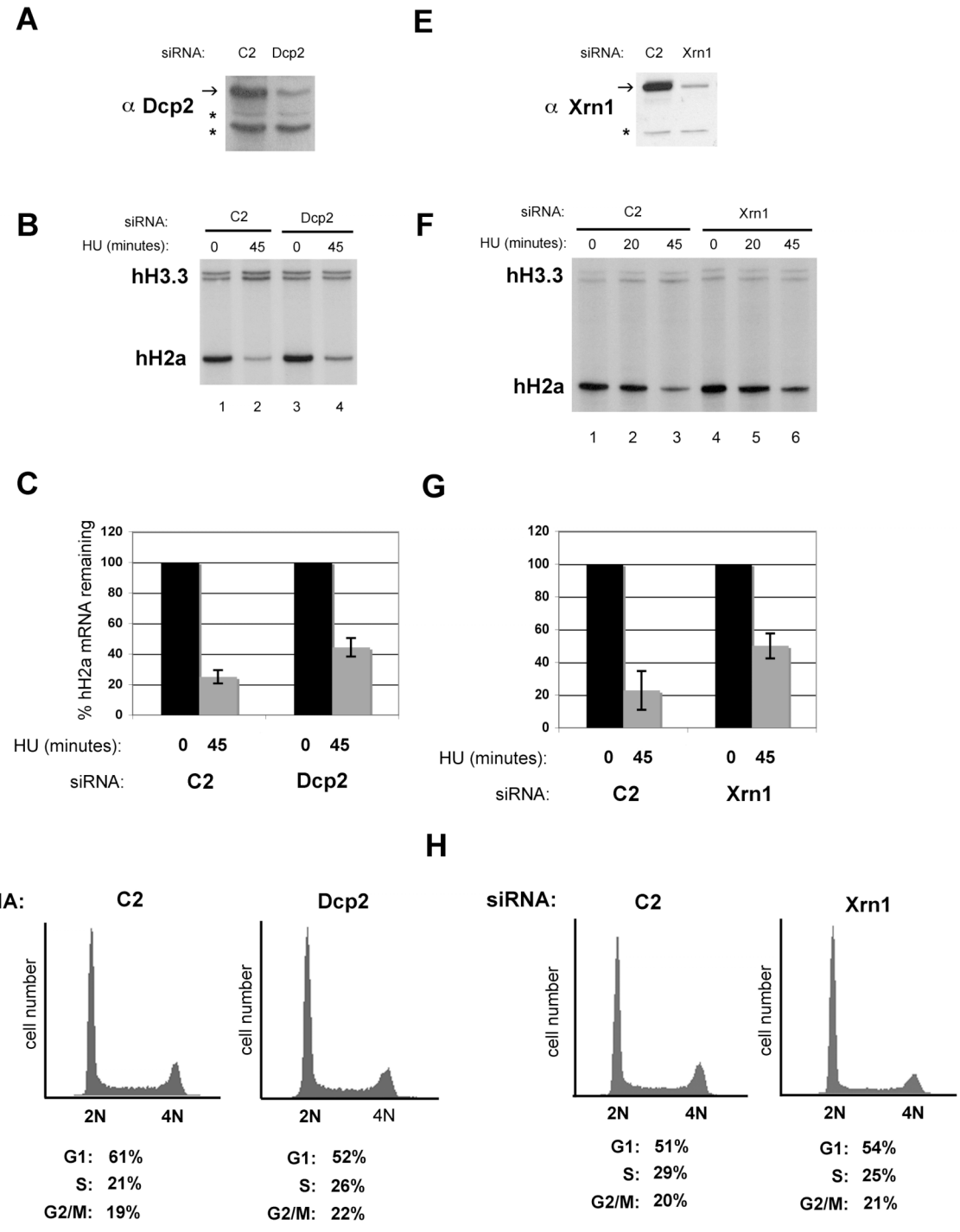
A
siRNA: C2 Dcp2
α Dcp2
E
siRNA: C2 Xrn1
α Xrn1
B
siRNA: C2 Dcp2
HU (minutes): 0 45 0 45
hH3.3
hH2a
1 2 3 4
F
siRNA: C2 Xrn1
HU (minutes): 0 20 45 0 20 45
hH3.3
hH2a
1 2 3 4 5 6
C
% hH2a mRNA remaining
120 100 80 60 40 20 0
HU (minutes): 0 45 0 45
siRNA: C2 Dcp2
G
120 100 80 60 40 20 0
HU (minutes): 0 45 0 45
siRNA: C2 Xrn1
D
siRNA: C2 Dcp2
cell number
2N 4N
G1: 61%
S: 21%
G2/M: 19%
G1: 52%
S: 26%
G2/M: 22%
H
siRNA: C2 Xrn1
cell number
2N 4N
G1: 51%
S: 29%
G2/M: 20%
G1: 54%
S: 25%
G2/M: 21%

Figure 13. Effect of knockdown of exosome components on histone mRNA degradation. (A, E) HeLa cells were treated with the indicated siRNAs to PM/Scl-100 (A-C) or Rrp41 (E-G) and treated with 5 mM HU and levels of each protein determined by Western blotting as in Figure 1 and 2. (B, F) 2 μg of total cell RNA from cells with PM/Scl100 knocked down (B) or Rrp41 knocked down (F) with two siRNAs (5 and 6) to Rrp41 was resolved by urea-acrylamide gel electrophoresis and probed with a mixture of histone H2a mRNA and 7SK snRNA probes as in Figure 1. (C, G) The average of 3 independent knockdowns to PM/Scl-100 (Panel C: ◆, C2; ■, PM/Scl-100) and Rrp41 (Panel G: ◆, C2; ■, Rrp41(1); -▲-, Rrp41(2)) is shown. (D and H) Cell cycle analysis of PM/Scl-100 and Rrp41 knockdowns.

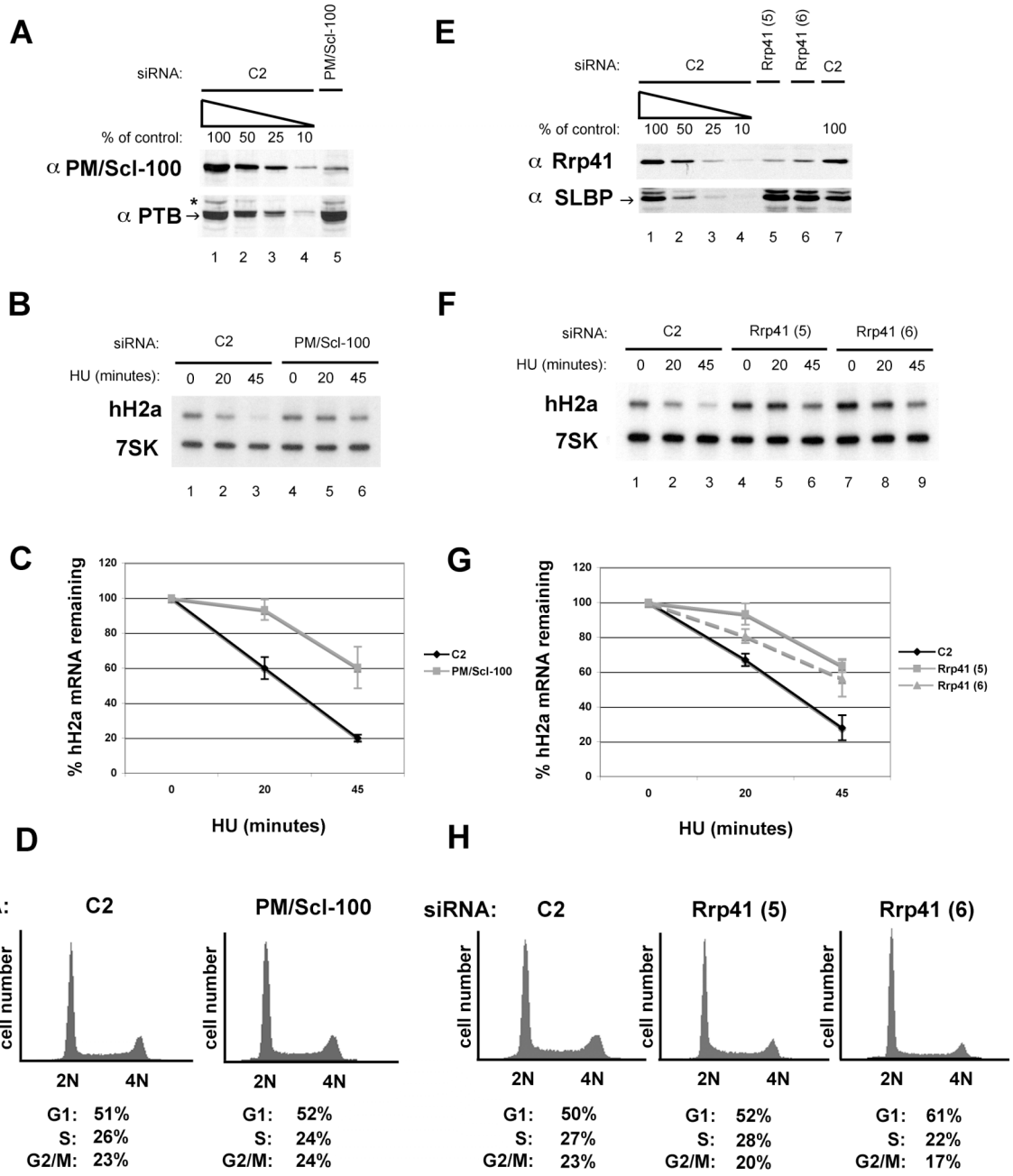
A
siRNA:
C2
PM/Scl-100
% of control:
100 50 25 10
α PM/Scl-100
α PTB →
*
1 2 3 4 5
B
siRNA:
C2
PM/Scl-100
HU (minutes):
0 20 45 0 20 45
hH2a
7SK
1 2 3 4 5 6
C
% hH2a mRNA remaining
120
100
80
60
40
20
0
0
20
45
HU (minutes)
C2
PM/Scl-100
D
siRNA:
C2
PM/Scl-100
cell number
2N
4N
G1: 51%
S: 26%
G2/M: 23%
G1: 52%
S: 24%
G2/M: 24%
E
siRNA:
C2
Rrp41 (5)
Rrp41 (6)
C2
% of control:
100 50 25 10
100
α Rrp41
α SLBP →
1 2 3 4 5 6 7
F
siRNA:
C2
Rrp41 (5)
Rrp41 (6)
HU (minutes):
0 20 45 0 20 45 0 20 45
hH2a
7SK
1 2 3 4 5 6 7 8 9
G
% hH2a mRNA remaining
120
100
80
60
40
20
0
0
20
45
HU (minutes)
C2
Rrp41 (5)
Rrp41 (6)
H
siRNA:
C2
Rrp41 (5)
Rrp41 (6)
cell number
2N
4N
G1: 50%
S: 27%
G2/M: 23%
G1: 52%
S: 28%
G2/M: 20%
G1: 61%
S: 22%
G2/M: 17%

Figure 14. Summary of 5'-3' decay and exosome RNAi experiments. Average fold stabilization of all independent experiments shown in Figures 1 through 3, with standard deviations indicated by vertical bars.

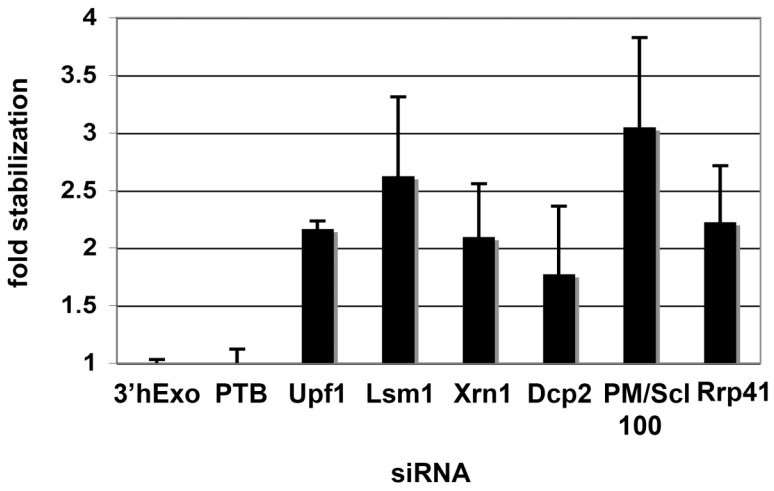
fold stabilization
4
3.5
3
2.5
2
1.5
1
3'hExo
PTB
Upf1
Lsm1
Xrn1
Dcp2
PM/Scl 100
Rrp41
siRNA

Figure 15. Detection of the 5' and 3' ends of capped histone H3 mRNA *in vivo* by cRT-PCR. (A) The cRT-PCR strategy to determine the ends of intact histone mRNA and degradation intermediates is shown (adapted from Couttet et al., 1997). (B) cRT-PCR reactions with and without decapping from total cell RNA were separated on 1.5% agarose gels and amplicons detected by ethidium bromide staining. Two human histone H3 mRNAs are visualized in the +TAP lanes. (C) Control cRT-PCR experiment to determine the 3' end of histone mRNA *in vitro*. Synthetic histone pre-mRNA was processed in a nuclear extract, and the unprocessed and processed RNAs were treated with TAP and subjected to cRT-PCR, and the products cloned and sequenced. All 4 clones of processed RNA sequenced ended at ACCCA. The arrow indicates the site cleaved *in vitro*. (D and E) cRT-PCR was performed on total cell RNA, the histone H3 products amplified, cloned and sequenced. *HIST2H3A/C* (panel D) or *HIST2H3D* (panel E) mRNAs that were capped were cloned by cRT-PCR. The number of times each sequence was obtained is indicated by a number in parentheses. (D) The 5' (top) and 3' (bottom) ends of capped (+TAP) *HIST2H3A/C* mRNAs. The genomic sequence of *HIST2H3A/C* is indicated on the top line. The sequences of the TA cloned cRT-PCR products are shown. (E) The 5' (top) and 3' (bottom) of the capped histone *HIST2H3D* mRNA. The genomic sequence of *HIST2H3D* is shown in the top lines. The number of times a particular clone was obtained is in parentheses. (F) The 3' end of histone mRNA is trimmed 2-3 nts *in vivo*.

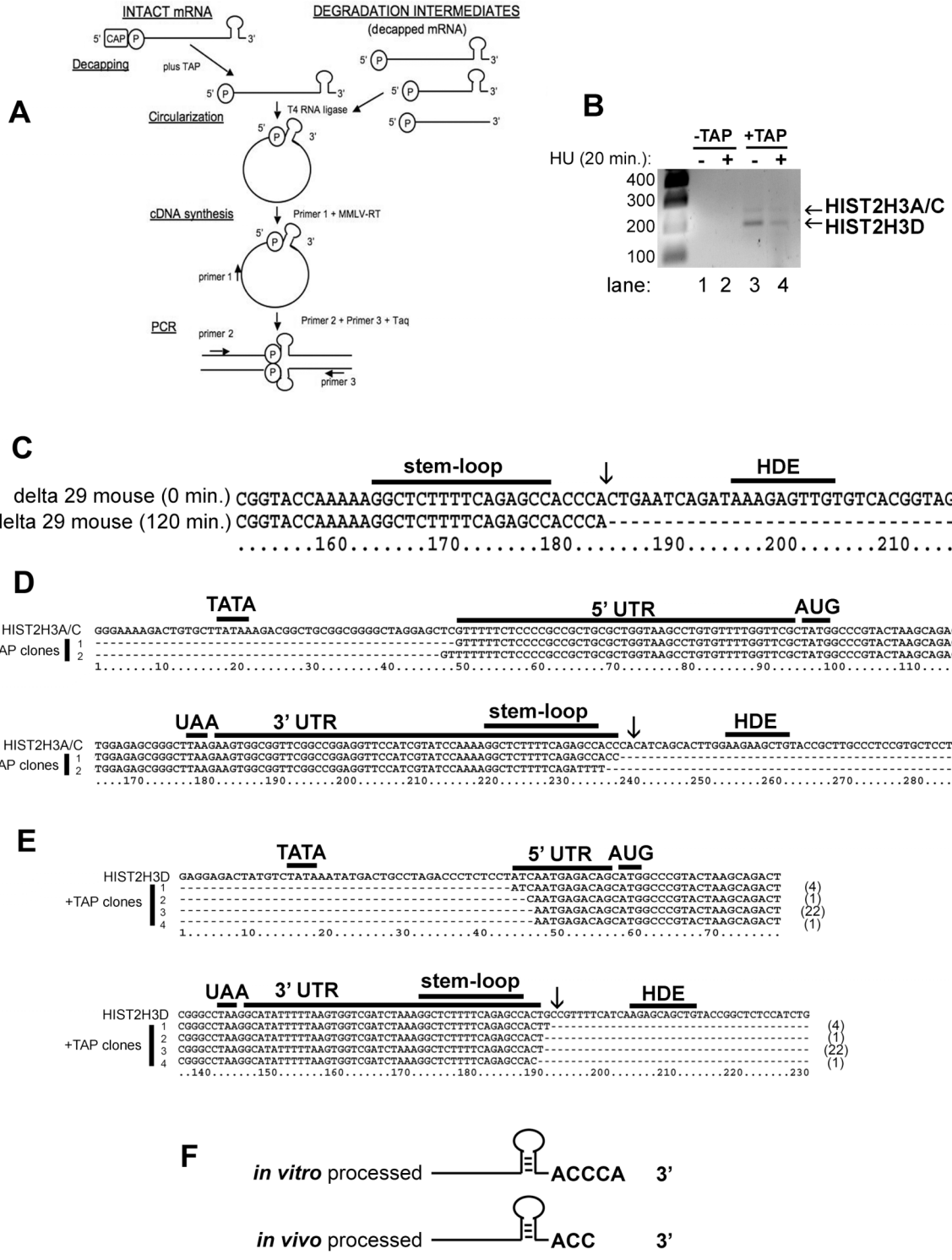
A
INTACT mRNA
DEGRADATION INTERMEDIATES
(decapped mRNA)
5' CAP P 3'
Decapping
plus TAP
5' P 3'
Circularization
T4 RNA ligase
cDNA synthesis
Primer 1 + MMLV-RT
primer 1
PCR
Primer 2 + Primer 3 + Taq
primer 2
primer 3
B
-TAP +TAP
HU (20 min.):
- + - +
400
300
200
100
lane: 1 2 3 4
←HIST2H3A/C
←HIST2H3D
C
stem-loop
HDE
delta 29 mouse (0 min.) CGGTACCAAAAAGGCTCTTTTCAGAGCCACCCACTGAATCAGATAAAGAGTTGTGTCACGGTAGC
delta 29 mouse (120 min.) CGGTACCAAAAAGGCTCTTTTCAGAGCCACCCA----------
.....160.....170.....180.....190.....200.....210.....
D
TATA
5' UTR
AUG
HIST2H3A/C GGGAAAAGACTGTGCTTATAAAGACGGCTGCGGCGGGGCTAGGAGCTCGTTTTTCTCCCCGCCGCTGCGCTGGTAAGCCTGTGTTTTGGTTCGCTATGGCCCGTACTAAGCAGACT
+TAP clones 1 ----------GTTTTTCTCCCCGCCGCTGCGCTGGTAAGCCTGTGTTTTGGTTCGCTATGGCCCGTACTAAGCAGACT (10)
2 ----------GTTTTTTTCTCCCCGCCGCTGCGCTGGTAAGCCTGTGTTTTGGTTCGCTATGGCCCGTACTAAGCAGACT (1)
1.....10.....20.....30.....40.....50.....60.....70.....80.....90.....100.....110.....
UAA
3' UTR
stem-loop
HDE
HIST2H3A/C TGGAGAGCGGGCTTAAGAAGTGGCGGTTCGGCCGGAGGTTCCATCGTATCCAAAAGGCTCTTTTCAGAGCCACCCACATCAGCACTTGGAAGAAGCTGTACCGCTTGCCCTCCGTGCTCCTCC
+TAP clones 1 TGGAGAGCGGGCTTAAGAAGTGGCGGTTCGGCCGGAGGTTCCATCGTATCCAAAAGGCTCTTTTCAGAGCCACC---------- (10)
2 TGGAGAGCGGGCTTAAGAAGTGGCGGTTCGGCCGGAGGTTCCATCGTATCCAAAAGGCTCTTTTCAGATTTT---------- (1)
....170.....180.....190.....200.....210.....220.....230.....240.....250.....260.....270.....280.....
E
TATA
5' UTR
AUG
HIST2H3D GAGGAGACTATGTCTATAAATATGACTGCCTAGACCCTCTCCTATCAATGAGACAGCATGGCCCGTACTAAGCAGACT
+TAP clones 1 ----------ATCAATGAGACAGCATGGCCCGTACTAAGCAGACT (4)
2 ----------CAATGAGACAGCATGGCCCGTACTAAGCAGACT (1)
3 ----------AATGAGACAGCATGGCCCGTACTAAGCAGACT (22)
4 ----------AATGAGACAGCATGGCCCGTACTAAGCAGACT (1)
1.....10.....20.....30.....40.....50.....60.....70.....
UAA
3' UTR
stem-loop
HDE
HIST2H3D CGGGCCTAAGGCATATTTTTAAGTGGTCGATCTAAAGGCTCTTTTCAGAGCCACTGCCGTTTTCATCAAGAGCAGCTGTACCGGCTCTCCATCTG
+TAP clones 1 CGGGCCTAAGGCATATTTTTAAGTGGTCGATCTAAAGGCTCTTTTCAGAGCCACTT---------- (4)
2 CGGGCCTAAGGCATATTTTTAAGTGGTCGATCTAAAGGCTCTTTTCAGAGCCACT---------- (1)
3 CGGGCCTAAGGCATATTTTTAAGTGGTCGATCTAAAGGCTCTTTTCAGAGCCACT---------- (22)
4 CGGGCCTAAGGCATATTTTTAAGTGGTCGATCTAAAGGCTCTTTTCAGAGCCAC---------- (1)
..140.....150.....160.....170.....180.....190.....200.....210.....220.....230
F
in vitro processed ACCCA 3'
in vivo processed ACC 3'

Figure 16. New histone H3 gene, *HIST2H3D*. A highly expressed human histone H3 gene was cloned. The previously unannotated H3 gene is found in the minor histone gene (*HIST2*) cluster on chromosome 1q21 from nucleotides 276048-275157. The TATA box is represented in the 5' end of the gene in bold letters. The major transcriptional start site is represented by the bold A depicted in blue and start codon in green. The termination codon is represented in red with the bold sequence following representing the conserved stemloop sequence at the 3' end. The cleavage site is represented by the two blue 'C's' where cleavage in nucleus is presumed to occur between them. The nts between the stemloop and cleavage site are underlined. The bold sequence downstream of the cleavage site represented the histone downstream element (HDE).

5’CTTCGGTCATTCATGGTATACAATGCATCTAACTTGCTGA
GCAAAATGCCAGACATGAAATAAATGTTAGCTATGGTAGAA
GAGCTACAGTAACAGGTAACCTGAAACAGGCTGATAGCTC
ATAGAAGGGCATGCTTGAATTCGGGGAAAAAAAAAATCTC
TGTTAAAATGGGATGCAAAACACTTTATACATTGCTTTTAC
AAAAGTTAGACTAATTTAAAGGAAAGTCTTCAAAAACAATC
CGTGATCGATAAAATTACAGAAAAAAATCAGGAAAGGGGG
AAATAATAAGGGAAGAAAGATTAGCAGAACAATCTTCCGC
CCCAGTAAAGAGGATTGAATTTTAACCAATGAGATCACAAG
TTTGAAAATTTCCTTTTCAGGCCCAATCAAGAGGAGACTAT
GTC**TATA**AATATGACTGCCTAGACCCTCTCCTATC**A**ATGAG
ACAGC**ATG**GCCCGTACTAAGCAGACTGCCCGCAAGTCGA
CCGGCGGCAAGGCCCCGAGGAAGCAGCTGGCTACCAAA
GCGGCCCGCAAGAGCGCGCCGGCCACGGGCGGGGTGAA
GAAGCCGCACCGCTACCGGCCCGGCACCGTGGCTCTGC
GGGAGATCCGGCGCTACCAGAAGTCTACGGAGCTGCTGA
TCCGCAAGCTGCCCTTCCAGCGGCTGGTACGCGAGATCG
CGCAGGACTTTAAGACGGACCTGCGCTTCCAGAGCTCGG
CCGTGATGGCGCTGCAGGAGGCCAGCGAGGCCTACCTG
GTGGGGCTGTTCGAAGACACGAACCTGTGCGCCATCCAT
GCCAAGCGCGTGACCATCATGCCCAAGGACATCCAGTTG
GCCCGCCGCATCCGCGGGGAGCGGGCC**TAA**GGCATATTT
TTAAGTGGTCGATCTAAA**GGCTCTTTTCAGAGCC**ACTG**CC**
GTTTTCATC**AAGAGCAGCTGT**ACCGGCTCTCCATCTGATG
TGCGTCTGCCTTGCGCAGCGGTCAGGGGCCAGGGGCACT
CGTGGTGGGTGA3’

Figure 17. Detection of uncapped histone mRNA by cRT-PCR upon inhibition of DNA synthesis reveals degradation intermediates with nonencoded uridines. (A and B) cRT-PCR was performed on total cell RNA in the absence of TAP (see Figure 15, lanes 1 and 2). The low levels of histone H3 mRNAs (A) *HIST2H3A/C* or (B) *HIST2H3D* that were not capped when treated with hydroxyurea were cloned and sequenced. Primer 2 and 3 represent sites where I targeted amplification towards the 5' and 3' ends. ORF sequences between these 2 oligonucleotides are missing. Numbers in parentheses are the number of times each clone was obtained. (C and D) The 3' ends from the largest *HIST2H3A/C* (panel C) and *HIST2H3D* (panel D) mRNA degradation intermediates are shown. The number of times each sequence was obtained is indicated by a number in parentheses. (E) Chromatogram from a *HIST2H3D* mRNA degradation intermediate containing 8 untemplated U's (T's in the DNA sequence). The 3' and 5' ends are ligated (arrow) together. (F) Summary of the distribution of various types of degradation intermediates observed.

A

HIST2H3A/C

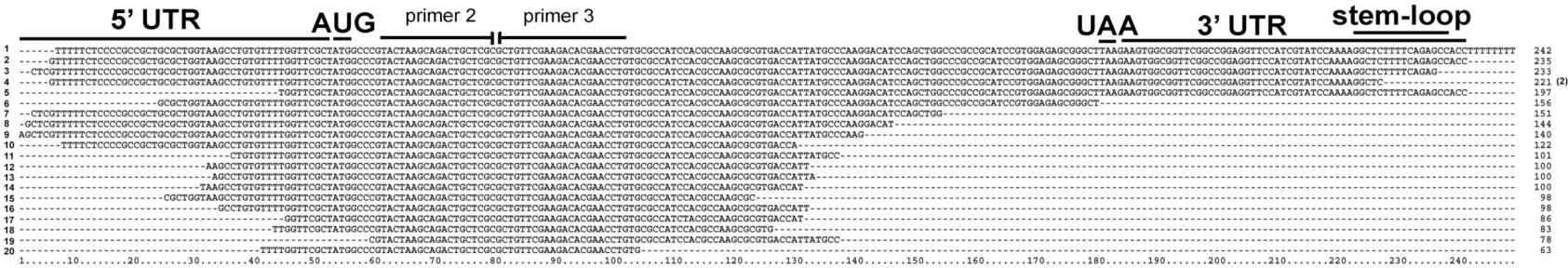

B

HIST2H3D

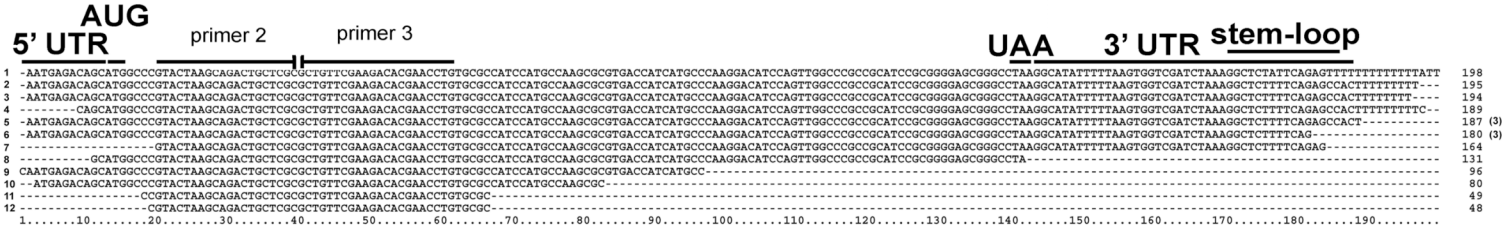

C HIST2H3A/C

stem-loop

```
CCAAAAGGCTCTTTTCAGAGCCACCTTTTTTTT   242
CCAAAAGGCTCTTTTCAGAGCCACC--------   235
CCAAAAGGCTCTTTTCAGAG-------------   233
CCAAAAGGCTC----------------------   221 (2)
CCAAAAGGCTCTTTTCAGAGCCACC--------   197
```

D HIST2H3D

stem-loop

```
AAAGGCTCTATTCAGAGTTTTTTTTTTTTTATT   198
AAAGGCTCTTTTCAGAGCCACTTTTTTTTT---   195
AAAGGCTCTTTTCAGAGCCACTTTTTTTTT----   194
AAAGGCTCTTTTCAGAGCCACTTTTTTTTTC--   189
AAAGGCTCTTTTCAGAGCCACT-----------   187 (3)
```

E

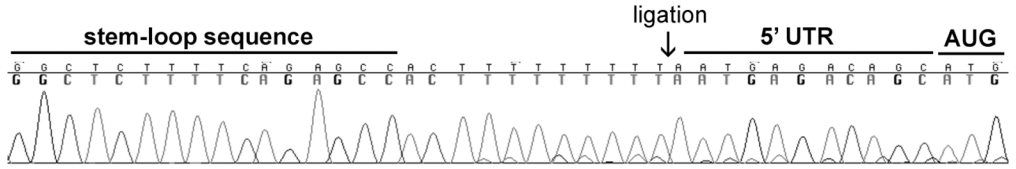

F

type of uncapped intermediate	percent of total clones
Full-length	10% (4 of 37)
5' shortened (3' intact)	3% (1 of 37)
3' shortened (5' intact)	30% (11 of 37)
Both 5' and 3' shortened	43% (16 of 37)
Oligo(U) tails on 3' end	14% (5 of 37)

Figure 18. Model of histone mRNA degradation.

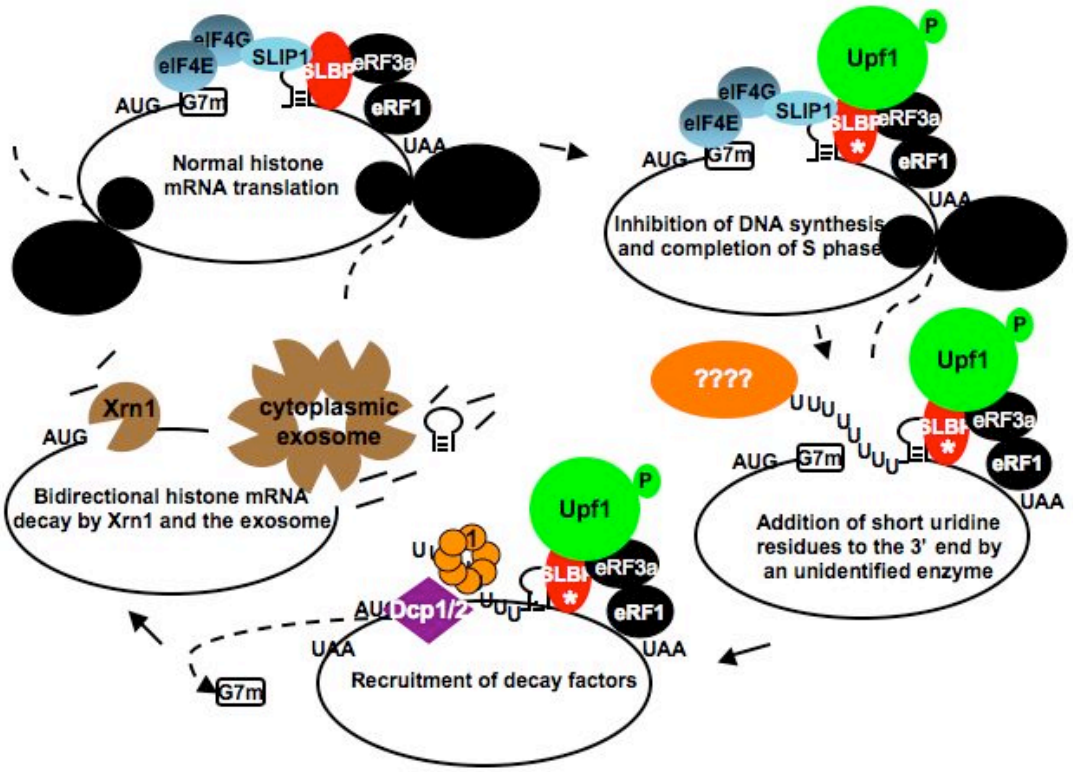
eIF4G
eIF4E
SLIP1
SLBP
eRF3a
eRF1
AUG
G7m
UAA
Normal histone mRNA translation
Upf1
P
Inhibition of DNA synthesis and completion of S phase
????
Addition of short uridine residues to the 3' end by an unidentified enzyme
Xrn1
cytoplasmic exosome
Bidirectional histone mRNA decay by Xrn1 and the exosome
Dcp1/2
Recruitment of decay factors

CHAPTER 3

DEGRADATION OF HISTONE mRNA REQUIRES OLIGOURIDYLATION

INTRODUCTION

Histone mRNAs are rapidly destabilized when cells are exposed to inhibitors of DNA synthesis and when cells are completing the DNA replication phase of the cell cycle. It is clear the unique 3' stemloop of metazoan replication-dependent histone mRNAs plays a critical role in regulating the rapid change in histone half-life (Graves et al., 1987; Pandey and Marzluff, 1987), although the precise mechanism is not known. The stemloop binding protein (SLBP) binds the stemloop and is a significant component in proper regulation of histone protein biogenesis. In addition to SLBP, other proteins such as the Lsm1-7 complex and the RNA helicase Upf1 have been shown to be bound to histone mRNA and the 3' mRNP that exists specifically under conditions when histone mRNA is degraded (Kaygun and Marzluff, 2005a; Mullen and Marzluff, 2008), (Chapter 2). The protein complex(es) that is (are) recruited to the 3' end of histone mRNA appears to play a fundamental role in specifically targeted histone mRNA for rapid degradation under the appropriate cellular stimuli. Following the recruitment of the appropriate positive regulators of histone mRNA degradation, histone mRNA molecules are targeted for bidirectional 5'-3' and 3'-5' degradation (Mullen and Marzluff, 2008), (Chapter 2).

In the last chapter I presented preliminary evidence showing the presence of short, untemplated uridine tracts on nearly full-length histone mRNA degradation intermediates. This preliminary evidence suggests it is possible the cell uses terminal uridylyltransferase (TUTase) activity to post-transcriptionally modify the 3' end of histone mRNA in the cytoplasm. This modification could provide a mechanism to specifically target histone mRNA for degradation. At the time I made this observation there were no cloned and characterized human enzymes with this activity. However, it has been recognized for over 45 years that enzyme fractions from carcinoma cells and rat liver could incorporate uridine triphosphate into RNA (Burdon and Smellie, 1961; Klemperer, 1963). Additionally, poliovirus encodes an RNA polymerase that requires a host factor required to prime viral replication (Dasgupta et al., 1980). Biochemical fractionation of HeLa cells suggested that the host factor is in fact a TUTase that adds uridines to the 75 nt long 3' poly(A) tail and this subsequently forms a hairpin that primes the viral RNA polymerase (Andrews and Baltimore, 1986).

The best example of the importance of TUTase activity occurs in the mitochondria of the kinetoplastid *Trypanosoma bruceii* (Shaw et al., 1988). RNA editing in trypanosomes involves the insertion or deletion of dozens to hundreds of uridylate residues by a complex series of enzymatic reactions that are carried out by enzymes encoded for in the nucleus (Stuart, 1991). First, a specified guide RNA (gRNA) targets a substrate RNA sequence that is subsequently cleaved by an endoncuclease (Adler and Hajduk, 1997). Next, either a TUTase adds a variable number of uridylate residues (Aphasizhev et al., 2003) or a 3'-U-exonuclease (Adler

and Hajduk, 1997) removes a variable number of uridylate residues. Finally an RNA ligase (TbMP52 or TbMP48), specified by the gRNA, joins the 5' and 3' ends (Madison-Antenucci et al., 2002). Together, the process of RNA editing in the mitochondria of trypanosomes functions to convert encrypted RNA sequences into functional open reading frames in order to assemble the electron transport machinery.

Another example of U-addition is the highly conserved splicesomal U6 snRNA. U6 snRNA is unique from other snRNAs in that uridine monophosphate residues are post-transcriptionally added to and removed from its 3' end, presumably as a final maturation step or to regulate its incorporation into the spliceosomal snRNP (Lund and Dahlberg, 1992; Rinke and Steitz, 1985). The U-stretches vary in length from 5-12 residues (Terns et al., 1992). Recent biochemical fractionation of HeLa extracts have purified a specific U6 snRNA TUTase activity (Trippe et al., 2003; Trippe et al., 1998), but at the time of my initial observation of short U stretches on the 3' end of histone mRNA (July 2006), the identity of the TUTase had not bee elucidated.

This changed in August of 2006 when the Benecke lab reported the cloning of the U6 TUTase from human cells (Trippe et al., 2006). The 93 kDa U6 TUTase enzyme is required for U6 snRNA maturation *in vitro* and *in vivo* and is required for cell viability. Importantly, the cloning of the U6 TUTase provided some of the first insight into the domain structure of what we are quickly realizing is an entire family of TUTase-like enzymes in eukaryotes. Specifically, U6 TUTase possesses a poly(A) polymerase associated-domain (PAPD) which is contained within a larger

overlapping topoisomerase-related function (TRF) domain (Trippe et al., 2006). These overlapping domains share significant sequence identity to the trypanosomal RET1 TUTase and to a lesser degree the canonical poly(A) polymerase α.

In this chapter I provide compelling evidence supporting a novel pathway for histone mRNA degradation that involves initial addition of uridines to the 3' end of histone mRNA. Treatment of cells with hydroxyurea (HU) results in a dramatic increase in oligouridylated histone mRNAs, and at the end of S-phase, cells also accumulate oligouridylated histone mRNAs. In addition, a functional RNAi screen against 7 putative TUTases present in human cells identifies 2 putative TUTases that attenuate histone mRNA degradation in response to inhibition of DNA synthesis. Epitope-tagged versions of these 2 TUTases are localized to the cytoplasm of human cells. Moreover, I present preliminary biochemical characterization of the TUTases believed to be involved in histone mRNA degradation. These data, taken together with that from Chapter 2, present a novel mechanism of histone mRNA degradation.

MATERIALS AND METHODS

Cell synchronization

To detect oligo(U) on histone mRNA in response to inhibition of DNA synthesis, I used synchronized HeLa cells (see Chapter 2 for detailed Materials and Methods). Fresh, warm media containing 5 mM HU was added 3 hours following release from the second thymidine block for 15, 30 and 60 minutes. I harvested total

cell RNA using the methods previously described in Chapter 2 and DNase-treated the RNA samples following isolation to eliminate genomic DNA contamination.

In order to detect oligo(U) tails on the 3' end of histone mRNA during the cell cycle (without inhibiting DNA replication) at the end of S phase, synchronized dishes were set up to follow the rapid degradation of histone mRNA at the end of S phase. The precise length of S-phase in cell synchrony experiments does vary from experiment to experiment (but is constant within an experiment) but typically I would observe histone mRNA rapidly disappear between 5-7 hours after release from the second thymidine block.

Reverse transcription of oligo(U) tails on the 3' end

RT reactions were performed on 4 μg of DNase-treated total RNA (Chomczynski and Sacchi, 1987) from the 0, 15, 30 and 60 minutes time points following HU treatment. MMLV-RT (Invitrogen) was used in these reactions following the manufacturer's protocol. The oligo(U) tail was primed with an oligo(dA) oligo containing a T7 sequence (Table 3) on the 5' end to use in the subsequent PCR step.

PCR

Two rounds of PCR totaling 60 cycles was required for detection of oligouridylated tails on the 3' end of histone mRNA. This likely reflects the very low abundance of these degradation intermediates. Histone genes have a high guanine and cytosine content (roughly 67% on average) and this made amplifying full-length histone cDNA initially difficult. Therefore, for the first round of PCR I used a GC-rich

Pfu DNA polymerase (Invitrogen) where I targeted specific histone mRNAs with an oligo targeting the 5' UTR and the T7 reverse primer (Table 3). The non-allelic copies of each of the 5 classes of replication-dependent histone genes have ORFs that have little divergence at the nucleotide level and almost none at the protein level (Marzluff et al., 2002) so targeting individual genes of each class of histone mRNA requires targeting the 5' UTR. For the first round, I performed 30 cycles (95° C for 30 seconds, 50-54° C for 30 seconds, and 72° C for 30 seconds) in a 50 μl PCR reaction containing 0.5 μl GC-rich DNA polymerase, 10 μl of 5X Buffer A supplied by the manufacturer (Invitrogen), 0.5 μl of each (5' UTR oligo and T7 reverse), 1-2 μl of oligo(dA) RT, and 37.5 μl water. No detectible amplicons from the first round of PCR using ethidium bromide staining were ever observed.

The second round of PCR used oligos that target the ORF of the respective histone mRNAs and the same T7 reverse oligo (Table 3). I used 1 μl from the first round of PCR and identical cycling strategies (30 cycles) as in the first round. This time however, Taq DNA polymerase, 5% DMSO, 10X Taq buffer (see above) was used in place of the GC-rich Pfu DNA polymerase. This allowed me the opportunity to T/A clone the amplicons to confirm the position of the oligo(U) tails present on the 3' end of histone mRNA following inhibition of DNA synthesis. PCR products were separated on 2% agarose gels containing ethidium bromide. Amplification of the histone H2A 3' end was performed using primer H2a/a O-1 (Table 3) and amplified a 188 bp product while the H2a/a O-2 primer amplified a product 15 bp larger. Both the H3 genes targeted amplified a product approximately 200 bp. Common to the H3 oligo (dA) RT-PCR is a contaminating band of approximately 130 bp. This

nonspecific band contains the 5' UTR oligo as well as the ORF oligo followed by a small amount of ORF sequence and then the T7 sequence. No nonencoded uridines are seen in the clones of this nonspecific band, which is present in large amounts only when no oligo(U) tails on histone mRNA were detected.

RNA interference

RNAi to TUTase mRNA was carried out as described in Chapter 2. The siRNA sequences to the various TUTases are listed in Table 4.

RT-PCR of TUTase mRNA

TUTases were downregulated by siRNA as described above. Total RNA was isolated by Trizol reagent (Sigma) and 2 μg of RNA was reverse transcribed with MMLV-RT (Invitrogen) and random primers. RT reactions were subjected to PCR with the oligos described in Table 5.

Cloning of TUTases

TUTases were cloned by PCR from cDNA clones or by RT-PCR from total HeLa RNA and cloned into pCDNA4-myc3 or pCDNA3-flag vectors. Accession numbers of the TUTases are the following: TUTase-1 (BAB13981), -2 (BC04758), -3 (Q8NDF8), -4 (XP_038288), -5 (AB005754), the U6 TUTase (BC110910) and TUTase-7 (BC032456).

Immunofluorescence and confocal microscopy

HeLa cells plated on coverslips were transiently transfected with 0.5 μg pCDNA4-myc3-FLAG plasmids encoding the ORF of TUTases-1 and -3 for 48 hours. Cells were prepared for immunofluorescence as described (Wagner and

Marzluff, 2006) and the N-terminal myc-epitope tag was detected with a monoclonal mouse anti-myc antibody (Upstate Biotechnology).

Purification of epitope-tagged TUTases from human cells

TUTase ORFs were cloned into a modified pcDNA4 vector containing a single N-terminal FLAG tag and a β-globin intron upstream of the epitope tag (courtesy of Yi Zhang, University of North Carolina at Chapel Hill). 293T cells were plated (3 x 10^6 cells) into 15 cm^2 dishes and 70 μg of plasmid DNA transfected into cells using Lipofectamine 2000 (Invitrogen) according to the manufacturer's suggestions and following similar large-scale transfections for protein purification (Cazalla et al., 2005). Cells were harvested 48 hours following transfection and purified using M2-FLAG antibody (single FLAG) conjugated protein resin (Sigma) similarly as previously described (Cazalla et al., 2005; Tsukada et al., 2006; Tsukada and Zhang, 2006).

Briefly, cells were pelleted at 1200 rpm for 5 minutes at 4°C and washed with PBS. Cell pellets were frozen on dry ice, thawed on ice and resuspended in 10 ml of F lysis buffer (20 mM Tris pH 7.9, 500 mM NaCl, 4 mM $MgCl_2$, 0.4 mM EDTA, and 20% glycerol). Resuspended pellets were homogenized in 40 ml dounces in 30 minutes by stroking 10 times then letting homogenates rest for 10 minutes and doing this a total of 3 times. Lysates were clarified by spinning at 11,000 rpm for 10 minutes and the supernatant recovered. Next, 6 ml of dilution buffer (20 mM Tris pH 7.9, 10% glycerol, and 0.02% NP40) was added to dilute the NaCl and then protein inputs taken. 0.5-1.0 ml of activated FLAG resin (Invitrogen) was washed with 5 ml of F lysis buffer, the lysate added to the resin, and rotated for 3 hours at 4°C.

Protein-bound resin was washed 3 times with 10 ml of F wash buffer (20 mM Tris pH 7.9, 150 mM NaCl, 2 mM $MgCl_2$, 0.2 mM EDTA, 15% glycerol and 0.01% NP40), then the resin transferred to a cold 1.5 ml microfuge tube. Elution was carried out with 0.3 ml of 0.2 mg/ml (single) FLAG peptide in wash buffer for 30 minutes at 4°C. Elution was repeated and fractions analyzed by silver staining and Western blot analysis using anti-M2-FLAG antibody (Sigma).

***In vitro* polymerization assays**

Purified TUTase protein was used in an *in vitro* reaction to test for poly(U)/oligo(U) activity as previously described (Kwak and Wickens, 2007). Briefly, 20 μl reactions were incubated at 30°C for 1 hour. Reactions contained 1 μCi of 32P α-UTP, an unlabelled 30 mer stemloop RNA, 20 mM Tris pH 7, 60 mM KCl, 0.2 mM EDTA, 0.5 mM DTT, 7.5 μg of BSA, 40 U RNase inhibitor (New England BioLabs), 1.1 mM $MgCl_2$, approximately 100-300 ng of purified SpCid1 (courtesty of Jae Eun Kwak and Marvin Wickens, University of Wisconsin at Madison) or purified TUTase-1, TUTase-3 (long isoform), or TUTase-7 (hCid1).

Protein Identification

Protein bands were excised from gels and subjected to automated in-gel digestion with trypsin on a Genomic Solutions ProGest digestor. After digestion, peptides were then extracted and spotted onto a MALDI target plate along with a solution of alpha-cyano 4-hydroxycinnamic acid matrix. Once dried, MS and MS/MS spectra (MS/MS fragmentation was attempted on the top 20 intensity ions in each MS spectrum, with those of trypsin excluded) were acquired in an automated fashion on an Applied Biosystems 4800 MALDI-TOF/TOF Proteomics Analyzer mass

spectrometer. The resulting peptide mass fingerprint and MS/MS sequence tag data were then searched against the MSDB and NCBI databases using the Applied Biosystems GPS Explorer software employing the Mascot search engine to obtain the protein identifications. Hits that met the Mascot significance threshold were reported.

RESULTS

Histone H2A and H3 mRNAs acquire oligo(U) tails after addition of hydroxyurea

In order to detect mRNAs containing oligouridylated tails added to the 3' end of histone mRNA, I developed a nested RT-PCR strategy, depicted in Figure 19A. First I primed reverse transcription with an oligonucleotide containing a T7 promoter sequence followed by 8 A's to make cDNAs from all RNAs containing an oligo(U) sequence. A specific primer targeting the 5' UTR of a histone gene and the T7 primer were used for the first round of PCR. The nested PCR reaction used a histone ORF primer with the same reverse T7 promoter primer. I targeted the same two H3 genes used in the cRT-PCR studies (Chapter 2) and in addition targeted an H2A mRNA (*HIST2H2AA*). I prepared total RNA at 0, 15, 30 and 60 min after initiating histone mRNA degradation by treating double thymidine blocked cells released for 3 hours with HU to inhibit DNA synthesis.

At 0 time there is no amplicon of oligouridylated histone mRNA detected from either the *HIST2H2AA* mRNA or the *HIST2H3A/C* and *HIST2H3D* mRNAs (Fig. 19B, lane 2). After 15 minutes a robust band is detected which subsequently declines in

intensity at 30 minutes and is almost entirely gone at 60 minutes coinciding with the near completion of histone mRNA degradation (Fig. 19B, lanes 3-5). I cloned the amplicons from the 0 and 15 minute time points. There was a striking difference in colony number on the transformed H2A plates, with only a few colonies present on the 0 minute plates compared to hundreds of colonies present on the 15 minute plates (Figure 19D), consistent with the increased amount of RT-PCR product after HU treatment. These results imply that my RT-PCR approach is semi-quantitative. I sequenced amplicons cloned after HU treatment and these all were derived from histone mRNAs containing oligo(U) tails at or near the 3' end of these histone mRNAs. They contained 8 U's (the number of U's in the primer) which were added either to the very terminal end (3 nts after the stemloop) of the mRNA or somewhere within the stem loop (Figure 19C). The latter observation suggests that multiple rounds of oligo(U) addition may occur near the 3' end of the mRNA, possibly because degradation may stall in the stemloop and the degradation must be primed again.

In the *HIST2H2A/C* (Fig. 19B, middle panel, lane 2) and the *HIST2H3D* (Fig. 19B, bottom panel, lanes 2 and 5) reactions, I detected a nonspecific band at the 0 time point which was absent after HU treatment for 15 or 30 min, but was present at 60 min when most of the histone mRNA has been degraded. I sequenced clones from the 0 time point of the H3 oligo(dA) RT-PCRs and found the nonspecific band was a primer dimer sequence containing the two histone primers and a small sequence of H3 ORF followed by the reverse T7 promoter primer (primer-dimer of 3 oligos). They did not contain any oligo(U) sequence.

In yeast, addition of adenosines to the 3' end of many RNAs is a prerequisite to degradation of RNAs by the exosome in the nucleus (LaCava et al., 2005; Vanacova et al., 2005). To test whether polyadenylation might also play a role in histone mRNA degradation I attempted to detect poly- or oligoadenylated histone mRNAs after inhibiting DNA replication by a similar strategy used to amplify the oligouridylated histone mRNAs. As a positive control for the oligo(dT) oligo I used SLBP knockdown cells that have been shown to result in accumulation of some polyadenylated histone mRNA as a result of misprocessing (Narita et al., 2007). I readily detected polyadenylated histone mRNAs in the SLBP knockdown cells (Figure 20A), but did not detect any oligoadenylated histone mRNAs in control cells or cells treated with HU (Figure 20B). In addition my unbiased sequencing of circularized histone mRNAs (Chapter 2) never yielded oligoadenylated mRNAs.

Oligouridylated histone mRNAs are present at the end of S-phase but not in mid S-phase

Histone mRNAs are rapidly degraded at the end of S-phase. To determine if the oligouridylation is present normally at the end of S phase I synchronized HeLa cells by double thymidine block (Whitfield et al., 2000). As a positive control I treated mid S-phase cells (3 hrs after release from the thymidine block) for 15 min with HU. I prepared whole cell lysates for Western analysis and total RNA for Northern blot analysis and oligo(dA) RT-PCR at various times beginning from the middle of S phase but focusing particular attention to the end of S phase. Figure 21A is a Western blot showing that SLBP protein levels are high in S phase and decrease rapidly upon completion of DNA synthesis and increase in abundance

again when cells approach the subsequent S phase (Figure 21A, lane 14), (Whitfield et al., 2000). I also determined cyclin A levels, a mitotic cyclin which is degraded at anaphase as cells exit mitosis. Northern blot analysis was performed for H2A mRNA using 7SK snRNA as a loading control (Figure 21B). Histone H2A mRNA is rapidly degraded upon the completion of S phase then re-accumulates upon entry into the subsequent S phase (Figure 21B, lane 15). Figure 21C shows the results from oligo(dA) RT-PCR at various times in S phase and upon the completion of DNA sythesis. At 0 and 3 hours following release from double thymidine block (DTB) there was little to no detection of olidouridylated *HIST2H2AA* or *HIST2H3D* mRNA (Figure 21C, lanes 1 and 2). When HU is added for 15 minutes at 3 hrs oligouridylated *HIST2H2AA* and *HIST2H3D* mRNA accumulated (Figure 21C, lane 3). Starting 5 hrs after release into S-phase I detected oligouridylated histone mRNA (Figure 21C, lane 4) and the amount increased at 5.5-6 hrs for both *HIST2H2AA* mRNA (Figure 21C, lane 5) and *HIST2H3D* mRNA (Figure 21C, lane 6). The levels of oligouridylated histone mRNAs declined at 6.5 hours and were no longer detectable at 7 hours during G2 phase. I sequenced oligouridylated RT-PCR products for both *HIST2H2AA* and *HIST2H3D* from the 5.5 and 6 hour time points. Consistent with the results after HU treatment (Figure 19B, 19C), I found oligouridylated tails present at the end of S phase on both the 3' end of the histone mRNA as well as within the stemloop sequence (Figure 21D). Note that the oligo(U) tails were often interrupted by another nucleotide, which has recently been determined to be characteristic of other terminal transferases (Kwak and Wickens, 2007).

Two putative cytoplasmic TUTases are required for efficient histone mRNA degradation

The addition of nontemplated uridines to the 3' end of histone mRNA requires a 3' terminal transferase activity. I searched the human genome with the assistance of Hemant Kelkar (University of North Carolina at Chapel Hill) for putative TUTase enzymes that contain the PAPD/TRF domain, a domain found in the human CID1 (Rissland et al., 2007) and U6 snRNA TUTase (Trippe et al., 2006). We identified 7 putative TUTases (one of them being the U6 TUTase) and I designed siRNAs targeting each one and knocked them down in HeLa cells. To demonstrate the efficiency of the siRNAs at the mRNA level I determined whether the siRNAs reduced the endogenous TUTase mRNA levels by RT-PCR. I assessed the knockdown at the RNA level using 7SK snRNA as a loading control (Figure 22A). In addtion, I assessed the degree of knockdown at the protein level by coexpressing myc-tagged TUTases and found that the siRNAs efficiently depleted the exogenously expressed TUTase-1, -3, and -5 (Figure 22B) by Western blotting. Knocking down the U6 TUTase was lethal as previously reported (Trippe et al., 2006). Of the remaining six TUTases, knocking down two (TUTase-1 and TUTase-3) reduced the rate of histone mRNA degradation after HU treatment (Figure 23A and 23B). Knocking down the other four enzymes, TUTases 2, 4, 5 and 7 (Figure 23A and 23B) had no effect on histone mRNA degradation.

Since histone mRNAs are degraded in the cytoplasm, I determined the subcellular localization of the TUTases-1 and -3 by transiently transfecting HeLa cells with various doses of myc-tagged plasmids encoding these proteins followed

by confocal immunofluorescence. TUTase-1 is exclusively cytoplasmic, while TUTase-3 is predominantly cytoplasmic but is also present in the nucleus in some cells (Figure 24). The localization is consistent with a role for these enzymes in histone mRNA degradation.

Note that the TRAMP complex that adds adenosines to nuclear RNAs to prime their degradation are in this same family of enzymes (Rissland et al., 2007; Vanacova et al., 2005). I could not definitively determine which of the human family members correspond to the Trf4/5 enzyme. However, since Trf4/Trf5 strictly nuclear, it is very unlikely that TUTase-1 or TUTase-3 are responsible for this activity. A more comprehensive evaluation of the evolution of eukaryotic TUTases is included in Chapter 5.

Preliminary biochemical characterization of TUTase-3 expressed in human 293T cells

I chose to focus on the initial biochemical characterization of TUTase-3 for reasons mentioned in the Discussion section. Baculoviral expression in Sf9 cells of histidine-tagged versions of a number of different TUTases was repeatedly unsuccessful and I could never observed detectable amounts of viral production or protein expression. For this reason I attempted to purify FLAG-tagged versions from human cells. Exogenously expressed FLAG-tagged TUTase-3 was purified from 293T cells and the eluted fractions analyzed by Western blot and silver staining (Figure 25A and 25B). A FLAG-tagged version of TUTase-7 was purified as a control. The Western blot analysis shown in Figure 25A demonstrates that I could purify detectible amounts of both TUTase-3 and TUTase-7.

In order to determine the quality of the purification I ran a duplicate gel and protein bands visualized by silver stain (Figure 25B). A number of protein bands were observed and another duplicate gel ran and sent to the UNC Michael Hooker-Duke Proteomics Facility for protein identification (see Materials and Methods). The results from these experiments confirmed the identity of both TUTase-3 and TUTase-7 and identified some common copurifying contaminants (Hsp70 and two different forms of tubulin). The TUTase-3 purification identified two potentially significant copurifying proteins: protein arginine methyltransferase-5 (PRMT-5) and methylosome protein variant 50.

Next, I wanted to determine if TUTase-3 had any detectible oligo(U)/poly(U) activity *in vitro*. I performed an *in vitro* polyuridylation assay (Kwak and Wickens, 2007) using the two protein fractions from TUTase-3 at increasing concentrations. A schematic of this assay is outlined in Figure 25C. I used a recombinantly purified version of *S. pombe* Cid1 expressed in *E. coli* as a positive control and the incubation in the absence of protein served as a negative control. Figure 25C, lane 2 clearly demonstrates the ability of SpCid1 to efficiently and nonspecifically extend a histone 3' end RNA substrate. The TUTase-3 fraction did not exhibit nearly as robust extension as the positive control, however upon increasing concentrations TUTase-3-dependent UTP incorporation is clearly present (Figure 25D, compare lanes 3 and 4, compare lanes 5, 6 and 7). These data supply preliminary evidence supporting the ability of TUTase-3 to add uridine residues *in vitro* to the 3' end of a histone RNA substrate.

DISCUSSION

Histone mRNAs are degraded by both the 5'-3' decay machinery and the cytoplasmic exosome. In this chapter I have presented data that corroborate the evidence provided by the cRT-PCR experiments (Chapter 2), that histone mRNAs acquire oligo(U) tails when histone mRNAs are degraded. The acquisition of the oligo(U) tails occurs both when DNA synthesis is inhibited as well as when cells are normally exiting S phase of the cell cycle.

Model of histone mRNA degradation

Histone mRNA degradation in the cytoplasm is triggered by inhibition of DNA replication in the nucleus and when cells complete DNA replicaton. Previous work together with these results, allow me to propose an updated model for histone mRNA degradation (Figure 26). The stemloop is the *cis* element responsible for histone mRNA degradation. It must be located an appropriate distance from the termination codon and requires ongoing translation (Graves et al., 1987; Kaygun and Marzluff, 2005b). The lab has postulated that inefficient translation termination is the critical event for triggering histone mRNA degradation (Kaygun and Marzluff, 2005b), as is the case for NMD in yeast (Amrani et al., 2004). Histone mRNA degradation requires Upf1 which interacts with SLBP at the 3' end of histone mRNA after treatment with HU (Kaygun and Marzluff, 2005a). I postulate that the recruitment of Upf1 results in the recruitment of the appropriate TUTase and oligouridylation of histone mRNA. Lsm1-7 then binds to the oligo(U) tail (and may be specifically recruited by the complex at the 3' end of the mRNA). Recent studies by Kiledjian and coworkers have shown that Lsm1-7 is the major complex that binds to oligo(U)

in HeLa cell lysates (Song and Kiledjian, 2007), consistent with the proposed role of Lsm1-7 in histone mRNA degradation.

Following oligouridylation it is likely that SLBP is still bound to the histone mRNA, since SLBP and Lsm1 coimmunoprecipitate from HU treated cells, although the association is sensitive to RNase consistent with the Lsm1 being bound to the oligo(U) tail rather than to SLBP. Once Lsm1-7 is bound, then the decapping complex can be recruited and histone mRNA is decapped and degradation initiated from the 5' end. Alternatively the exosome may be recruited and the mRNA degraded from the 3' end. My data strongly suggests that both of these events occur on most mRNAs, resulting in simultaneous degradation of the same molecule 5' to 3' and 3' to 5'. I cloned decay intermediates of single molecules by cRT-PCR, and obtained histone RNAs that had both their 5' and 3' ends shortened, demonstrating that individual molecules of histone mRNA are degraded from both the 5' end and the 3' end (Chapter 2).

Initially 3' to 5' degradation may be relatively inefficient (possibly because of the presence of SLBP bound to the stemloop), and I detect intermediates in which degradation has proceeded into the stem, and then the RNA is oligouridylated at that site. These molecules likely arise from stalling (and dissociation) of the exosome, requiring oligouridylation to reinitiate degradation 3' to 5'.

Candidate TUTases for histone mRNA degradation

There are a group of genes initially thought to encode poly(A) polymerases that were clearly distinct from the canonical poly(A) polymerase that adds poly(A) tails to mRNAs. These enzymes, such as Cid1 in *S. pombe*, were thought to be

poly(A) polymerases because they had some homology to the metazoan Gld2 enzymes, which are responsible for cytoplasmic polyadenylation of mRNA in metazoan oocytes (Kwak et al., 2004; Stevenson and Norbury, 2006). It is now clear that at least some of these enzymes are also uridylyl transferases (Kwak and Wickens, 2007). *S. cerevisiae* lacks any proteins that are similar to Cid1, and has two family members, Trf4 and Trf5 which are clearly nuclear while many of the Cid1-related proteins are cytoplasmic (Stevenson and Norbury, 2006).

Hemant Kelkar and I identified 7 human genes that encode putative terminal uridylyl transferases (TUTases) based on their homology to the U6 terminal transferase and the *S. pombe* Cid1 enzyme, and the same enzymes were very recently identified by Kwak and Wickens (2007). Knocking down 2 of these enzymes, TUTase-1 and TUTase-3, but not the other five (including TUTase-7, the Cid1 homolog), resulted in a reduced rate of histone mRNA degradation (Figure 23). These two enzymes are cytoplasmic, and I postulate that one or both of them may be required for the oligouridylation that initiates histone mRNA degradation. It is possible that one enzyme is responsible for the initial terminal addition and the other is required for the addition to the partially degraded stem, which may be necessary to effectively complete histone mRNA degradation.

Benecke and coworkers recently isolated the enzyme that adds oligo(U) tails to U6 snRNA, an essential reaction in the maturation of U6 snRNA (Trippe et al., 2006). TUTase-1 has been previously implicated as the mitochondrial poly(A) polymerase (Nagaike et al., 2005). However, Norbury and coworkers have shown that *S. pombe* Cid1 can add either uridine or adenosine to RNA *in vitro* and that the

specificity is likely conferred by proteins associated with the TUTase, since Cid1 complexes immunoprecipitated from cells exclusively add uridine *in vitro* (Rissland et al., 2007). Thus it is possible that TUTase-1 has multiple functions in the cell. It is also possible our identification of TUTase-1 was a false positive. For this reason, my initial biochemical characterization began with TUTase-3.

The potential interaction of TUTase-3 with PRMT5 and the methylosome requires additional functional studies. This possibility is interesting since PRMT5 and other methyltransferases have been implicated in the maturation of Sm class RNPs (Gonsalvez et al., 2007) including the histone-specific U7 snRNP (Azzouz et al., 2005b). The initial *in vitro* uridylation activity exhibited by TUTase-3 is suggestive of its activity *in vivo*. However, higher quantities of purified protein must be achieved in order to appropriately perform the experiment. This is complicated by the fact that the C-terminal region of all the TUTases is highly unstructured and likely underlies the difficulty to achieve satisfactory recombinant expression in both *E. coli* and insect cells. Additional future work into this technical problem will contribute significantly to understanding the biochemisty of these enzymes.

Is oligouridylation important for other mRNA degradation pathways?

While addition of oligo(U) to a specific subset of mRNAs to initiate RNA degradation has not been previously reported in eukaryotic cells, there are examples of a potential role for oligouridylation in degradation of mRNAs following siRNA cleavage, and of terminal addition of nucleotides to prime degradation of RNAs in both the eukaryotic nucleus and in prokaryotes. Shen and Goodman reported that following miRNA cleavage of mRNAs in plants, mouse and Epstein-Barr virus, they

could detect oligouridylated mRNA fragments corresponding to the 5' cleavage products (Shen and Goodman, 2004). They suggested these were intermediates in the degradation of the 5' mRNA fragments produced by miRNA cleavage. In the alga *Chlamydomonas reinhardtii*, Ibrahim and colleagues suggested the MUT68 protein, a poly(A) polymerase (CID12 ortholog in *S. pombe*) was responsible for oligoadenylation of RISC-induced cleavage products (Ibrahim et al., 2006) prior to cleavage. There is extensive evidence that degradation of improperly processed tRNAs and rRNAs are degraded in the nucleus by addition of oligo(A) by the Trf4/Trf5 complex followed by recruitment of the exosome (LaCava et al., 2005; Vanacova et al., 2005).

Bacterial mRNA degradation is initiated by addition of oligo(A) to the 3' end of the mRNAs by a poly(A) polymerase which is homologous to Trf5. This oligo(A) tail can then bind the Hfq protein, a homologue of the eukaryotic Sm proteins (Valentin-Hansen et al., 2004), and recruit the degradosome, a bacterial homologue of the exosome (Blum et al., 1999). In bacterial mRNA degradation, there is addition of oligonucleotides to the 3' end of the RNA whenever the degradosome pauses or is blocked by secondary structure of the mRNA. In bacteria this addition is catalyzed by polynucleotide phosphorylase (PNPase), which adds nucleotides non-specifically (although A's predominate since ATP is the most abundant nucleotide) (Mohanty and Kushner, 2000). It is thought that the single-stranded tail then serves as a platform for the degradosome to reinitiate degradation of the mRNA, and that cycles of nucleotide addition followed by exonucleolytic degradation are characteristic of bacterial mRNA degradation (Kushner, 2004). Note that I also isolated mRNAs

which had oligo(U) tails added to mRNAs that had part of the stem sequence removed. It is possible that these result from partial degradation of histone mRNA, followed by stalling of the exosome, and then addition of oligo(U) to the degradation intermediate, allowing completion of mRNA degradation in a manner similar to that found in degradation of bacterial mRNAs.

Summary

The evidence I have presented in this chapter points to oligouridylation as an initiating event in histone mRNA degradation. However, it remains unknown how the TUTase(s) are specifically recruited to the 3' end of histone mRNA. Nonetheless, it is an exciting time in RNA biology with the challenges that await the field to further our understanding of how terminal uridylyl transferase activity in the cytoplasm functions to regulate gene expression.

Table 3. Oligonucleotides used in oligo(dA) RT-PCR detection of oligouridylated histone H2A and H3 mRNA.

Oligo name	Specific Gene Target	Application	Sequence (5' – 3')
H2a/a 5'	*HIST2H2AA* (5' UTR)	Oligo (dA) RT-PCR (1^{st})	GACTACTATCGCTGTCATGTCTG
H3/2a/2c 5'	*HIST2H3A* (5' UTR) *HIST2H3C* (5' UTR)	Oligo (dA) RT-PCR (1^{st})	GGTAAGCCCTGTGTTTTGGTTCGC
H3/2d 5'	*HIST2H3D* (5' UTR)	Oligo (dA) RT-PCR (1^{st})	GAGACAGCATGGCCCGTACTAAG
H2a/a O-1	*HIST2H2AA* (C-term of ORF)	Oligo (dA) RT-PCR (2^{nd})	GAACTGAACAAGCCTGCTGGGCAAG
H2a/a O-2	*HIST2H2AA* (C-term of ORF	Oligo (dA) RT-PCR (2^{nd})	CCTGCAGCTAGCGATCCG
T7 oligo(dA)	N/A	Oligo (dA) RT	GTAATACGACTCACTATAGGGAAAAAAAA
T7 oligo(dT)	N/A	Oligo (dT) RT	GTAATACGACTCACTATAGGGTTTTTTTTT
T7 reverse	N/A	Oligo (dA) RT-PCR (1^{st} & 2^{nd})	GTAATACGACTCACTATAGGG

Table 4. siRNA sequences used to knock down TUTases. The table below details the sequences targeting the open reading frames of the indicated target TUTase mRNA. All siRNAs were synthesized from Dharmacon with d(T)d(T) ends.

Target	Sequence	Reference
C2	5’-GGUCCGGCUCCCCCAAAUG-3’	(Wagner and Garcia-Blanco, 2002)
TUTase-1	5’-CGAGCACAUUCACUAACAA-3’	This paper
TUTase-2	5’-CGUUAGUGCUGGUGAUUAA-3’	This paper
TUTase-3	5’-GGACGACACUUCAAUUAUU-3’	This paper
TUTase-4	5’-UGAUAGUGCUUCAGGAAUU-3’	This paper
TUTase-5	5’-CUACGGUACCAAUAAUAAA-3’	This paper
U6 TUTase	5’-GCAGCCAAUUACUGCCGAA-3’	(Trippe et al., 2006)
TUTase-7	5’-GAAAAGAGGCACAAGAAAA-3	This paper

Table 5. Oligonucleotides for RT-PCR of endogenous TUTase mRNA. Sense and antisense primers are indicated.

Target	Oligo sequence
TUTase-1	sense: 5’-GAAGATCCTGTCTGTGTTAGGAG-3’, antisense: 5’-GGAAGGTCGATCTGTATCTTCC-3’
TUTase-2	sense: 5’-GCAGACTTGTCTAGAGCTGTG-3’, antisense: 5’-CTCGAATCAGCTGAGGTCTCTC-3’
TUTase-3	sense: 5’-GAGTAACAGATGAAGTTGCCAC-3’), antisense: 5’-GTTTGAGTTGTACCTTGGAAGC-3’
TUTase-4	sense: 5’-GGCAACCAGTTTACAGGCAATAGC-3’ antisense: 5’-CGTCCGATACGTCTTCAATTCC-3’
TUTase-5	sense: 5’-GGTCCTATCCAAACAGAGACG-3’ antisense: 5’-GTTCCTTCTACACCAGCTTGTC-3’
TUTase-7	sense: 5’-GGTTATAGGTGGCAAGACACAAG-3’ antisense: 5’-CAGCCTCTGTTCCAAGTTCTC-3’

Figure 19. Detection of oligouridylated histone mRNAs after inhibition of DNA synthesis. (A) RT-PCR strategy to detect oligo(U)-containing histone mRNA molecules. Total RNA from HeLa cells was primed for cDNA synthesis using an oligo(dA) primer fused to a T7 sequence. Two rounds of PCR (30 cycles each) were performed using oligos targeting the 5' UTR (1^{st} round) or the ORF (2^{nd} round) and a primer complementary to the T7 sequence. (B) Oligo(dA) RT-PCR from *HIST2H2AA*, *HIST2H3A/C* and *HIST2H3D* treated with HU for 0, 15, 30 and 60 minutes. The products were resolved by agarose gel electrophoresis and detected by ethidium bromide staining. * indicates a non-specific band. (C) Sequences from cloned oligo(dA) RT-PCR reactions from the *HIST2H3D* mRNA when treated with HU for 15 minutes. The number in parentheses at the 3' end of each sequence represents the number of clones observed. (D) *HIST2H2AA* clones from nested oligo(dA) RT-PCR reactions. 2 μl of PCR product (0 minutes HU, 15 minutes HU) from the second round of PCR (+Taq) were TA cloned, transformed and plated onto kanamycin-containing LB agar plates.

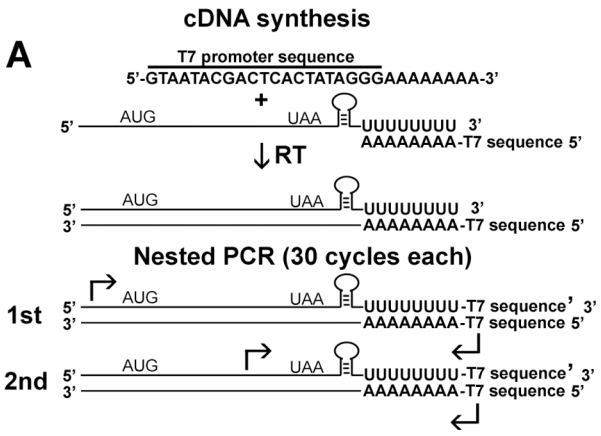

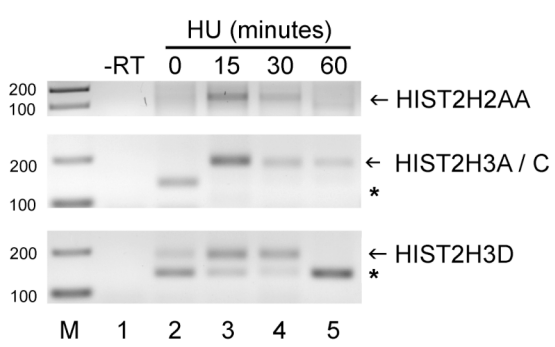

C

stem-loop

```
AAAGGCTCTTTTCAGAGCCACTTTTTTTT  (3)
AAAGGCTCTTTTCAGATTTTTTTT       (1)
AAAGGCTCTTTTCAGTTTTTTTT        (2)
AAAGGCTCTTTTCAGTTTATTTTTTTT    (2)
AAAGGCTCTTTTTTTT               (1)
```

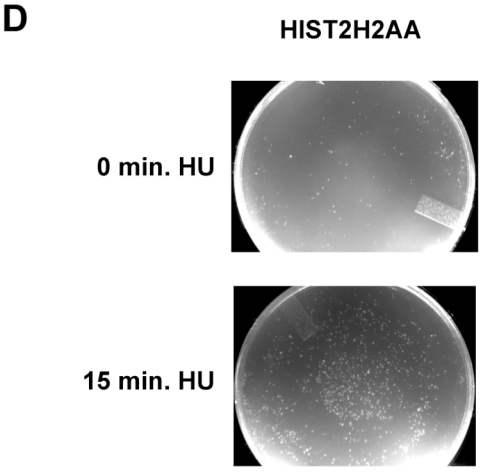

Figure 20. Oligo(dT) RT-PCR controls. (A) Positive control for oligo(dT) RT-PCR. Knockdown of SLBP results in polyadenylated *HIST2H2AA* mRNA due to misprocessing of the pre-mRNA. Total RNA was subjected to oligo(dT) cellulose selection and 500 ng of the elution was random primed for reverse transcription. 2 μl of RT reaction was used for PCR similarly as in Figure 19. (B) Oligo(dT) control for *HIST2H2AA* mRNA from cells treated with hydroxyurea. Total RNA from the experiments performed in Figure 19 were random primed and subjected to MMLV reverse transcriptase. PCR was performed identically to that in Figure 19 to detect *HIST2H2AA* mRNA. The 110 bp product is too small to be *HIST2H2AA* mRNA and does not change in response to HU treatment.

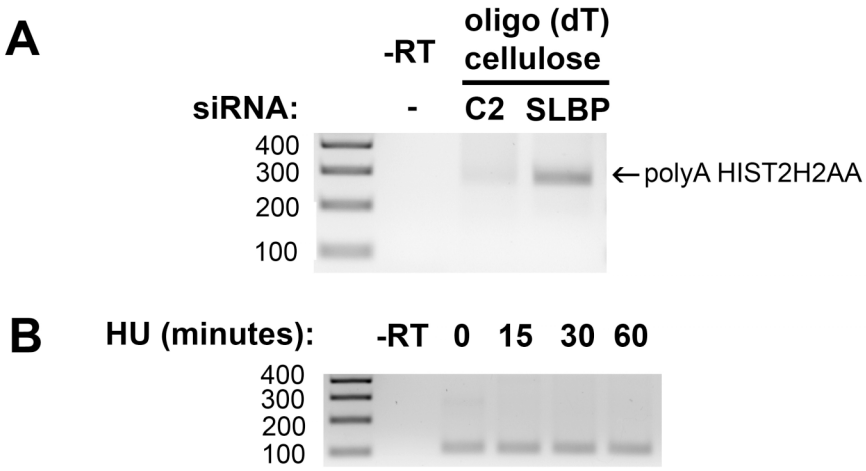
A
-RT
oligo (dT) cellulose
siRNA:
-
C2
SLBP
400
300
200
100
← polyA HIST2H2AA
B
HU (minutes):
-RT
0
15
30
60
400
300
200
100

Figure 21. Detection of oligouridylated histone mRNAs at the end of S phase. (A) HeLa cells were synchronized by double thymidine block (DTB) and released into S phase and protein samples collected at the indicated times. Western blot analysis of SLBP and cyclin A was performed. (B) Total RNA was isolated from the same cells as in (A) and H2a mRNA and 7SK RNA levels measured by Northern blotting. (C) Oligo(dA) RT-PCR on total RNA from the middle and end of S phase into G2 phase of the cell cycle. Total RNA from the indicated time points following release from DTB was subjected to the RT-PCR strategy depicted in (Figure 19A) to detect *HIST2H2AA* and *HIST2H3D* mRNA and resolved on a 2.0% agarose gel. HU was added at 3 hours for 15 minutes in lane 3 as a positive control for the oligo(dA) RT-PCR. (D) The oligo(dA) primed RT-PCR products from the 5.5 and 6.0 hour time points were cloned and a number of clones from the *HIST2H2AA* and *HIST2H3D* mRNAs were cloned and sequenced.

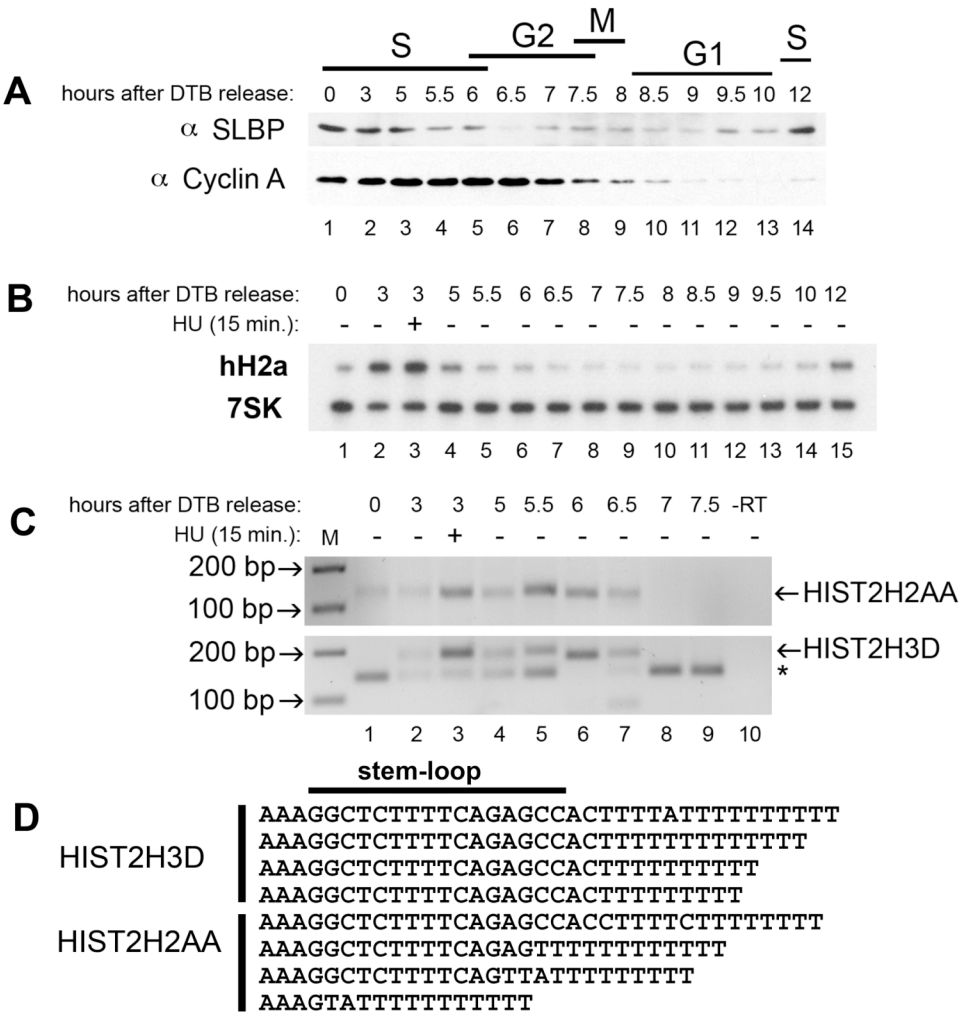
A
S
G2
M
G1
S
hours after DTB release: 0 3 5 5.5 6 6.5 7 7.5 8 8.5 9 9.5 10 12
α SLBP
α Cyclin A
1 2 3 4 5 6 7 8 9 10 11 12 13 14
B
hours after DTB release: 0 3 3 5 5.5 6 6.5 7 7.5 8 8.5 9 9.5 10 12
HU (15 min.): - - + - - - - - - - - - - - -
hH2a
7SK
1 2 3 4 5 6 7 8 9 10 11 12 13 14 15
C
hours after DTB release: 0 3 3 5 5.5 6 6.5 7 7.5 -RT
HU (15 min.): M - - + - - - - - - -
200 bp→
100 bp→
←HIST2H2AA
200 bp→
100 bp→
←HIST2H3D
*
1 2 3 4 5 6 7 8 9 10
stem-loop
D
HIST2H3D
AAAGGCTCTTTTCAGAGCCACTTTTATTTTTTTTTT
AAAGGCTCTTTTCAGAGCCACTTTTTTTTTTTTT
AAAGGCTCTTTTCAGAGCCACTTTTTTTTTT
AAAGGCTCTTTTCAGAGCCACTTTTTTTTT
HIST2H2AA
AAAGGCTCTTTTCAGAGCCACCTTTTCTTTTTTTT
AAAGGCTCTTTTCAGAGTTTTTTTTTTTT
AAAGGCTCTTTTCAGTTATTTTTTTTT
AAAGTATTTTTTTTTTT

Figure 22. RNAi to 6 of 7 putative TUTases present in the human genome is effective both at the mRNA and protein level. (A) The 7 TUTases were knocked down using specific siRNAs as in the experiments described in Chapter 2. Endogenous TUTase mRNA levels were measured by RT-PCR. 2 μg of total RNA was random primed and subjected to MMLV reverse transcriptase followed by PCR. The degree of knockdown, relative to 7SK RNA as a control, estimated by ImageQuant software is indicated. (B) A representative experiment to determine the efficacy of TUTase-1, -3, and -5 siRNAs to knock down an exogenously expressed version of each TUTase. Myc epitope-tagged TUTases were cloned and transfected at the time of the second hit of siRNA (Materials and Methods). Protein lysates were harvested 48 hours following the second hit and probed by Western using an anti-myc antibody. Upf1 was used as a loading control. Note: The missing TUTase is the U6 snRNA TUTase. As previously reported, treatment of cells with siRNA to U6 TUTase is lethal to human cells (Trippe et al., 2006).

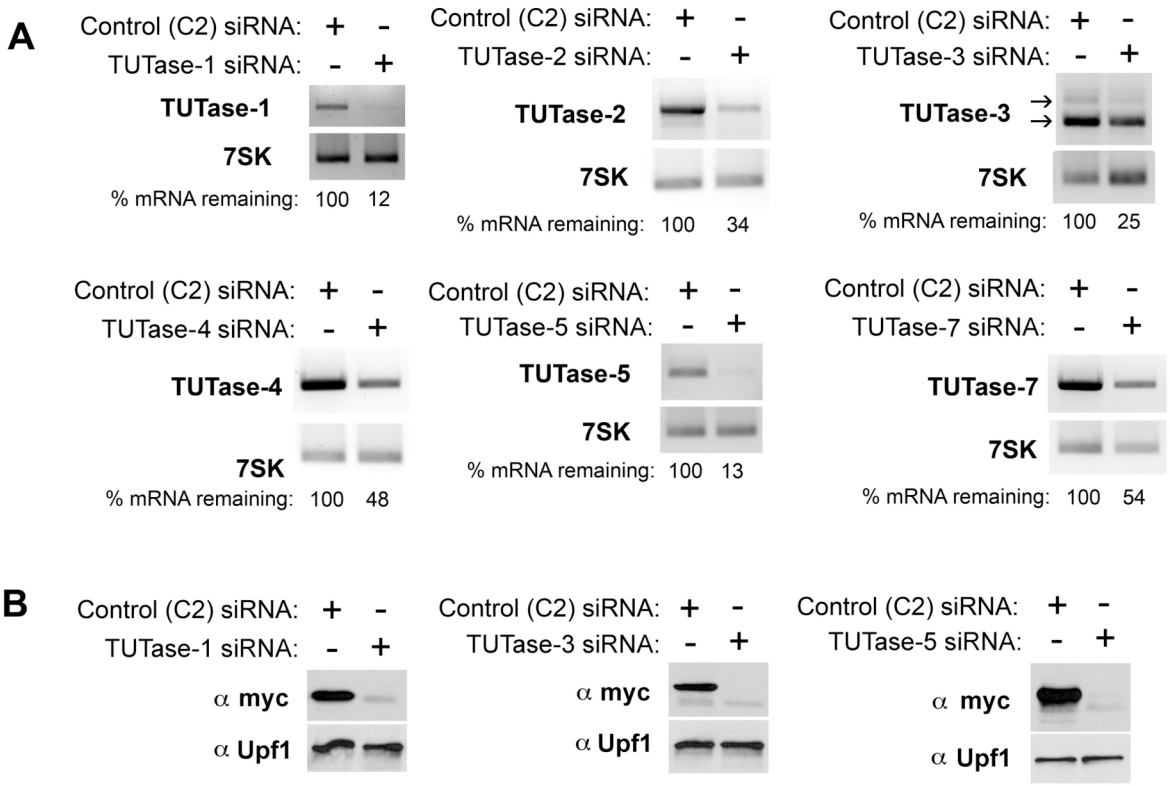
A
Control (C2) siRNA: + -
TUTase-1 siRNA: - +
TUTase-1
7SK
% mRNA remaining: 100 12
Control (C2) siRNA: + -
TUTase-2 siRNA: - +
TUTase-2
7SK
% mRNA remaining: 100 34
Control (C2) siRNA: + -
TUTase-3 siRNA: - +
TUTase-3
7SK
% mRNA remaining: 100 25
Control (C2) siRNA: + -
TUTase-4 siRNA: - +
TUTase-4
7SK
% mRNA remaining: 100 48
Control (C2) siRNA: + -
TUTase-5 siRNA: - +
TUTase-5
7SK
% mRNA remaining: 100 13
Control (C2) siRNA: + -
TUTase-7 siRNA: - +
TUTase-7
7SK
% mRNA remaining: 100 54
B
Control (C2) siRNA: + -
TUTase-1 siRNA: - +
α myc
α Upf1
Control (C2) siRNA: + -
TUTase-3 siRNA: - +
α myc
α Upf1
Control (C2) siRNA: + -
TUTase-5 siRNA: - +
α myc
α Upf1

Figure 23. RNAi screen to seven TUTases present in the human genome identifies two putative TUTase involved in histone mRNA degradation. (A) Knockdown of TUTases-1 and -3 stabilizes histone H2a degradation following inhibition of DNA synthesis by HU. A representative experiment demonstrating the effect on histone mRNA degradation when TUTase-1 and TUTase-3 are knocked down. 2 μg of total cell RNA from cells treated with 5 mM HU was resolved by urea acrylamide gel electrophoresis and analyzed with a mixture of histone H2a mRNA and 7SK snRNA probes. The Western blot in Figure 22B demonstrating the efficacy of the siRNAs at the protein level is paired with this experiment. (B) The rate of degradation of histone mRNA in 3 independent experiments where the different TUTases were knocked down. Lsm1 was included as a positive control. Standard deviations are represented by vertical bars. The U6 TUTase is essential for cell viability and the effect on histone mRNA degradation could not be determined (see text for details).

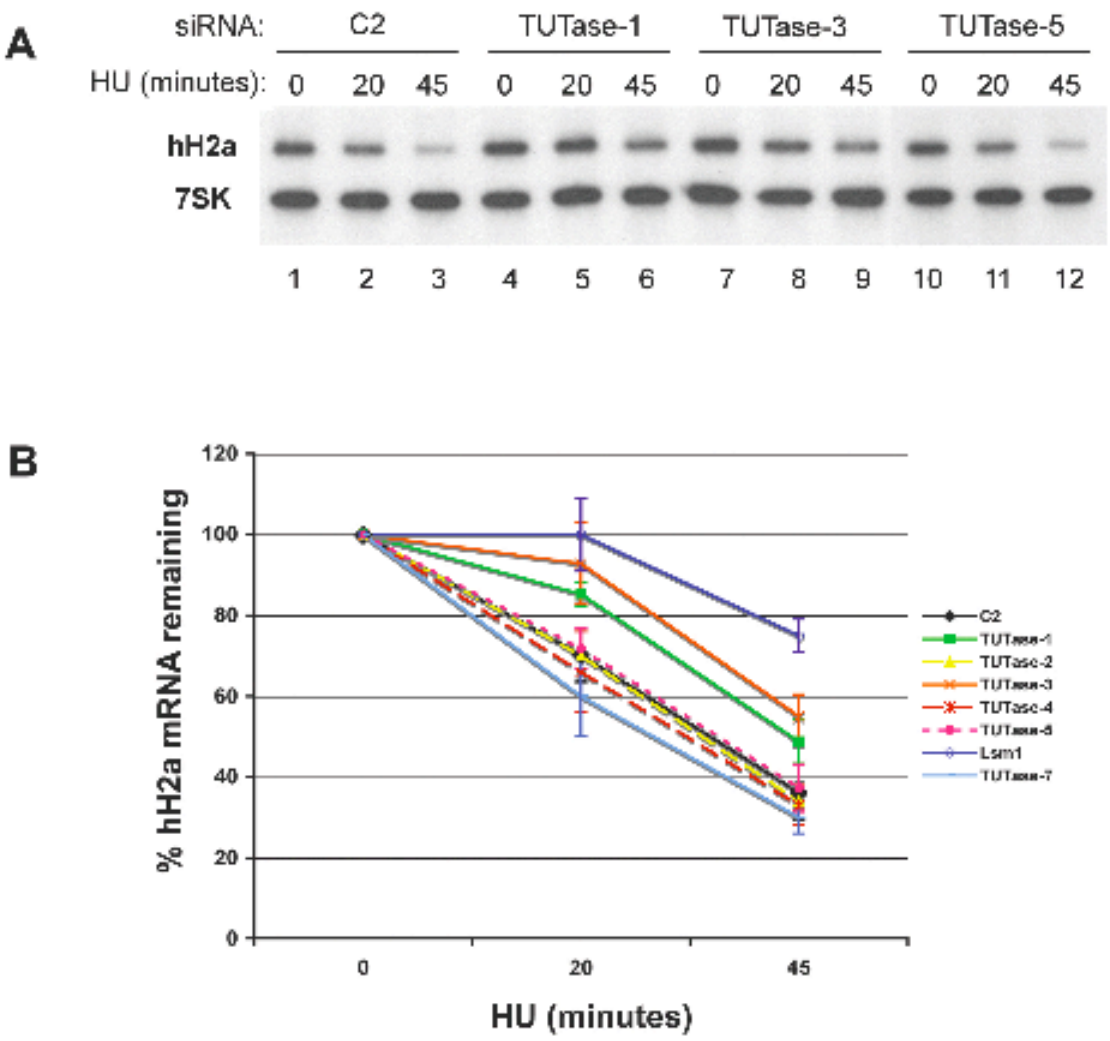
A
siRNA:
C2
TUTase-1
TUTase-3
TUTase-5
HU (minutes):
0 20 45 0 20 45 0 20 45 0 20 45
hH2a
7SK
1 2 3 4 5 6 7 8 9 10 11 12
B
% hH2a mRNA remaining
120
100
80
60
40
20
0
0
20
45
HU (minutes)
C2
TUTase-1
TUTase-2
TUTase-3
TUTase-4
TUTase-5
Lsm1
TUTase-7

Figure 24. TUTase-1 and TUTase-3 are predominantly localized to the cytoplasm of HeLa cells. TUTase-1 and -3 are localized predominantly in the cytoplasm of HeLa cells. Cells were transfected with myc-tagged clones of TUTase-1 or TUTase-3 and the tagged proteins detected by immunofluorescence (red) 48 hours following transfection using an anti-myc antibody.

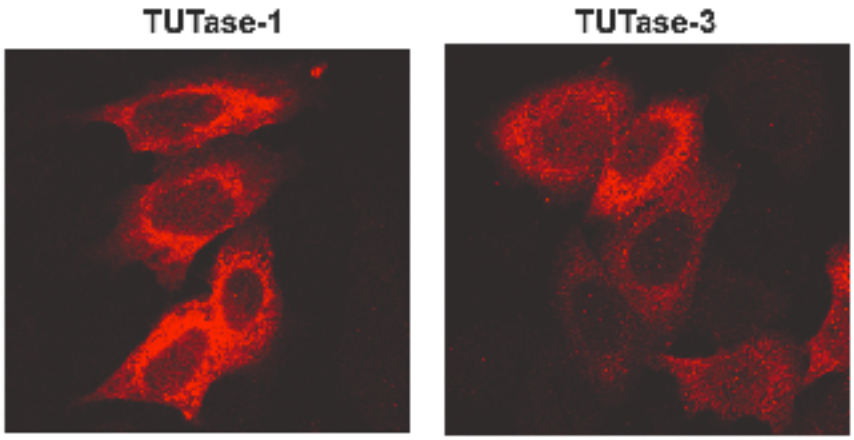
TUTase-1
TUTase-3

Figure 25. Biochemical characterization of TUTase-3. (A) FLAG-tagged versions of TUTase-3 and TUTase-7 were batch purified from 293T cells. Indicated percentages of total protein lysate are indicated. 8% of the total elution volume is present in lanes 5-8. 12% SDS-polyacrylamide gels were run, transferred, and the membrane probed for FLAG-tagged TUTases using an anti-M2-FLAG monoclonal antibody. (B) Silver stain of fraction 2 from (A) and protein identification carried out by mass spectrometry (see Materials and Methods). (C) Schematic of *in vitro* oligo/polyuridylation assay to assess TUTase-3 activity. (D) TUTase-3 shows oligouridylation activity *in vitro*. Increasing concentrations of TUTase-3 protein fractions from (A) were used in the *in vitro* assay (lanes 3-7). Lane 1 has no protein added and lane 2 contains 200 ng of recombinantly expressed *S. pombe* Cid1 as a positive control. The arrow indicates increasing incorporation of UTP with increasing concentrations of TUTase-3.

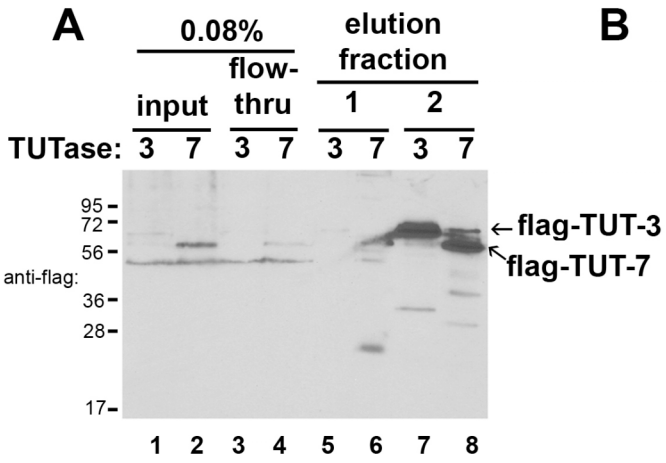
A
0.08%
elution fraction
input
flow-thru
1
2
TUTase: 3 7 3 7 3 7 3 7
95
72
56
anti-flag:
36
28
17
1 2 3 4 5 6 7 8
flag-TUT-3
flag-TUT-7

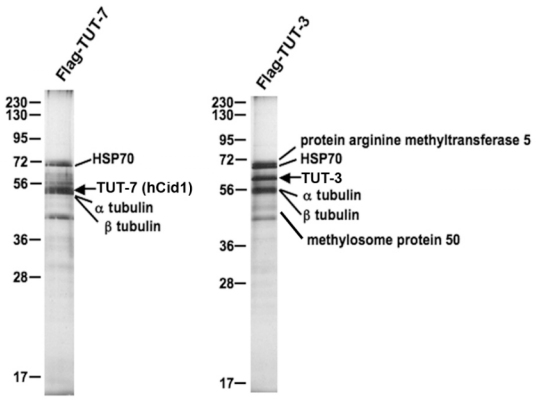
B
Flag-TUT-7
230
130
95
72
56
36
28
17
HSP70
TUT-7 (hCid1)
α tubulin
β tubulin
Flag-TUT-3
protein arginine methyltransferase 5
HSP70
TUT-3
α tubulin
β tubulin
methylosome protein 50

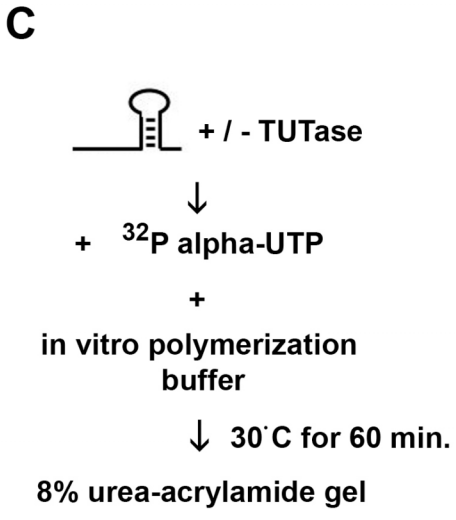
C
+ / - TUTase
+ 32P alpha-UTP
+
in vitro polymerization buffer
30˚C for 60 min.
8% urea-acrylamide gel

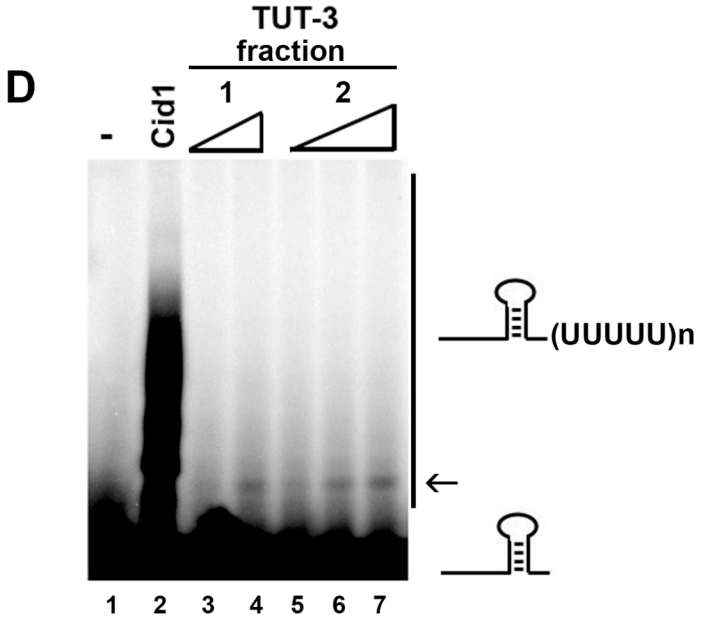
D
TUT-3 fraction
-
Cid1
1
2
(UUUUU)n
1 2 3 4 5 6 7

Figure 26. Current model of histone mRNA degradation.

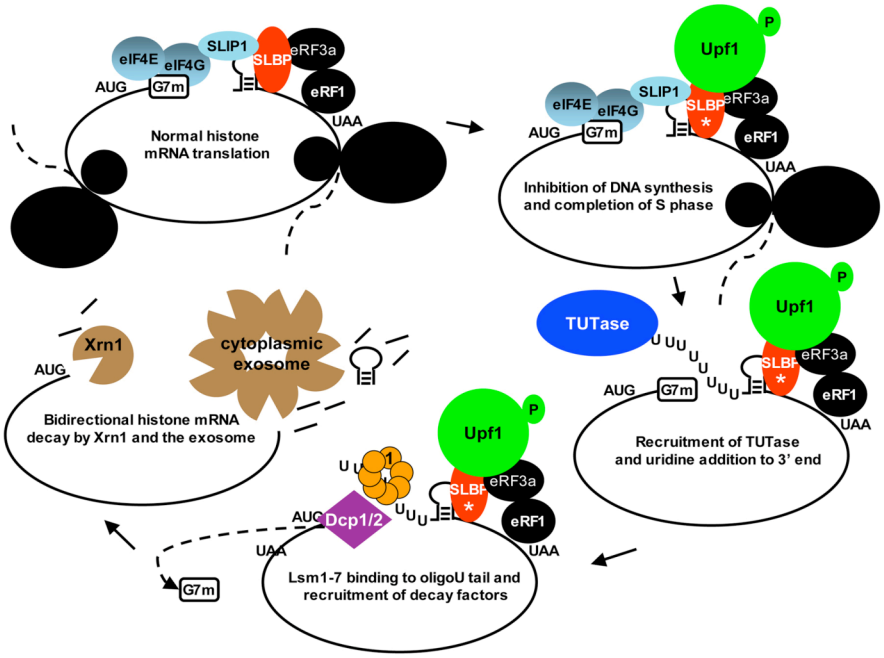
eIF4E
eIF4G
SLIP1
SLBP
eRF3a
eRF1
AUG
G7m
UAA
Normal histone mRNA translation
Upf1
P
Inhibition of DNA synthesis and completion of S phase
TUTase
Recruitment of TUTase and uridine addition to 3' end
Xrn1
cytoplasmic exosome
Bidirectional histone mRNA decay by Xrn1 and the exosome
Dcp1/2
Lsm1-7 binding to oligoU tail and recruitment of decay factors

CHAPTER 4

EXPRESSION OF STEMLOOP BINDING PROTEIN (SLBP) IS CRITICAL FOR PROPER METABOLISM OF HISTONE mRNA, INCLUDING PROPER HISTONE mRNA TURNOVER

INTRODUCTION

The replication-dependent histone mRNAs are the only eukaryotic cellular mRNAs that are not polyadenylated, ending instead in a conserved stemloop (Marzluff, 2005). These mRNAs lack any introns and undergo a single processing reaction cleaving the nascent pre-mRNA from the DNA template. The cleavage reaction requires the stemloop (SL) 5' of the cleavage site and a purine-rich region, the histone downstream element (HDE) located about 10 nts 3' of the cleavage site (Marzluff and Duronio, 2002). The HDE basepairs to a small nuclear RNA termed the U7snRNA, which is a component of the ribonucleoparticle the U7snRNP (Mowry et al., 1989; Mowry and Steitz, 1987). The stem loop binding protein (SLBP) binds to the SL and helps stabilize the interaction of U7 snRNP with the pre-mRNA. Several lines of evidence support this model. First, pulldown of biotinylated histone pre-mRNA from nuclear extracts results in the concomitant pulldown of the U7snRNA (Dominski et al., 1995). The U7snRNA fails to come down with histone pre-mRNA if SLBP is immunodepleted from the extract. Second, *in vitro* processing

of histone pre-mRNA is absolutely dependent on SLBP if the HDE is weakened in its capacity to basepair to U7 snRNA (Dominski et al., 1999). If the HDE can basepair strongly with the U7snRNA, the need of SLBP for the cleavage reaction is abrogated resulting in SLBP-independent processing of the pre-mRNA (Dominski et al., 2001; Dominski et al., 1999; Scharl and Steitz, 1994). Finally, a presumed bridging factor has been identified (ZFP100) that interacts with both the SLBP/SL complex as well as the U7snRNP specific Sm-like protein, Lsm11 (Azzouz et al., 2005a; Dominski et al., 2002; Wagner et al., 2006).

The requirement of SLBP for *in vitro* processing of histone pre-mRNA is not absolute, but rather conditional. Extracts depleted of SLBP are incapable of processing the H1t histone pre-mRNA but are fully competent to process the H2A-614 histone pre-mRNA (Dominski et al., 2001). The differences between these two substrates lie in the ability of the U7 snRNP to basepair to the HDE. H2A-614 can form several more hydrogen bonds with the U7 snRNA than H1t, thus a substrate with a high affinity for the U7 snRNP does not require SLBP for processing. The major evidence in support of a role for SLBP in processing *in vivo* is from studies in *Drosophila*. It has been found that flies that are hypomorphic or null for SLBP have significant (although not exclusive) misprocessing of endogenous histone pre-mRNA (Lanzotti et al., 2002) and RNAi-mediated knockdown of SLBP in S2 cells phenocopies this misprocessing (Wagner et al., 2007). In these flies, the normal cleavage site is not recognized and the polymerase transcribes down to cryptic cleavage and polyadenylation sites resulting in the formation of polyadenylated histone mRNA (Lanzotti et al., 2002). Flies that are null for the U7snRNA gene

contain exclusively polyadenylated histone mRNA (Godfrey et al., 2006). Surprisingly, these flies are viable but males and females are sterile. The former result suggests the presence of a poly(A) tail on histone mRNA is permissive for fly development but may be toxic for proper spermatogenesis and oogenesis. The cause of this toxicity is not known.

Once the U7snRNP is bound to the HDE, a cleavage factor is recruited containing at least CPSF73, CPSF100, and Symplekin (Dominski et al., 2005a; Kolev and Steitz, 2005). CPSF73 is the endonuclease that cleaves the histone pre-mRNA from the DNA template (Dominski et al., 2005a). Other CPSFs and CstFs are not required for histone pre-mRNA processing although biochemical data suggests that they might be associated with the cleavage factor (Kolev and Steitz, 2005). Regardless, the molecular interactions between the cleavage factor and the U7snRNP/SLBP/SL complex have not been elucidated.

The molecular events that follow processing in the nucleus and are prior to the translation of histone mRNA in the cytoplasm are less understood. What is clear is that the histone mRNA is rapidly exported and this export in S2 cells is dependent on the expression of Nxf1, which is the fly homolog of the RNA export factor TAP (Erkmann et al., 2005a). Early in S phase, SLBP localization is strictly nuclear, presumably participating in the processing reaction at the Cajal Body (Marzluff and Duronio, 2002) although discrete localization of SLBP at the Cajal Body has not been observed. As S phase progresses, SLBP begins to accumulate in the cytoplasm and is present along with histone mRNA in the large polyribosome fraction on glycerol gradients (Whitfield et al., 2004). The correlation of SLBP and

histone mRNA localization on polysomes is likely a functional interaction as the treatment of HeLa cells with cycloheximde results in an increase in SLBP on polyribosomes and a decrease in the nucleus (Whitfield et al., 2004). Inhibition of DNA replication with HU results in a rapid degradation of histone mRNA and rapid relocalization of SLBP to the nucleus (Whitfield et al., 2004). Furthermore, SLBP interacts with a novel protein called SLIP1, which interacts with eIF4G and plays a role in translating histone mRNA and possibly other cellular mRNAs (Cakmakci et al., 2008). In *Xenopus* oocytes, the expression of SLBP protein stimulates the translation of luciferase reporter genes ending in a stemloop (Sanchez and Marzluff, 2002). These data are all consistent with a role of SLBP in the translation of histone mRNA.

In late S phase, as DNA replication is concluding, the levels of histone mRNA are downregulated as are thelevels of SLBP protein. This reduction in histone message is a result of rapid decay of the existing histone mRNA pool in the cytoplasm, reduced transcription of the histone genes, and the reduced processing efficiency of the histone pre-mRNA, and the (Chapter 1). The reduced transcription of histone genes is likely a consequence of reduced CyclinE-cdk2 activity on the histone transcription factor NPAT, whose localization to histone genes is dependent on its phosphorylation status (Ma et al., 2000). Reduced processing efficiency seen in very late S phase or G2 phase is due to a reduced level of SLBP as G2 nuclear extracts, which are unable to process a histone pre-mRNA *in vitro*, can be restored to full processing activity by supplementation with recombinant SLBP (Dominski et al., 1999).

The rapid decay of existing histone mRNA is executed through a surprising mechanism that I described in Chapters 2 and 3 (Mullen and Marzluff, 2008). In late S phase, histone mRNA is oliguridylated at the 3' end resulting in a histone mRNA containing 8-15 uridines. It is not clear if SLBP is required for this reaction. SLBP is known to be destroyed in late S phase through phosphorylation of two threonine residues and mutation of these residues to alanines results in robust expression throughout the end of S phase as well as G2 phase (Zheng et al., 2003). Surprisingly, in the presence of this stable mutant SLBP, histone mRNA is still degraded appropriately and with similar kinetics consistent with SLBP being required for histone mRNA degradation.

In order to understand the critical roles of SLBP in cells, Kelly Sullivan, Eric Wager and myself knocked down SLBP using RNA interference in U2OS cells. Previously, Eric Wagner and the Müller lab had shown independently that this treatment in HeLa cells results in a reduction in the rate of cell growth and an accumulation of cells in S-phase (Wagner et al., 2005; Zhao et al., 2004). However, a thorough molecular analysis of the histone mRNA has not been done. Here I present data from Kelly, Eric and myself that show the major lesion in histone mRNA metabolism as a result of knocking down SLBP is not in histone pre-mRNA processing, but in the export of histone mRNA to the cytoplasm. Loss of SLBP results in a reduction in the amount of histone protein synthesis, and hence chromatin assembly, which leads to a decreased rate of DNA replication and activation of an S-phase cell cycle checkpoint response. Over the course of SLBP knockdown there is a reduction in the histone:DNA ratio in the cells. The rapid

alteration of histone mRNA half-life in response to hydroxyurea is also impaired in SLBP knockdown cells since the normal site of histone mRNA degradation is the cytoplasm. Together these results implicate SLBP as having a critical histone mRNA export function necessary for proper histone gene expression and cell division.

MATERIALS AND METHODS

RNA interference

RNAi was performed using a two-hit method as previously described using Lipofectamine 2000 (Invitrogen) (Mullen and Marzluff, 2008; Wagner and Garcia-Blanco, 2002). Briefly, 110,000 U2OS or 95,000 HeLa cells were plated into 24 well plates and the following day, siRNAs were transfected into cells. A day following the first hit of siRNA, cells were replated into 6 well dishes, allowed to grow an additional day and then transfected with the second hit of siRNA. Cells were harvested 48-72 hours following the second hit for analysis. The siRNA sequences of the C2 (control) and S2 (SLBP) were the same as previously described (Wagner et al., 2005).

DNA synthesis and mitotic index measurements by FACS

I quantified the percentage of bromodeoxyuridine (BrdU) labeled cells in S phase and phospho-histone H3 in mitosis as previously described (Doherty et al., 2003). The HU controls for these assays were done by incubating cells in a final concentration of 5 mM HU for 1 hour. To measure DNA synthesis in S phase, RNAi-treated cells were pulsed with a 1 mM stock solution of BrdU (10 μM final

concentration) for 1 hour. Cells were harvested with trypsin and spun down at 1,400 rpm for 5 min. at room temperature. The supernatant was removed and the cell pellet was resuspended in 1.5 ml cold PBS with vortexing. The resuspended cell pellet was then fixed by adding 3 ml of cold 100% ethanol. Cells were pelleted briefly by centrifuging at 1000 rpm for 5 min. in the cold room. The supernatant was aspirated and the cell pellet was incubated with 3 ml of 0.08% pepsin in 0.1 N HCl and incubated at 37°C for 20 min. Pelleted nuclei were suspended in 1.5 ml of 2 N HCl and incubated at 37°C for 20 min. Next, 3 ml of 0.1 M sodium borate was added to neutralize the pH and the nuclei pelleted. Nuclei were washed with 2 ml of IFA (10 mM HEPES pH 7.4, 150 mM NaCl, 4% FBS, 0.1% NaN_3) plus 0.5% Tween-20 and incubated in the dark, on ice for 30 minutes and then pelleted. Nuclei were resuspended with 100 μl of a solution containing α-BrdU antibody conjugated to FITC (Becton Dickinson) diluted 1:5 in IFA plus 0.5% Tween-20 and incubated in the dark, at room temperature for 2 hours. Following the incubation, 2 ml of IFA plus 0.5% Tween-20 was added and nuclei pelleted. Nuclei were resuspended with 500 μl of the IFA plus 0.5% Tween solution containing 5 μg/ml RNase A and 50 μg/ml propidium iodide. Nuclei were incubated overnight at 4°C and analyzed on a Becton-Dickinson (Becton Dickinson) FACScan using Summit Software (Dako Cytomation).

To measure mitotic index by phospho-histone H3, RNAi treated cells were harvested as above and fixed with 1% formaldehyde in PBS for 30 minutes. Fixed cells were pelleted at 1200 rpm for 5 minutes at 4°C and the supernatant removed. Cells were resuspended in 1.5 ml PBS and then 3 ml of cold 100% ethanol was

added and cells stored at 4°C overnight. The fixed cells were pelleted by centrifugation at 1,200 rpm for 5 min. at 4°C. The supernatant was removed and cell pellets washed with 2 ml IFA plus 0.5% Tween and then centrifuged. Washed cells were resuspended in 100 μl of a solution containing 0.5 μg of phospho-histone H3 (serine 10) antibody (Upstate Biotechnology) and 5 μg/ml RNase A in IFA plus 0.5% Tween-20 for 2 hours at room temperature. Following the incubation 2 ml of IFA plus 0.5% Tween-20 was added, the cells centrifuged, and the supernatant removed. The cell pellet was resuspended in 100 μl of the IFA plus 0.5% Tween-20 solution containing an anti-rabbit secondary antibody conjugated to FITC (Santa Cruz Biotechnology) for 1 hour at room temperature. Following the incubation, 2 ml of IFA plus 0.5% Tween-20 was added and the cells centrifuged. The secondary antibody was removed and the cell pellet resuspended in 500 μl of the IFA plus 0.5% Tween solution containing 5 μg/ml RNase A and 50 μg/ml propidium iodide. Cells were analyzed by FACS as above.

Northern blot analysis and S1 nuclease protection assays

Northern blot analysis to replication-dependent histone genes and 7SK snRNA was performed as described previously (Mullen and Marzluff, 2008). Briefly, 2 μg of total RNA was run on 6% urea-polyacrylamide gels, transferred to Hybond N+ nitrocellulose (Amersham Biosciences), and probed in QuickHyb (Stratagene) overnight at 60°C. Probes were generated by random primed, α^{32}P-dCTP labeling (PrimeIt II Kit, Stratagene) of PCR products generated to the ORF of cloned histone genes.

S1 nuclease protection assays to map the 3' ends of histone H2A (*HIST2H2AA*) and H3 (*HIST2H3A/C*) were performed as previously described (Kaygun and Marzluff, 2005a). Briefly, 5-20 μg of total RNA was hybridized to 3' end-labeled probes at 56°C overnight and then digested with S1 nuclease (Promega) at room temperate for 60 minutes. H2A probes for 3' end labeling were generated by AscI (New England BioLabs) restriction enzyme digestion of a cloned *HIST2H2AA* plasmid and probes for H3 were generated by BssHI (New England BioLabs) restriction enzyme digestion of a cloned *HISTH3A/C* plasmid. Digested plasmid DNA was 3' end labeled with α^{32}P-dCTP and Klenow (New England BioLabs) as previously described. Protected fragments were resolved on 6% urea-polyacrylamide gels.

Western blot analysis

Protein lysates from RNAi treated cells were harvested and the concentrations quantified using Bradford reagent (BioRad). Primary antibodies used in this study include SLBP anti-rabbit, symplekin anti-rabbit (BD Biosciences), fibrillarin anti-mouse (Abcam), Hsp90 anti-mouse (Cell Signaling Technology), histone H3 anti- (Abcam).

Labeling and acid extraction of RNAi-treated cells

Pulse labeling experiments were performed as previously described (Whitfield et al., 2000). Breifly, cells were starved for 45 minutes in media lacking methionine prior to being pulsed for 15 min. in media supplemented with ^{35}S methionine. Cells were washed in PBS, collected by scraping and pelleted by centrifugation. Pellets were resuspended in nuclear isolation buffer (250 mM sucrose, 1 mM $CaCl_2$, 2 mM

$MgCl_2$, 1% Triton X-100, 10 mM Tris pH 8.0, 2 mM PMSF) and lysed on ice for 1 hour. Nuclear pellets were acid extracted with HCl for 30 min. Proteins were TCA precipitated overnight at -20° C, washed in acetone, and resuspended in SDS loading buffer. Protiens were resolved on a 15% polyacrylamide gel and relative histone amounts were quantified by PhosphorIMage analysis (GE Healthcare) and ImageQuant software.

Cell fractionation

HeLa cells were fractionated as previously described (Lerner and Nicchitta, 2006; Lerner et al., 2003) and RNA isolated by Trizol reagent (Invitrogen).

Histone mRNA degradation

HeLa cells were treated with a final concentration of 5 mM hydroxyurea for various times as described previously (Kaygun and Marzluff, 2005a; Mullen and Marzluff, 2008). Total RNA from samples were isolated using Trizol reagent (Invitrogen). We used PhosphorImager (GE Healthcare) analysis to calculate the percent of histone H2a mRNA remaining following HU treatment. H2a mRNA levels were normalized to levels of the 7SK snRNA loading control.

***In Situ* hybridization**

In situ hybridizations were performed similarly as described (Erkmann et al., 2005a). RNAi treated cells were grown on coverslips and washed with PBS and fixed in 3.7% PFA in PBS for 10 minutes at room temperature. Cells were then washed again and permeabilized in 0.5% Triton X-100 in PBS. Pre-hybridization was performed for 10 minutes at 37°C using a solution of 4x SSC and 50% formamide pre-heated to 37°C. Cover slips were inverted onto a 5-10 µl drop of

hybridization solution (50% deionixed formamide, 10% dextran sulfate, 1x Denhardt's solution, 4x SSC, 1 mg/ml E. coli tRNA) containing 1 ng/µl DIG labeled H2A or H3 probe. Probes were denatured for 5 min. at 80ºC and cooled on ice prior to addition to hybridization solution. Hybridizations were performed overnight at 37ºC in a humidified chamber. Cells were washed once with 2X SSC at 37 ºC, 3X 60% formamide in 0.2x SSC at 37ºC, 2X SSC at room temperature, and three times with 0.5% Tween-20 in 4X SSC. Coverslips were inverted onto 8 µl drops of 0.5% Tween-20 in 4X SSC containing mouse Cy3 α-DIG antibody diluted 1:200 and incubated at 37ºC for 1 hour in a humidified chamber. Coverslips were washed 3X with 0.5% Tween-20 in 4X SSC and inverted onto 8 µl drops of with 0.5% Tween-20 in 4X SSC containing Cy-3 α-mouse secondary antibody diluted 1:200. Secondary incubation was performed for 45 minutes at 37ºC in a humidified chamber. Coverslips were washed 3 times with 0.5% Tween-20 in 4X SSC before being fixed with 3.7% PFA in PBS for 5 minutes at room temperature. After a PBS wash, conversplips were DAPI stained and mounted onto slides using Fluorsave reagent (Calbiochem). Images were acquired using a Zeiss LSM 510 confocal microsocope and analyzed using ImageJ software.

RESULTS

SLBP knockdown cells are viable and continue to increase in number but at a slower rate than normal

SLBP has been shown previously to have roles in a number of different processes involved in the metabolism of histone mRNA (Marzluff, 2005; Marzluff and

Duronio, 2002). In the current study, Kelly Sullivan, Eric Wagner and myself set out to determine the essential function(s) of SLBP by transiently knocking it down in U2OS cells using a double-stranded siRNA that specifically targets SLBP mRNA. Kelly and Eric began by performing an RNAi timecourse experiment to gain insight determine the length of time following the second hit of siRNA at which we could assay cells for histone mRNA metabolic defects, while still maintaining efficient SLBP knockdown. In Figure 27A, Eric Wagner used Western blotting to monitor SLBP protein levels over various times throughout the RNAi transfection. U2OS cells were plated in 24 well dishes and the following day, transfected with either control (C2) or SLBP (S2) siRNA. The day after the first transfection (24 hours, Figure 27A, lanes 1-3), SLBP protein levels were slightly lower in C2 treated cells after 24 hours than in untransfected cells (Figure 27A, compare lanes 1 and 2). This decrease is likely due to the high cell density used to achieve effective transfection. The expression of SLBP protein is limited to S-phase while many of the cells are confluence-arrested at the 24 hour time point, leaving fewer cells in S-phase. The 24 hour time point in Figure 27A represents when we split the cells out of the 24 wells, and replated them into 6-well tissue culture dishes. After 48 hours, we transfected another dose of siRNA and waited up to 3 days after (120 hours) to assay for defects in histone mRNA metabolism. It is clear that from 72 to 120 hours following the initial hit of siRNA, SLBP proteins levels are markedly downregulated (Figure 27A, lanes 4-11).

As previously shown, knockdown of SLBP to this level results in an increase in the number of cells in S-phase (Wagner et al., 2005). Kelly Sullivan next wanted

to determine the cell number during each of these conditions since it appeared that SLBP knockdown cells were not growing as well as the C2 control cells. Cell number was determined using a hemacytometer following trypsinization and viability assessed by Trypan Blue staining. Figure 27B is a graphical representation of the total number of cells in the SLBP knockdown wells compared to the C2 negative controls. Although the cells remained viable and continued to increase in number, they did so at a slower rate than normal. It is apparent from this data there are 30-40% fewer cells in the SLBP (S2) knockdown population due to their slower rate of growth.

Reducing the levels of SLBP decreases the rate of DNA synthesis and activates an S-phase cell cycle checkpoint

Since SLBP knockdown cells did not appear to be growing as well as control cells, and since Eric had previously shown there was an accumulation of SLBP knockdown cells in S phase, I sought to determine the biological mechanism responsible for these preliminary phenotypes. To assess the ability of SLBP knockdown cells to synthesize DNA, I pulsed U2OS cells that had been transfected with control (C2) or SLBP (S2) siRNA with bromodeoxyuridine (BrdU), a thymidine analog, for 30 minutes and analyzed incorporation by FACS. As a control I treated cells transfected with C2 (control) siRNA with 5 mM hydroxyurea (HU) for 1 hour to block DNA replication. The DNA content as measured by propidium iodide staining revealed what Eric had observed previously that SLBP knockdown cells accumulated in S-phase of the cell cycle (Figure 28A, top panel). From the FACS analysis of BrdU-incorporation (Figure 28A, bottom panel), it is clear that SLBP

knockdown cells do not incorporate BrdU as much as control cells. In the control RNAi (C2) cells, there is efficient incorporation of BrdU as detected by a FITC-conjugated antibody to BrdU. The characteristic arc of BrdU incorporation is present in the control cells, with only a small percentage of cells under the arc not incorporating BrdU. In contrast, the SLBP knockdown cells (S2) have a markedly lower BrdU-FTIC signal overall and lack the characteristic arc observed in control cells (Figure 28A, bottom panel), suggesting to me that their rate of DNA synthesis is reduced. In support of this, a C2 control-treated set of cells treated with HU lacks any incorporation of BrdU since DNA synthesis has been inhibited.

I also used the BrdU FACS analysis to better quantify the cell cycle phase distribution in the SLBP knockdown cells compared to the C2 control (Figure 28B). I quantified the G1 and G2 phases as the populations at 2N and 4N (respectively) that do not incorporate BrdU. I separated S phase into two phases, early and late, by quantifying the two populations that represent these points during DNA replication as those cells expressing incorporated BrdU. It is apparent from this representation of the data (Figure 28B) that S2 cells accumulate most BrdU in the early part of S phase and are having difficulty completing S phase since there are more late S phase levels compared to control, while levels of G2 cells are reduced by 40%.

The BrdU FACS analysis (Figure 28A and 28B) suggested that cells were not synthesizing DNA as efficiently as control cells and that cells were having difficulty completing S phase of the cell cycle. To support these data, I determined the mitotic rate of SLBP knockdown cells using an antibody to phosphorylated histone H3 (serine 10) as a mitotic marker. Positive cells were measured by FACS and positive

cells quantified as a percentage of the control (Figure 28C). It is clear from the mitotic index data that SLBP knockdown cells are going through mitosis at approximately half the rate of C2 control cells, consistent with the 50% reduction in growth rate. This reduction is comparable to C2 control cells that were treated with HU for 1 hour, further lending support that SLBP knockdown cells are not synthesizing DNA efficiently.

In order to assess the degree of knockdown in these experiments, I used Western blotting of SLBP knockdown lysate and compared it to a serial dilution series of the C2 control lysate (Figure 28D). As can be seen from Figure 28D, the level of knockdown of SLBP was greater than 95%. This level of knockdown using the S2 siRNA was typical for experiments carried out 48 to 72 hours following the second transfection of siRNA.

I next determined whether the reduced rate of DNA replication resulted in activation of the S-phase checkpoint, a consequence of defective chromosome replication, damaged DNA, and environmental stress (Sancar et al., 2004). I was particularly interested in this since it has been shown previously that overexpression of a dominant negative chromatin assembly factor 1 (CAF1) produces a similar DNA replication phenotype as knocking down SLBP (Ye et al., 2003a). I hypothesized that reducing the levels of SLBP might ultimately result in impaired histone protein biosynthesis and hence mimic the defective chromatin assembly phenotype since the chromatin assembly machinery would not have enough histone proteins to properly assemble chromatin.

I assessed the phosphorylation of Chk1, a kinase that is activated by the ATR kinase when DNA replication stress is sensed in S-phase cells. As a control, I again used C2 control cells treated with HU for 1 hour since HU treatment is known to activate the DNA replication checkpoint and result in Chk1 phosphorylation (Sancar et al., 2004). There was increased Chk1 phosphorylation on both serine 345 (S345) and serine 317 (S317) in response to SLBP knockdown (Figure 28E). The levels of Chk1 phosphorylation on both of these serine residues was similar to that present in the HU-treated C2 siRNA population, supporting the notion that reducing the levels of SLBP results in a DNA replication phenotype that is directly sensed by the cell cycle checkpoint sensor and effector molecules. I did not detect phosphorylated Chk2 under these conditions using an antibody to threonine 68.

Histone mRNA levels are reduced in SLBP knockdown cells and the majority that remains is properly processed

Since SLBP is essential for histone mRNA biosynthesis, I used Northern blots to determine histone mRNA levels for all four, core replication-dependent histone genes as well as for the linker histone H1 (Figure 29A). I used radiolabeled probes generated by PCR targeting the open reading frame (ORF) to detect histones H2A, H2B, H3, H4 and H1 and used 7SK snRNA as a loading control. The Northern blots shown in Figure 29A indicated that the abundance of histone H2A, H2B, H3, and H4 is reduced only about 50% in the SLBP knockdown cells when compared to the C2 negative control. This is consistent with a previous report (Zhao et al., 2004) where we observe roughly half (ranging from 37% to 70%) as much histone mRNA in the SLBP knockdown cells compared to the control siRNA. The exception was histone

H1 mRNA, where steady state levels appeared to be approximately 10% higher than the control. It was quite surprising that I saw histone mRNA accumulate at all since SLBP is required for histone mRNA processing.

It was particularly interesting to observe a slower migrating band in the histone H4 Northern blot (Figure 29A, fourth panel). I hypothesized this represented misprocessed histone mRNA since the role of SLBP in histone pre-mRNA processing has been recently established in flies and human cells (Lanzotti et al., 2002; Narita et al., 2007). I therefore performed both S1 nuclease protection assays and Northern blots using total cell RNA and oligo(dT) selected total cell RNA, respectively. I was able to detect a small amount of misprocessed histone H2A mRNA by S1 nuclease protection assay but not histone H3 (Figure 29B). Northern analysis to histone H4, using oligo(dT) selected RNA, revealed that the slower migrating band shown in Figure 29C was indeed misprocessed, polyadenylated histone H4 mRNA. Despite the observation of some misprocessed histone H3 and H2A mRNA, most of the histone mRNA that was present was properly processed.

Histone protein levels are reduced in SLBP knockdown cells and the normal regulation of histone mRNA degradation is impaired.

The results from the above experiments were surprising since there existed a reasonable amount of properly processed histone mRNA for all the core histone genes, including the linker histone H1 gene. Previous structure-function studies on SLBP have shown the protein to possess a critical domain essential for histone mRNA translation (Cakmakci et al., 2008; Sanchez and Marzluff, 2002). Due to the modest decrease in properly processed histone mRNA in SLBP knockdown cells,

Kelly Sullivan hypothesized that perhaps the translation function of SLBP was more important for histone metabolism than its pre-mRNA processing function. He therefore investigated the levels of histone protein in SLBP knockdown cells. Figure 30A shows Western blot analysis from whole cell protein lysates. He performed the Western blot with a serial dilution of the control C2 siRNA lysate to estimate differences between the control (C2) and SLBP siRNA (S2) treated cells, using Symplekin, a scaffold protein involved in 3' end formation (Kolev and Steitz, 2005), as a loading control. The levels of SLBP were decreased by more than 90% of the control C2 lysate (Figure 30A). When Kelly probed using an anti-histone H3 antibody, he could see that in the SLBP knockdown cells, total histone H3 was reduced by 50-75% relative to the level seen in control treated cells (Figure 30A).

To directly test the SLBP knockdown cells' ability to translate histone mRNA Kelly Sullivan next pulse-labeled them by adding ^{35}S-labeled methionine in the culture media for 15 minutes as previously described (Cakmakci et al., 2008; Whitfield et al., 2000). Both the Coomassie stain and autoradiograph of this experiment are presented in Figure 30B. The Coomassie stain (Figure 30B, left panel) is consistent with a reduction in total protein levels for all four core histones, consistent with the previous Western results for histone H3. The autoradiograph of the same experiment (Figure 30B, right panel) further demonstrates that in fact the rates of translation for histones H2A and H3 are decreased by approximately 40% in the SLBP knockdown cells when compared to control C2 cells. We concluded that the amount of histone mRNA (properly processed or misprocessed) present in the SLBP knockdown cells is not enough to meet the histone protein demands of the

replicating U2OS cell and, at least in part, contributes to the DNA replication and growth defects we observed.

Histone mRNA half-life is coordinately regulated with the rate of DNA synthesis, whereupon the completion of S phase or inhibition of DNA synthesis results in rapid degradation of histone mRNA. Histone mRNA degradation is a regulated process that involves the addition of an oligo(U) tail to the 3' end in order to recruit specific decay factors for rapid, bidirectional decay of the mRNA (Chapters 2 and 3). Since reducing SLBP protein levels produced defects in DNA synthesis and normal histone gene expression, I asked if downregulation of SLBP had an effect on histone mRNA degradation. I inhibited DNA replication with 5 mM HU in both C2 control cells and SLBP knockdown cells for 30 and 60 minutes. A representative Northern blot analysis of histone H2A mRNA is presented in Figure 30C (left panel) and reveals the rate of histone mRNA degradation is decreased when SLBP protein levels are downregulated by siRNA. 7SK snRNA is used as a loading control to normalize the percentage of histone H2a mRNA remaining following the two time points of HU treatment. Histone mRNA in the C2 control is rapidly degraded at the 30 minute time point and is barely detectible at the 60 minute time point (Figure 30C, lanes 2 and 3). In the SLBP knockdown cells, histone mRNA degradation is stabilized roughly 1.6 fold on average at the 30 minute time point (Figure 30C, graph on right which represents 3 independent experiments) and roughly 2.3 fold at the 60 minute time point (Figure 30C). Together these data support the evidence obtained from examining histone mRNA levels in the SLBP knockdown, that the decreased amount of histone mRNA corresponds to a

decreased pool of histone protein in the cell. Moreover, the HU time course experiments suggest that SLBP is necessary for histone mRNA degradation and in its absence the normal pathway of histone mRNA degradation is impaired.

In situ hybridization to histone mRNA reveals that histone mRNA is retained in the nucleus in SLBP knockdown cells

We next wanted to determine the subcellular localization of the properly processed histone mRNA in SLBP knockdown cells. To address this question further, Kelly Sullivan performed *in situ* hybridization on control and SLBP knockdown cells with histone H3 mRNA using paraformaldehyde-fixed U2OS cells. In untransfected and the control C2 siRNA cells, histone H3 and H2A mRNA localization revealed a halo-like appearance in the cytoplasm in both U2OS and HeLa cells (respectively), surrounding the perinuclear region of the cell (Figure 32A and 32B). This is consistent with histone mRNA's presence on the endoplasmic reticulum (ER), since S1 nuclease protection assays I performed to histone H2A and H3 on RNA from subcellular fractionations, reveals that replication-dependent histone mRNAs are exclusively localized to the ER and not in the remaining cytosol (Figure 31). In contrast, when SLBP protein levels are dramatically reduced, *in situ* hybridization to histone H3 mRNA reveals a strong, if not exclusive, localization to the nucleus of cells (Figure 32C, bottom panel in red). This pattern was also observed in SLBP knockdown cells when *in situ* hybridization to histone H2A was performed (Figure 32B). Interestingly the histone mRNA that accumulates in the nucleus is properly processed, as the misprocessed RNA which is polyadenylated is presumably exported via the conventional poly(A) RNA export pathway. As a

control to demonstrate the specificity of the *in situ* hybridization probes, Kelly synchronized HeLa cells by double-thymidine block and released them into S phase for 3 hours. He added HU for 0, 15, 30 and 60 minutes and harvested cells for *in situ* hybridization. Figure 32A demonstrates the presence and localization of H2A mRNA and its disappearance as time of HU exposure increases.

As an alternative approach to confirm the presence of histone mRNA in the nucleus, Kelly Sullivan and Eric Wagner fractionated C2 control and S2 knockdown cells into nuclear and cytoplasmic fractions. They harvested protein and total RNA from these fractions as well as from a portion of the starting material. Figure 32D presents a Western blot showing relative cellular fractionation. Hsp90 and fibrillarin were used as cytoplasmic and nuclear markers respectively (Figure 32D). Consistent with their reported subcellular localization, Kelly and Eric see almost all the fibrillarin protein concentrate to the nuclear fraction whereas they see almost exclusive cytoplasmic localization of Hsp90 (Figure 32D).

Kelly and Eric next analyzed the RNA portions of the fractionation and simultaneously probed for histone H3 and U1 snRNA as a control using probes generated by PCR (Figure 32E). Consistent with the nuclear localization of splicosomal snRNA, they observed that U1 was concentrated in the nuclear fraction of both the C2 control and S2 knockdown (Figure 32E, lanes 2 and 5). A residual amount of U1 was detected in the cytoplasm (Figure 32E, lanes 3 and 6). Histone H3 mRNA was concentrated in the cytoplasm of C2 control cells (Figure 32E, lane 3) but its abundance diminished from the cytoplasm when SLBP was knocked down (S2, Figure 32E, compare lanes 3 and 6). Comparison of the ratio of histone H3 in

the nucleus and cytoplasm from the C2 and S2 RNAi treatments, reveals it is apparent that the ratio of histone H3 mRNA is greater in the nuclear fraction of the S2 knockdown when compared to the ratio of the compartments in the C2 control cells (Figure 32E). Sequestration of histone mRNA in the nucleus upon loss of SLBP is consistent with the decrease in histone protein synthesis due to decreased translation. Several factors may influence the stability of histone mRNA in SLBP knockdown cells; first, translation is required for degradation of the mRNA and second, the normal compartment for degradation is the cytoplasm.

DISCUSSION

SLBP plays a role in a number of different aspects of histone mRNA metabolism (Marzluff and Duronio, 2002). Null flies for SLBP are embryonic lethal and the larva produces only polyadenylated mRNAs (Godfrey et al., 2006) and hypomorphic flies produce histone mRNAs that are polyadenylated and not cell cycle regulated (Lanzotti et al., 2002). Evidence from worms and flies suggests SLBP expression is necessary for histone gene expression in early embryonic development since depletion of SLBP results in chromatin condensation defects in these embryos (Pettitt et al., 2002; Sullivan et al., 2001). Recent evidence from human cells has demonstrated that SLBP and the transcription negative elongation factor (NELF) function together to properly process replication-dependent histone genes in a cotranscriptional manner (Narita et al., 2007). Additionally, RNAi to SLBP results in an S phase and cell growth defect (Wagner et al., 2005; Zhao et al., 2004). Moreover, the role of SLBP in translation has been documented (Cakmakci et al.,

2008; Sanchez and Marzluff, 2002). Although a number of studies have defined distinct roles for SLBP in various aspects of histone mRNA metabolism, no comprehensive molecular study in human cells exists. In this study we used RNAi to SLBP to determine the critical function of SLBP in human cells. I was particularly interested in the role of SLBP in histone mRNA degradation.

In this chapter, I have presented a number of different findings from our studies. First, SLBP plays a surprisingly minor role in proper histone gene expression since reduction of SLBP protein by 98% decreased the amount of total histone mRNA in the cell by 50% and results in only a small portion of histone mRNA becomes polyadenylated. Second, histone mRNA translation is reduced in SLBP knockdown cells and total histone H3 protein levels in the cells are consequently decreased. Third, since SLBP participates in a number of aspects that ensure proper histone gene expression, the biological effect on the DNA synthesis machinery results in a cell growth defect that activates an S-phase checkpoint. Next, reduced expression of SLBP attenuates the cell's ability to rapidly degrade processed histone mRNA in response to inhibition of DNA synthesis. Most surprisingly, SLBP expression is critical for proper histone mRNA export since reducing SLBP protein levels resulted in the aberrant accumulation of histone mRNA in the nucleus. This latter result clearly underlies the aforementioned phenotypes we observed and argues that one of the critical functions of SLBP in human cells is to accompany histone mRNA to the cytoplasm where its translation and half-life can be properly regulated to ensure sufficient histone protein levels are produced for the chromatin assembly machinery.

Eukaryotic mRNA export is coupled to transcription, pre-mRNA processing and 3' end formation

Evidence over the past decade has revealed direct links between the distinct processes of gene expression (Maniatis and Reed, 2002). Together with mRNA surveillance systems such as nonsense-mediated decay and the general nuclear and cytoplasmic decay pathways (Chapter 1), coupling of even the earliest (e.g. transcription and 5' capping) and latest steps (e.g. mRNA export and translation) in gene expression ensures the proper expression of genes (Maquat, 2004; Maquat and Carmichael, 2001). Evidence from the Silver lab has demonstrated that the yeast mRNA export hnRNP protein Npl3 (Nab1) and another export factor Yra1 are cotranscriptionally recruited to chromatin at early and late steps, respectively, in the transcriptional process (Lei et al., 2001). Other evidence suggests that transcription and pre-mRNA splicing are coupled (Ge et al., 1998; Goldstrohm et al., 2001; Lai et al., 2001). Huang and Steitz have described two serine/arginine-rich (SR) splicing factors SRp20 and 9G8 that bind a 22 nt sequence element in the ORF of the intronless histone H2A gene and are required for proper mRNA export of mRNAs containing this conserved sequence (Huang and Steitz, 2001). SR proteins are evolutionarily conserved splicing factors in metazoans that shuttle between the nucleus and cytoplasm (Graveley, 2000). Recent genome-wide evidence from the Silver lab has found that both the DNA and RNA surveillance systems are coupled to global mRNA export when both nucleic acids are damaged by UV irradiation (Casolari et al., 2004; Hieronymus et al., 2004). The evidence we have gathered by reducing the expression of SLBP by RNAi in human cells provides an example of an

RNA binding protein involved in both 3' end processing and translation of histone mRNAs that is required for proper mRNA export, likely by coupling 3' end formation with efficient mRNA export.

Model of SLBP function in histone mRNA metabolism

Figure 33 presents a model of SLBP-dependent histone mRNA export. Normally, when sufficient levels of SLBP are present in the nucleus, SLBP functions first to cotranscriptionally process the 3' end of histone mRNAs (Narita et al., 2007). The SR protein 9G8 and SLBP bound to histone mRNA likely form an mRNP that together or independently interact with the mRNA export protein TAP to facilitate transit through the nuclear pore complex (Erkmann et al., 2005a; Huang and Steitz, 2001). The exported mRNA is initiated for translation in the cytoplasm where 9G8 is displaced by the initiating ribosome. SLBP remains bound to the mRNA, likely to regulate efficient translation termination and efficient ribosome recycling (Kaygun and Marzluff, 2005b). When normal histone mRNA is translated and SLBP is present, then the rapid alteration of histone mRNA half-life at the end of S phase or upon inhibition of DNA synthesis is intact.

When the expression of SLBP is reduced to very low levels the remaining SLBP must be utilized exclusively for processing. There is an accumulation of misprocessed, polyadenylated histone mRNA that is not cell cycle regulated suggesting limited SLBP results in efficient processing (Lanzotti et al., 2002; Narita et al., 2007), (Figure 29). The remaining amount of SLBP (1-4% of control) still present within the nucleus provides some pre-mRNA processing function (Dominski et al., 2001) or possibly another snRNP (Friend et al., 2007). We postulate that as a

result of the reduced levels of SLBP, SLBP dissociates from the histone mRNA, resulting in improper export even though the mRNA accumulates to substantial levels. However, in the absence of wild-type levels of SLBP protein there is an insufficient amount of SLBP protein to recruit 9G8 protein binding to the mRNA for 9G8/SLBP-dependent export. Alternatively, 9G8 binding may be unimpaired but not sufficient for proper histone mRNA export and that the SLBP/TAP interaction is additionally required to recruit histone mRNA to the nuclear pore complex and out of the cytoplasm.

The fate of nuclear-retained histone mRNA

Reducing the expression of SLBP results in a nuclear-retained histone mRNAs (Figure 32). The nuclear exosome functions to eliminate defective noncoding RNAs such as pre-tRNAs, pre-snoRNAs, pre-rRNAs, U6 snRNA, and 5S rRNA (Houseley et al., 2006). The degradation of these RNAs in budding yeast is mediated by the TRAMP complex of proteins that function to polyadenylate the 3' end to specifically target their degradation in the nucleus by the exosome (LaCava et al., 2005). The polyadenylation is carried out by the two noncanonical poly(A) polymerases, Trf4 and Trf5, found in *S. cerevisiae* (Houseley et al., 2007; Houseley and Tollervey, 2006; LaCava et al., 2005).

In this chapter, when SLBP was knocked down the rate of histone mRNA degradation in response to HU was reduced (Figure 30). This data taken together with the nuclear localization of histone mRNA under these conditions (Figure 32), suggest that histone mRNA is mislocalized and no longer has access to the cytoplasmic machinery required to regulate its rapid degradation (Chapter 2).

However it is clear that histone mRNA does turnover, just not as rapidly as a control-treated cell. The small amount of misprocessed histone mRNA likely is exported to the cytoplasm via the poly(A)-dependent export pathway but is not cell cycle regulated. It therefore could be possible that the properly processed, nuclear-retained histone mRNA is being degraded within the nucleus by the nuclear exosome. These mRNAs would likely be either polyadenylated or polyuridylated to direct specific targeting of the histone mRNA for degradation by the exosome. Continued investigation into this possibility is required to determine the fate of nuclear-retained histone mRNA as well as to the precise machanism that prevents histone mRNA from leaving the nucleus in the absence of SLBP. However, unlike defective mRNAs the processed histone mRNA are surprisingly stable in the nucleus.

Figure 27. SLBP knockdown cells are viable but grow at a slower rate than control cells. (A) SLBP protein is efficiently knocked down in U2OS cells using a double-hit method to deliver siRNA. U2OS cells were transfected in 24 well dishes with siRNAs to either control (C2) or SLBP (S2). The day following the first transfection (24 hours), cells were split into 6 well dishes and transfected with a second dose of siRNA (48 hours) and followed for 3 days (72 hours to 120 hours). Protein lysates were prepared at each indicated time point to monitor SLBP protein levels. (B) Total cell number of control (C2) and SLBP (S2) RNAi populations. siRNAs were delivered to U2OS cells as in (A) and enumerated at the indicated time points.

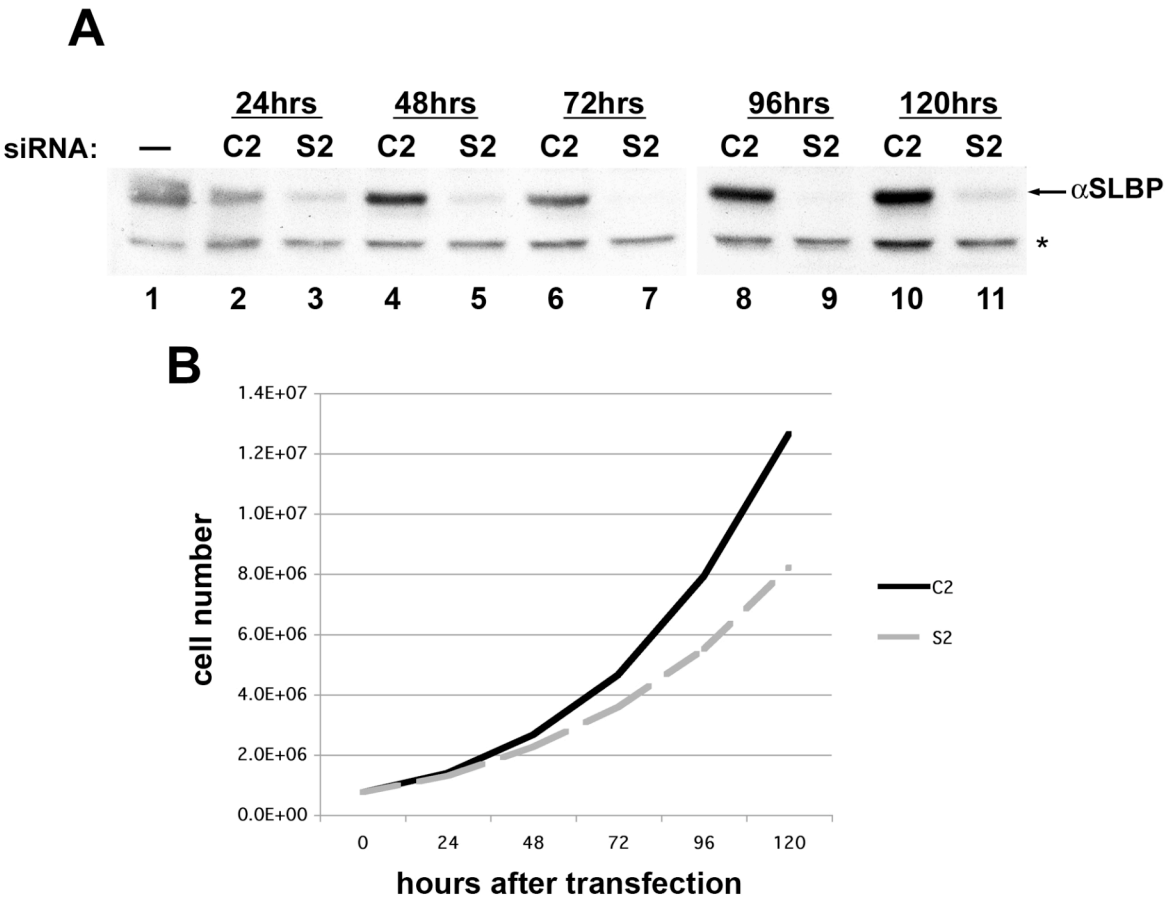
A
24hrs
48hrs
72hrs
96hrs
120hrs
siRNA:
—
C2
S2
C2
S2
C2
S2
C2
S2
C2
S2
αSLBP
*
1
2
3
4
5
6
7
8
9
10
11
B
1.4E+07
1.2E+07
1.0E+07
8.0E+06
6.0E+06
4.0E+06
2.0E+06
0.0E+00
cell number
0
24
48
72
96
120
hours after transfection
C2
S2

Figure 28. RNAi to SLBP results in cell cycle defects and activation of Chk1 kinase. (A) The rate of DNA synthesis in SLBP knockdown cells is decreased. C2 and S2 treated U2OS cells were grown in a final concentration of 10 μM bromodeoxyuridine (BrdU) for 1 hour and harvested for DNA synthesis or mitotic index assays. Hydroxyurea (HU, 5 mM) was added as a control to a parallel culture of C2 cells during BrdU incorporation (1 h). Cells were fixed and BrdU incorporation detected with an anti-BrdU antibody conjugated to FITC. Labeled cells were analyzed using a FACScan device and Summit software. (B) SLBP knockdown cells accumulate in S phase. Cell cycle phase distribution (G1, early and late S phase, and G2/M) was quantified from the data in (A), (C2, grey bars; S2, black bars) from 3 independent experiments. Quantities are expressed as a percentage of the C2 control cells. (C) Mitotic index in SLBP knockdown cells is reduced. Parallel cultures from (A) were fixed, stained with an antibody to the mitotic marker phospho-histone H3, and the antibody detected with a secondary antibody conjugated to FITC. Cells were analyzed similarly as in (A) and the population of cells with fluorescent signal above the G2 population was quantified. Quantities are expressed as a percentage of the C2 control cells. (D) SLBP protein is markedly reduced in U2OS cells. Western blot analysis on cell lysates from (A) is shown. A serial dilution of the C2 control lysate was performed as indicated and compared to the SLBP (S2) protein lysates. The asterisk indicates a cross reacting band that serves as a loading control. (E) SLBP knockdown results in the activation of a Chk1-dependent cell cycle checkpoint. Protein lysates from (A) were analyzed for the predominant signal transduction pathway that responds to replication stress. Total

Chk1 protein and phospho-specific Chk1 (serines 317 and 345) was analyzed by Western blot analysis. HU was used a positive control for Chk1 activation.

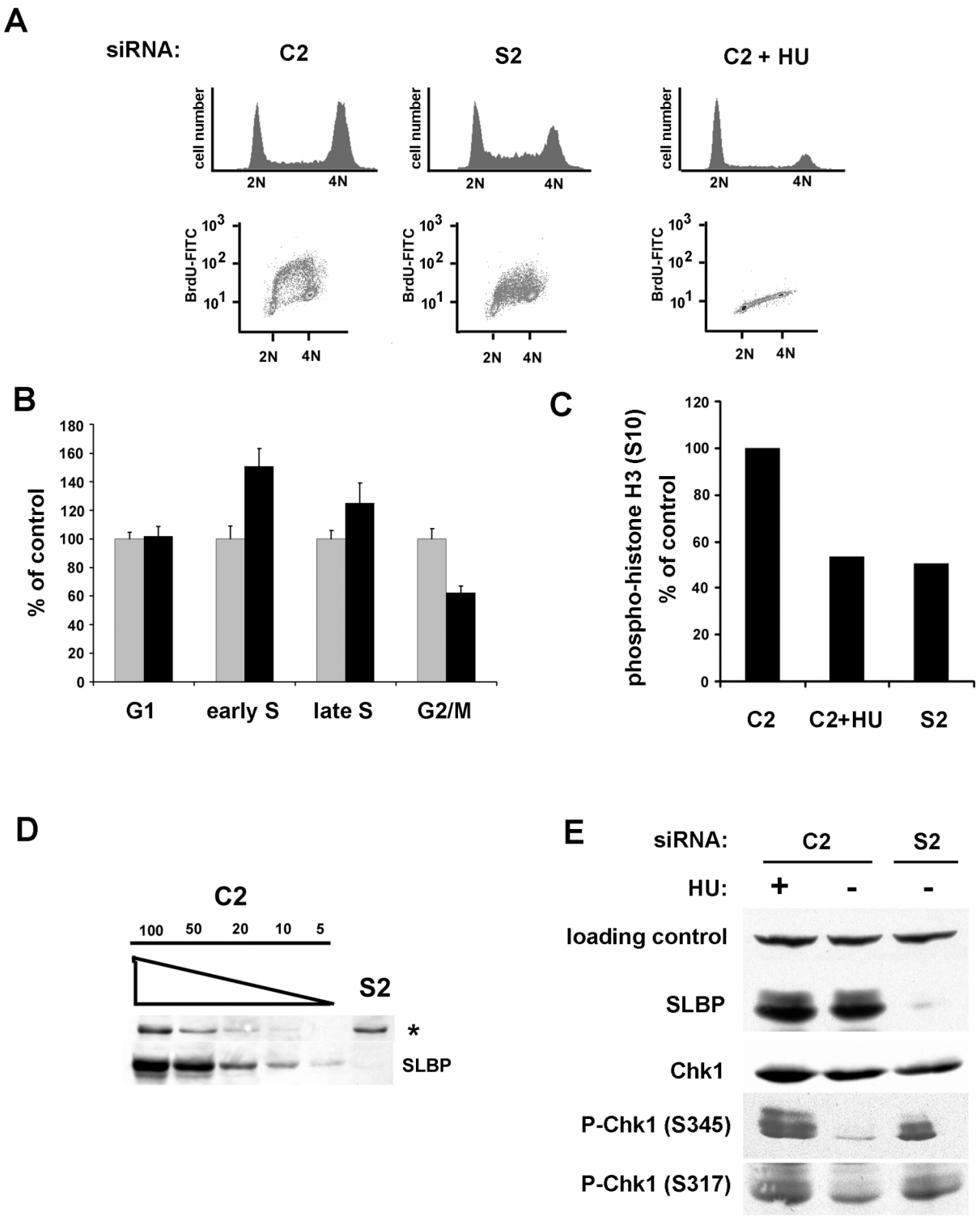
A
siRNA:
C2
S2
C2 + HU
cell number
2N
4N
BrdU-FITC
B
% of control
G1
early S
late S
G2/M
C
phospho-histone H3 (S10)
% of control
C2
C2+HU
S2
D
C2
100
50
20
10
5
S2
*
SLBP
E
siRNA:
C2
S2
HU:
+
-
-
loading control
SLBP
Chk1
P-Chk1 (S345)
P-Chk1 (S317)

Figure 29. Histone mRNA levels in SLBP knockdown cells are reduced and only a small portion of the mRNA is misprocessed and polyadenylated. (A) Histone mRNA levels are decreased in S2 treated cells. Northern blot analysis was performed on 2 μg of total RNA from C2 and S2 treated cells. 7SK snRNA is used as a loading control. A slowly migrating product reacting with the histone H4 probe is detected. The percentage of histone mRNA present in the S2 treated cells was quantified using PhosphorImager analysis and ImageQuant software and normalizing mRNA to the 7SK snRNA levels. (B) S1 nuclease protection assays to map the 3' ends of histone H2A (*HIST2H2AA*) and histone H3 (*HIST2H3A/C*). The asterisk (*) on the H2A gel reveals a small amount of polyadenylation. (C) Oligo(dT) selected total RNA reveals histone H4 is polyadenylated in SLBP knockdown cells. Northern blot analysis to histone H4 was performed on total RNA and RNA that had been oligo(dT) selected. The asterisk (*) signifies polyadenylation.

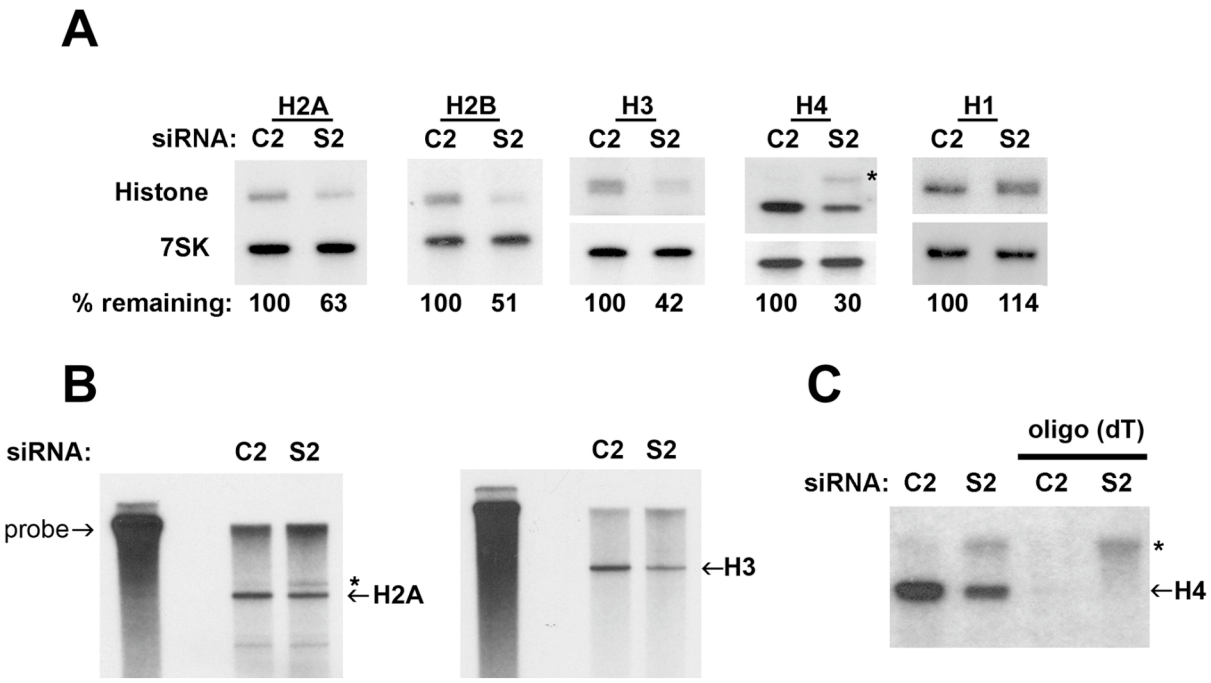
A
H2A
H2B
H3
H4
H1
siRNA: C2 S2 C2 S2 C2 S2 C2 S2 C2 S2
Histone
7SK
*
% remaining: 100 63 100 51 100 42 100 30 100 114
B
siRNA: C2 S2
probe→
*
←H2A
C2 S2
←H3
C
oligo (dT)
siRNA: C2 S2 C2 S2
*
←H4

Figure 30. Histone protein levels are decreased in SLBP knockdown cells and the normal histone mRNA degradation in response to HU is impaired. (A) Total histone H3 protein levels are decreased in SLBP knockdown cells. A serial dilution Western blot analysis of C2 and S2 protein lysates is shown. Antibodies to SLBP and histone H3 protein are used and an antibody to Symplekin is used as a loading control. (B) Total histone protein as well as histone mRNA translation is reduced in SLBP knockdown cells. U2OS cells were treated as in (A) but pulse-labeled with ^{35}S-methionine following growth in media depleted of methionine. Cells were harvested and nuclear pellets acid-extracted and proteins resolved on 15% polyacrylamide. Gels were Coommassie stained (left panel) or ^{35}S detected by PhosphorImage analysis (right panel). The core histone proteins are indicated (arrows) and the percent H2A/H3 proteins expressed as a percentage compared to the control (C2). (C) Histone H2A mRNA is not degraded as efficiently in SLBP knockdown cells compared to control cells. HeLa cells were treated with the indicated siRNAs and a Northern analysis performed (left panel) with probes to H2A mRNA and 7SK snRNA as a loading control. The right panel represents the results from 3 independent experiments. Standard deviations are represented by vertical bars.

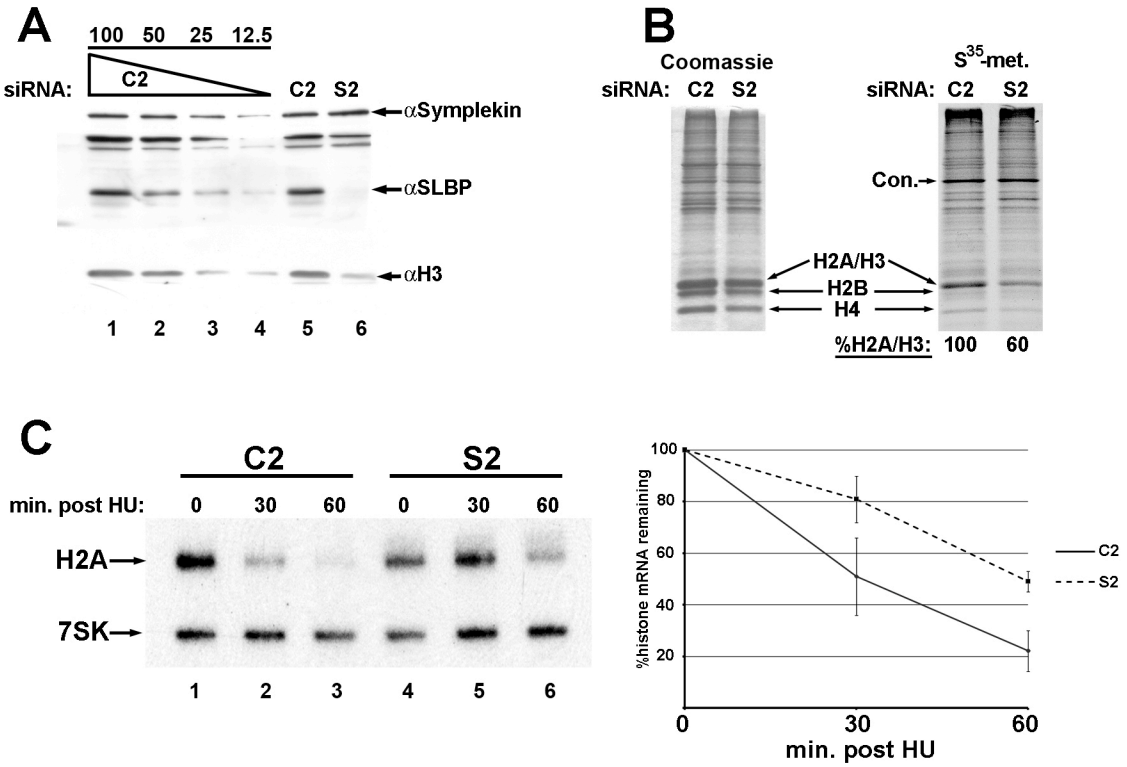
A
100 50 25 12.5
siRNA: C2 C2 S2
αSymplekin
αSLBP
αH3
1 2 3 4 5 6
B
Coomassie
S35-met.
siRNA: C2 S2
siRNA: C2 S2
Con.
H2A/H3
H2B
H4
%H2A/H3: 100 60
C
C2
S2
min. post HU: 0 30 60 0 30 60
H2A
7SK
1 2 3 4 5 6
%histone mRNA remaining
100
80
60
40
20
0
30
60
min. post HU
C2
S2

Figure 31. Properly processed replication-dependent histone mRNAs are localized to the endoplasmic reticulum. S1 nuclease protection assay to histone H2A, H3 and H3.3 mRNA. Total RNA from the ER and non-ER fractions (cytosol) of HeLa cell fractionations were simultaneously probed for the polyadenylated histone H3.3 mRNA and either replication-dependent histone H2A or H3 mRNA.

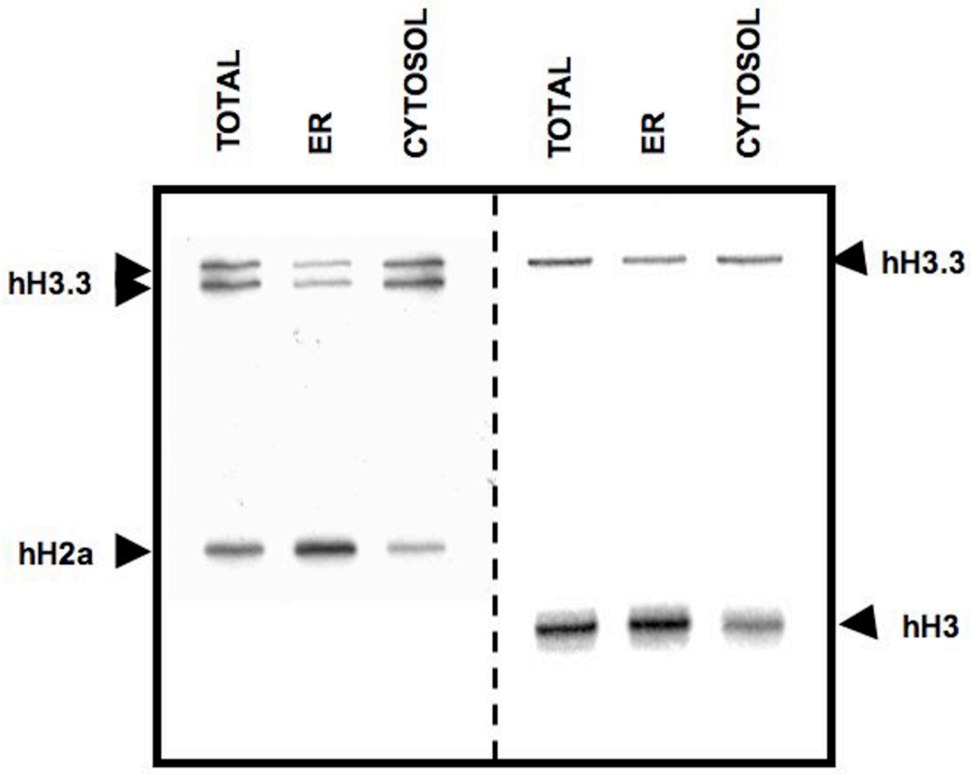
TOTAL
ER
CYTOSOL
TOTAL
ER
CYTOSOL
hH3.3
hH2a
hH3.3
hH3

Figure 32. Histone mRNA in SLBP knockdown cells is retained in the nucleus. (A) *In situ* hybridization to H2A mRNA is specific to the target histone mRNA. HeLa cells synchronized by double-thymidine block were released into S phase for 3 hours and treated with 5 mM hydroxyurea (HU) for 0, 15, 30 and 60 minutes. Cells were fixed and prepared for *in situ* hybridization. DAPI (blue), histone H2A mRNA (red). (B) Histone H3 mRNA is localized to the nucleus/nucleoli of HeLa cells when SLBP is knocked down. Logarithmically growing HeLa cells were treated with the indicated siRNAs and *in situ* hybridization performed to H3 mRNA. (C) Histone H3 mRNA is localized to the nucleus of U2OS cells when SLBP is knocked down. U2OS cells were treated with the indicated siRNAs and *in situ* hybridization performed to H3 mRNA as in (B). (D) Western blot control of fractionated U2OS cells treated with siRNA in (E). Total, nuclear, and cytoplasmic protein fractions were separated by 12% polyacrylamide gel electrophoresis and probed for Hsp90 and fibrillarin. (E) Histone H3 mRNA is enriched in the nuclear fraction of SLBP knockdown cells. Total RNA from cell fractionations from (D) were analyzed by Northern blot analysis and histone H3 mRNA and U1 snRNA simultaneously detected using a mixture of radiolabelled probes.

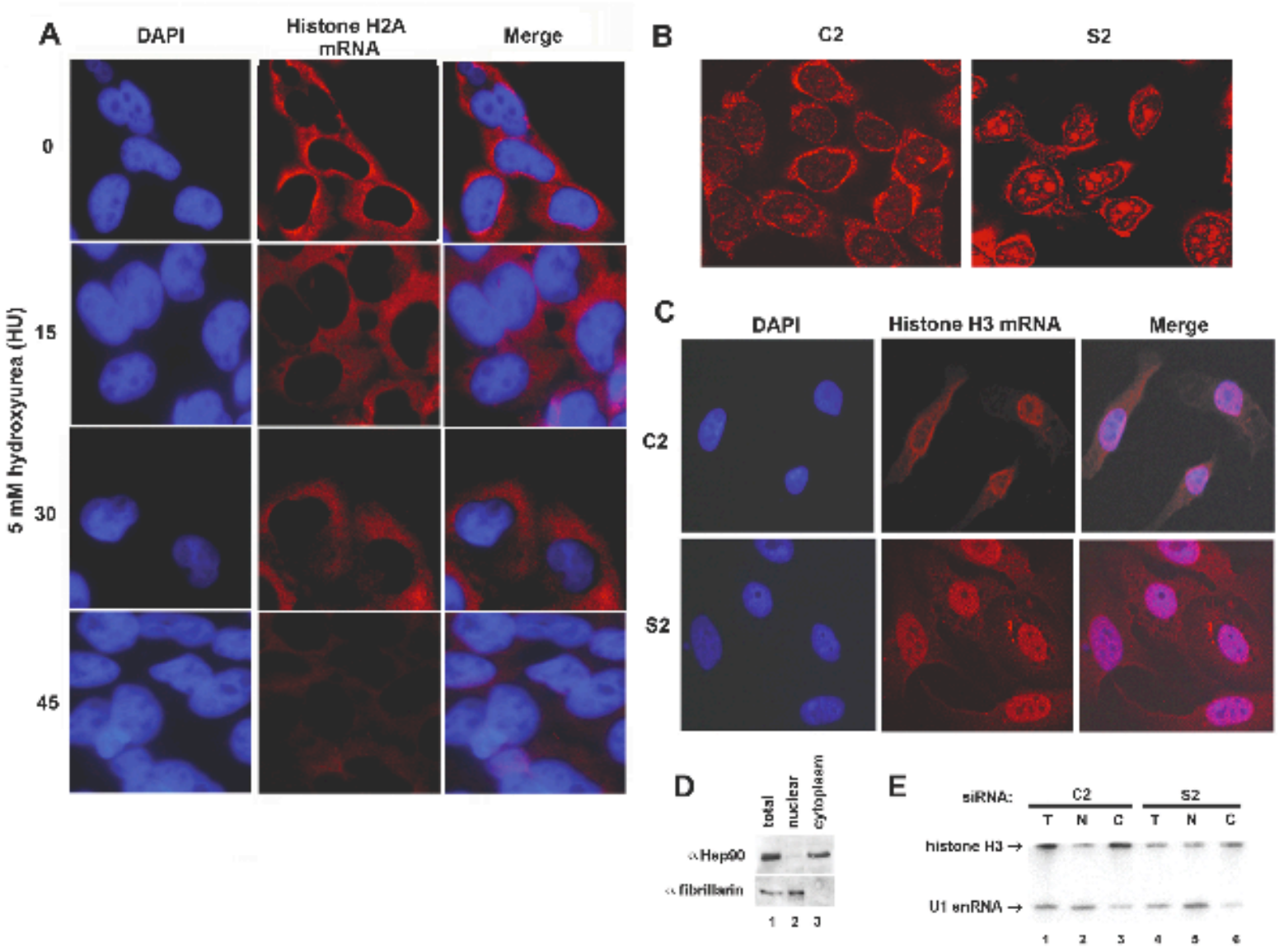
A
DAPI
Histone H2A mRNA
Merge
5 mM hydroxyurea (HU)
0
15
30
45
B
C2
S2
C
DAPI
Histone H3 mRNA
Merge
C2
S2
D
total
nuclear
cytoplasm
Hep90
fibrillarin
1 2 3
E
siRNA:
C2
S2
T N C T N C
histone H3
U1 snRNA
1 2 3 4 5 6

Figure 33. Model of SLBP-dependent histone mRNA export.

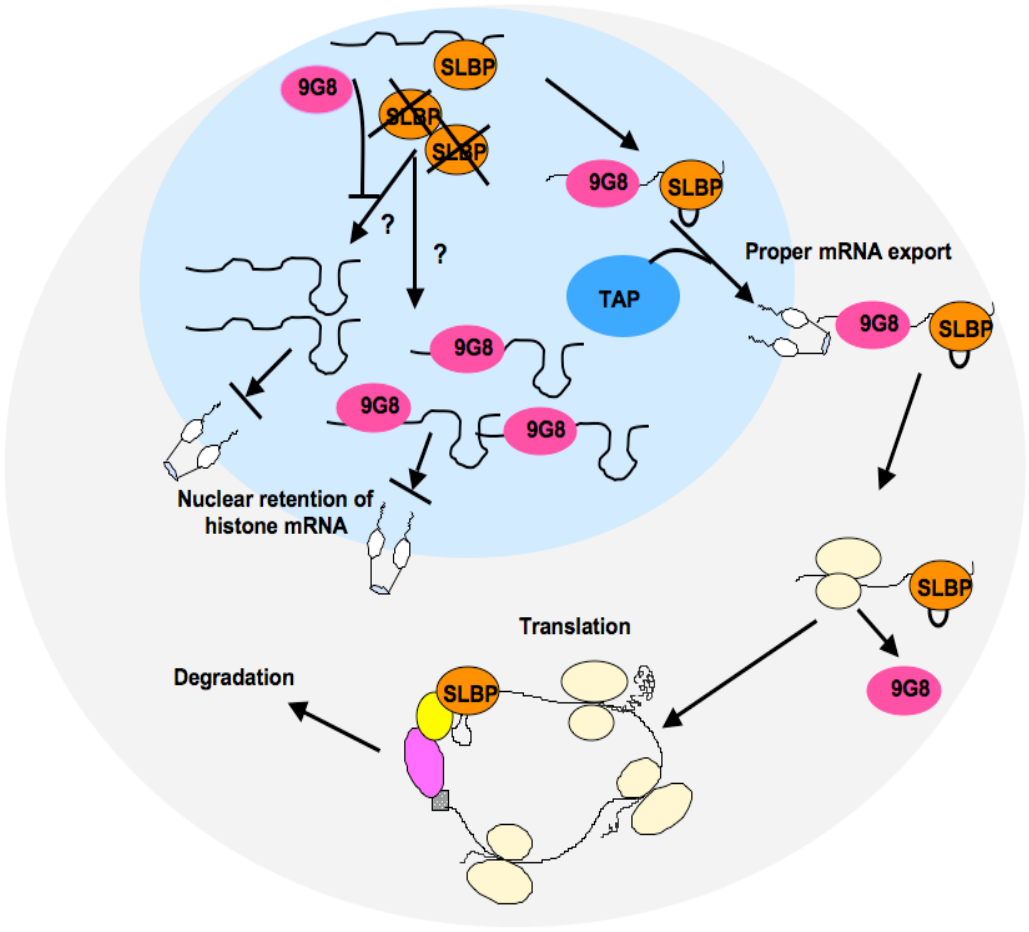
SLBP
9G8
SLBP
SLBP
?
?
9G8
SLBP
Proper mRNA export
TAP
9G8
SLBP
9G8
9G8
Nuclear retention of
histone mRNA
SLBP
Translation
9G8
Degradation
SLBP

CHAPTER 5

SUMMARY AND CONCLUSIONS

INTRODUCTION

The post-transcriptional regulation of histone mRNA metabolism in metazoans serves an important role in regulating histone protein synthesis to ensure proper chromatin formation. Evidence from fungi to humans clearly shows that altered histone gene expression is detrimental to the eukaryotic cell (Meeks-Wagner and Hartwell, 1986; Sullivan et al., 2001; Zhao et al., 2004). The rapid change in histone mRNA half-life that occurs when DNA replication is complete or when DNA synthesis is inhibited provides the cell the ability to balance the appropriate levels of histone protein synthesis with the demands of DNA synthesis. In this final chapter, I summarize the major findings from my dissertation and highlight some of the intriguing questions that my data raises. Additionally, I will provide a brief overview of the family of enzymes that possess terminal uridyltransferase activity and discuss the exciting, potentially widespread, contributions these enzymes may play in gene expression.

In this dissertation I have described evidence that has revealed a surprising mechanism of how histone mRNA degradation is regulated (Chapters 2 and 3). Together it suggests the initial step in histone mRNA degradation is the addition of

short uridine tails to the 3' end of histone mRNA. The addition of the oligo(U) tail is carried out by an enzyme with terminal uridyltransferase activity, likely by TUTase-1 and/or TUTase-3 (Chapter 3). Direct evidence from cRT-PCR and cloning experiments provide compelling data that individual molecules of histone mRNA are simultaneously degraded from both the 5' and 3' ends (Chapter 2). Although I have identified a number of the components required for histone mRNA degradation (Chapters 2 and 3), how all the parts specifically function to regulate histone mRNA degradation is not clear.

LSM1-7: AN UNLIKELY PLAYER IN HISTONE mRNA DEGRADATION

The Lsm1-7 complex is a positive regulator of decapping and 5'-3' degradation in eukaryotes (Tharun et al., 2000; Tharun and Parker, 2001). Surprisingly, Lsm1 is required for histone mRNA degradation (Chapter 2). RNAi-mediated knockdown of Lsm1 resulted in a dramatic stabilization of histone mRNA when DNA synthesis was inhibited (Chapter 2). I was very surprised by this evidence since genetic studies show the Lsm1-7 complex functions following deadenylation and prior to decapping (Tharun and Parker, 2001). Biochemical experiments have shown Sm-like proteins have an affinity to A-rich and U-rich RNA sequences and in support of this, Lsm1-7 has been shown to bind to short stretches of adenine or uridine and mixtures of both (AU-rich) (Chowdhury et al., 2007; Wilusz and Wilusz, 2005). Since replication-dependent histone mRNAs are not polyadenylated and do not contain remarkable AU-rich elements in the 3' UTR, the initial finding was puzzling. It was the Lsm1 finding that subsequently allowed me to

develop a hypothesis-driven approach to further understand histone mRNA degradation.

The initial finding prompted me to ask if Lsm1 (and likely the Lsm1-7 complex) was present in a complex with SLBP at the 3' end of histone mRNA under conditions where histone mRNA is rapidly degraded. Immunoprecipitation of an HA-tagged SLBP coprecipitated Lsm1 in a hydroxyurea-dependent manner, but this interaction was sensitive to RNase treatment suggesting Lsm1-7 binds directly to the 3' end of histone mRNA (Chapter 2). I initially hypothesized Lsm1-7 was either binding the 3' stemloop or somewhere else in the 3' UTR. Based on the literature at the time, it was also possible that A tails were added (Kwak et al., 2004; LaCava et al., 2005; Sanchez and Marzluff, 2004). Scant evidence also suggested it was possible that short U tails could also be added post-transcriptionally to regulate mRNA stability (Shen and Goodman, 2004). To determine precisely the 3' end of histone mRNA under conditions where histone mRNA was degraded, I used a cRT-PCR and cloning strategy. As discussed in chapters 2 and 3 of this dissertation the cRT-PCR approach combined with a complimentary oligo(dA) RT-PCR strategy produced a number of interesting findings, including the immutable presence of 8-15 nonencoded uridine residues on the 3' end of histone mRNA degradation intermediates that were decapped, but nearly full-length (Chapter 2). Together this evidence provided a model in which the oligo(U) tail is added and Lsm1-7 subsequently binds the oligo(U) tail to regulate the recruitment of the 5'-3' and 3'-5' degradation machinery (Chapter 3).

REPLICATION-DEPENDENT HISTONE mRNA DEGRADATION: EVOLUTIONARY REMNANTS OF BACTERIAL mRNA DEGRADATION?

The mechanism of histone mRNA degradation is strikingly reminiscent of the bacterial mRNA degradation pathway. Bacterial mRNAs often have structured stemloop structures on the 3' end, presumably to function in protecting the 3' end from degradation (Kushner, 2004). Bacterial mRNA degradation is initiated by polyadenylation of the 3' end where the poly(A) tail length is regulated by PNPase (Kushner, 2004). The activity of PNPase and the Sm-like heptameric complex Hfq recruit subsequent degradation from the 3' end by the degradosome, an exosome-like complex of 3'-5' exonucleases (Mohanty and Kushner, 2000; Wilusz and Wilusz, 2005). Multiple rounds of adenylation followed degradation are required to degrade the highly structured 3' ends present on bacterial mRNAs, and this readenylation functions to re-prime the degradosome.

The above mechanism is analogous to the strategy human cells use to rapidly degrade replication-dependent histone mRNA. In place of the addition of a poly(A) tail to target bacterial mRNAs for degradation, histone mRNAs are oligouridylated to specify their targeted destruction. In both pathways, an Sm-like complex associates with the nontemplated addition of A or U to the 3' end and this protein complex (Hfq or Lsm1-7) subsequently coordinates the recruitment of the degradation machinery. Moreover, I frequently obtained clones that had oligo(U) tails added within the stemloop sequence, suggesting that the human exosome likely needs to be re-primed to degrade through the structured 3' end of histone mRNAs, as has also been reported for bacterial mRNAs.

As Carol and Jeff Wilusz have suggested (Wilusz and Wilusz, 2008), the mechanism of histone mRNA degradation may also function to regulate the stability of structured noncoding RNAs such as rRNA and tRNAs, that are also not polyadenylated. Another interesting possibility proposed (Wilusz and Wilusz, 2008), is that oligouridylation could additionally act as an innate immune defense mechanism against flaviviruses such as Hepatitis C, Dengue, and West Nile viruses. The viral transcripts of these viruses are not polyadenylated but rather have stabilizing secondary structures at their 3' end (Gritsun and Gould, 2007). It is possible the host cell uses the same machinery used to degrade histone mRNA to also prevent viral infection by flaviviruses. In addition to the above speculation, there is a good likelihood that other mRNAs in the cell are substrates for 3' oligouridylation. Most cDNA libraries that exist were produced by oligo(dT)-primed reverse transcription to obtain expressed mRNAs that were polyadenylated. It would be interesting to ponder the potential abundance of clones that would exist if cDNA libraries from different cell types were to be made by oligo(dA)-primed reverse transcription.

BIDIRECTIONAL DECAY IN MAMMALS: THE PREDOMINANT MECHANISM?

In Chapter 2 I showed that individual histone mRNA molecules are simultaneously degraded from both the 5' and 3' ends. The functional requirement of components from both pathways (Lsm1, Dcp2, Xrn1, Rrp41, PM/Scl-100) as well as trapping histone mRNA degradation intermediates by cRT-PCR and cloning provided this evidence (Chapters 2 and 3). Although this provides the first direct

evidence for bidirectional decay of a physiologically important mRNA, two other reports suggest that mammalian cells use both pathways for mRNA degradation (Lejeune et al., 2003; Murray and Schoenberg, 2007). Even though both pathways exist in budding yeast, the 5'-3' pathway has been suggested to predominate (Cao and Parker, 2001, 2003). Despite the estimated importance of the 5'-3' pathway in yeast, evidence suggests the 5'-3' and 3'-5' are partially redundant (He et al., 2003; Houalla et al., 2006). There also likely exists some redundancy in humans, but the small amount of evidence that exists at this time points to the mammalian cell utilizing both pathways in a concerted manner to rapidly and efficiently degrade mRNA (Lejeune et al., 2003; Mullen and Marzluff, 2008; Murray and Schoenberg, 2007). Bidirectional decay might simply be a necessary requirement of mammals due to the increased size of mammalian genomes compared to fungi. The increased genome size combined with the increased importance of alternative splicing in mammals likely presents a more complex set of total mRNAs in need of regulation. Bidirectional mRNA degradation may then represent an efficient mammalian strategy to rapidly and irreversibly eliminate the expression of a given mRNA. This could be particularly important in the nervous system where mRNA translation and stability contribute to the synaptic plasticity that underlies learning and memory (Giorgi et al., 2007; Schratt et al., 2006; Sutton and Schuman, 2006).

A FAMILY OF POLY(A) POLYMERASES / TERMINAL URIDYLTRANSFERASES EXISTS IN EUKARYOTES

The past 18 months have revealed the presence of a family of noncanonical poly(A) polymerases in eukaryotes that contain members that are not poly(A) polymerases at all, but are instead terminal uridyltransferases (Kwak and Wickens, 2007; Rissland et al., 2007; Trippe et al., 2006). In this section I will review the known functions of this family enzymes that exist in both yeast and humans and attempt to provide insight into the TUTases identified that potentially add oligo(U) to the 3' end of histone mRNAs.

Budding Yeast

Two noncanonical poly(A) polymerases (PAPs) exist in the genome in *S. cerevisiae* (Houseley et al., 2007; Houseley and Tollervey, 2006). This number is small in contrast to *S. pombe* and humans where their genomes possess 6 and 7 related proteins, respectively (Tables 6 and 7). The two PAPs present in *S. cerevisiae* include Trf4 and Trf5 that collectively function in a nuclear RNA surveillance complex known as TRAMP (Houseley et al., 2007; Houseley and Tollervey, 2006). The TRAMP complex is composed of Trf4, Trf5, Air1, Air2, and Mtr4 and together polyadenylate aberrant noncoding RNAs in the nucleus for subsequent degradation by the exosome (LaCava et al., 2005). *S. cerevisiae* Trf4 and Trf5 are strictly localized to the nucleus, particularly the nucleolus (Dez et al., 2006).

Fission Yeast

The fission yeast *S. pombe* has evolved 6 similar enzymes (Table 6). The majority of theses enzymes are localized in both the nucleus and cytoplasm, with some possessing strict cytoplasmic localization (Table 6). None of the members exhibit the strict nuclear localization observed by Trf4 and Trf5 in budding yeast, suggesting more diverse roles for these enzymes in the cytoplasm. The founding and best-characterized member of this family of proteins is Cid1 (caffeine-induced death suppressor), which was originally identified in a screen to identify components of the replication checkpoint (Wang et al., 1999). It was originally suspected Cid1 was a DNA polymerase that somehow functioned in regulating DNA synthesis and the replication checkpoint (Wang et al., 1999). However, Cid1 is strictly localized to the cytoplasm (Read et al., 2002). Later work then showed Cid1 functioned to stabilize subsets of mRNAs in the cytoplasm by polyadenylation upon replication stress such as hydroxyurea exposure and DNA damage (Read et al., 2002). However in this same paper Read and colleagues showed that in addition to possessing substantial poly(A) activity *in vitro*, recombinantly expressed and purified Cid1 possessed substantial poly(U) activity, but not poly(C) or poly(G) (Read et al., 2002). The significance of the poly(U) activity was overlooked until Rissland, Norbury and coworkers recently resolved this biochemical complexity (Rissland et al., 2007). It was shown that when Cid1 was purified from *S. pombe* cells and not from *E. coli*, Cid1 purified from yeast was now strictly a poly(U) polymerase *in vitro* and possessed minimal, unremarkable poly(A) activity (Rissland et al., 2007). These results strongly imply that copurifying cofactors that originate from intact yeast

cells are responsible for dictating the uridine specificity of Cid1 *in vivo*. No convincing physiologic target mRNA substrates of Cid1 have been characterized.

The Moazed lab has defined the nuclear roles for Cid12 and Cid14, although both proteins also localize to the cytoplasm (Table 6). Cid12 and Cid14 function in distinct processes that work to silence heterochromatin in *S. pombe* (Buhler et al., 2007; Buhler et al., 2006; Motamedi et al., 2004). Cid12 functions as a poly(A) polymerase in an RNA-directed RNA polymerase complex (RDRC) that also contains the RNA helicase Hrr1 (similar to human Upf1), the histone methyltransferase Clr4, and the RNA-dependent RNA polymerase Rdp1 (Motamedi et al., 2004). The RDRC complex interacts with the RNAi-induced transcriptional silencing complex (RITS) that together function to silence noncoding centromeric transcripts (Motamedi et al., 2004). In an alternative pathway to silence centromeric transcripts, Cid14 is present in a TRAMP-like complex with Air1 and Mtr4 in the nucleus and has been show to polyadenylate centromeric transcripts for direct degradation by the exosome (Buhler et al., 2007; Buhler et al., 2006). Cid14 polyadenylated transcripts can also be silenced by the Cid12-containing RDRC dependent mechanism (Buhler et al., 2007; Buhler et al., 2006).

Cid13 has been shown to be a cytoplasmic poly(A) polymerase that is important in DNA replication and genome maintenance (Saitoh et al., 2002). Saitoh and coworkers have shown that Cid13 functions to stabilize *SUC22* mRNA, which encodes a subunit of ribonucleotide reductase that maintains the pool of dNTPs present in the cell (Saitoh et al., 2002). When wild-type fission yeast are treated with HU over time, the length of *SUC22* poly(A) tail length increases, suggesting Cid13

stabilizes a small set of mRNAs in the cell upon replication stress. In support of this, yeast mutant for Cid13 have slightly shorter *SUC22* poly(A) tails (Saitoh et al., 2002). Additionally, myc-tagged Cid13 purified from yeast cells has poly(A) polymerase activity *in vitro*, but not any remarkable poly(U), (C), or (G) activity (Saitoh et al., 2002). The above evidence from fission yeast implies a recurring role for the Cid-family of enzymes in DNA replication, replication stress, and genome integrity. Although it is not clear which Cid protein the TUTases (TUTase-1, TUTase-3) in humans I identified represent, it is possible there exists an evolutionary significance to these similarities. Modulation of gene expression at the post-transcriptional level could be a widespread mechanism for the eukaryotic cell to fine tune the complex process of DNA replication to ensure the fidelity of both the DNA and chromatin formation.

Cid11 and Cid16 have no defined roles in fission yeast. However a genome-wide cellular localization study has shown that Cid11 is localized to both the cytoplasm and nucleus while Cid16 is localized strictly to the cytoplasm (Matsuyama et al., 2006). As I have explained, a number of studies conducted in fission yeast have revealed significant poly(A) activity *in vitro* for the Cid1 family of proteins and because of these studies it has led to the initial characterization of these enzymes as noncanonical poly(A) polymerases (Stevenson and Norbury, 2006). However, recent evidence from *Xenopus* oocytes (Kwak and Wickens, 2007) and even more recent from human cells (Gonzales et al., 2008; Mellman et al., 2008; Mullen and Marzluff, 2008), ensure the story is much more exciting.

Metazoans

Homologs of the “noncanonical poly(A) polymerases” that exist in fission yeast are also found in higher eukaryotes. Kwak and Wickens identified several homologs in plants, worms, and humans and tested their ability to add poly(A), (U), (C) and (G) using a combination of an MS2-tethering assay in Xenopus oocytes and molecular biology (Kwak and Wickens, 2007). Surprisingly, they found that 3 of the 7 PAPD-containing proteins in humans (TUTase-4, -7 and the U6 TUTase) exhibited poly(U) polymerase activity in their *Xenopus* system and *in vitro* using purified peptides (Kwak and Wickens, 2007), (Table 7). In Chapter 3, I identified TUTase-1 and TUTase-3 as putative TUTases that are required for histone mRNA degradation (Mullen and Marzluff, 2008) and provided preliminary biochemical activity demonstrating TUTase-3 had oligo(U) activity *in vitro* (Chapter 3).

Attempts to predict the closest orthologs of TUTase-1 and TUTase-3 in fission yeast by sequence alignment and phylogenetic analysis has not revealed any definitive insight into their potential function (Figure 34). SpCid1 and TUTase-7 have been shown to be functional homologs (Rissland et al., 2007), although significant sequence divergence exists and prevents them from reliably grouping with one another in phylogenetic analyses (Figure 34), at least using distrance matrix algorithms. Based on Figure 34, the closest *S. pombe* relatives appear to be Cid14 and Cid12. Cid14 has been shown to function in a nuclear TRAMP-like complex to silence heterochromatin at centromeres (Buhler et al., 2007; Buhler et al., 2006). However, Cid14 is also localized to the cytoplasm (the site of histone mRNA degradation in human cells) and no cytoplasmic role for Cid14 exists at this time.

Cid12 functions in the nucleus in the RDRC-RITS complex to polyadenylate centromeric repeat transcripts for subsequent silencing of ongoing centromeric transcripts via the production of small dsRNAs (Motamedi et al., 2004). Interestingly, recombinantly expressed and purified Cid12 exhibits robust poly(U) activity *in vitro* (but not poly(C) or poly(G)), in addition to the established poly(A) activity (Mario Halic and Danesh Moazed, personal communication). Therefore, it is possible the unpublished poly(U) activity of Cid12 could be reserved for its function in the cytoplasm.

TUTase-1 reproducibly scored positively in an RNAi screen to the 7 putative TUTases in the human genome (Chapter 3). TUTase-1 has been fairly well characterized in humans to be a poly(A) polymerase that is required for polyadenylation of mitchonridal mRNAs (hmtPAP) (Nagaike et al., 2005; Tomecki et al., 2004). Many mitochondrial mRNAs terminate in a single U and polyadenylation in the mitochondria has been suggested to provide the UAA stop codon (Slomovic et al., 2005). hmtPAP/TUTase-1 has also been shown to colocalize in subcellular foci that overlap with a mitochondrial marker (Nagaike et al., 2005; Tomecki et al., 2004). Moroever, it has been predicted that Cid16 represents the homolog of hmtPAP/TUTase-1 (Table 5) (Stevenson and Norbury, 2006). The phylogenetic tree in Figure 34 supports this prediction since TUTase-1 closely groups with SpCid16. It is possible that TUTase-1 screened falsely positive in my RNAi screen (Chapter 3). Like many of the PAPD-containing proteins, hmtPAP/TUTase-1 lacks an RNA recognition motif (RRM) and these enzymes likely require other cofactors to impart their RNA specificity. That said, it is equally possible that TUTase-1 has dual

functions in the cell, one being outside of the mitochondria and specified by a unique set of proteins that define its specificity. Equally possible is that TUTase-1 functions in the mitochondria to coordinate the replication of mitochondrial DNA and its proper packaging. Further work is required to determine the role TUTase-1 plays in histone mRNA degradation.

The best characterized of the human PAPD-containing enzymes is the U6 TUTase. Trippe and coworkers cloned and characterized the U6 TUTase and showed that the U6 TUTase specifically added uridine residues to the U6 snRNA (Trippe et al., 2006). Most recently however, a thought provoking study from Mellman and coworkers suggest the U6 TUTase can also function as a poly(A) polymerase (Mellman et al., 2008). StarPAP is the same enzyme as the U6 TUTase and can be regulated to be a PAP by phosphatidylinositol 4,5 bisphosphate (PtdIns4,5P_2), a phospholipid that functions in lipid signaling in the cell (Mellman et al., 2008). Only when starPAP is bound to PtdIns4,5P_2, but not other phospholipids, does starPAP exhibit poly(A) polymerase activity *in vitro* (Mellman et al., 2008). In agreement with Trippe et al., starPAP also possesses poly(U) activity *in vitro* but when bound by PtdIns4,5P_2, starPAP exhibits exclusive ATP incorporation (Mellman et al., 2008).

The group shows starPAP is required as an alternative PAP when human cells are exposed to oxidative stress (Mellman et al., 2008). starPAP interacts with the cleavage and polyadenylation stimulating factors (CPSFs; CPSF73, CPFS100, and Symplekin as well as RNA pol II) and is required to polyadenylate and stabilize particular mRNAs that encode factors essential to elicit the cell's oxidative stress

response (Mellman et al., 2008). Strangely, their functional experiments using RNAi did not result in the cell lethality that I and Trippe et al. had observed when knocking down the U6 TUTase (Mullen and Marzluff, 2008; Tsukada et al., 2006). It is possible their transfection efficiency or siRNA sequence resulted in inefficient knockdown of starPAP/U6 TUTase and this serendipitously provided an ideal hypomorphic phenotype to elucidate the enzyme's role in alternative nuclear polyadenylation.

It is interesting to speculate that phospholipids play critical functions in regulating RNA enzymes. Recent crystallographic studies from Macbeth and Bass have revealed the adenosine deaminase 2 (ADAR2), an RNA editing enzyme in eukaryotes, contains an inositol hexakisphosphate (IP_6) molecule that is buried in the enzyme core and contributes to the protein fold (Macbeth et al., 2005). Functional experiments show that the amino acids that make contact with IP_6 as well as IP_6 itself are required for ADAR2 editing activity (Macbeth et al., 2005). Therefore, it could be possible that lipid signaling events that sense the end of S phase or the inhibition of DNA replication could impact the enzymatic activity of TUTase-1 and/or TUTase-3 to specifically add uridine residues to the 3' end of histone mRNAs as well as potentially other unidentified mRNA substrates.

SUMMARY

My dissertation has revealed new insight into the mechanism that regulates the rapid degradation of histone mRNA. Despite the fact that we now know a number of the factors that regulate histone mRNA degradation, we still do not know

specifically how translation termination factors, Upf1, a TUTase, Lsm1-7 and the 5'-3' and 3'-5' degradation enzymes specifically function to result in efficient decay of histone mRNA. It is likely the SURF complex containing SMG-1, Upf1, eRF3, and eRF1 is recruited to the 3' end of histone mRNA when translation is terminated under conditions when histone mRNA is signaled for degradation. The RNA helicase activity of Upf1 could help remodel the mRNP present on the 3' end of histone mRNA by interacting with SLBP and provide the TUTase access to the 3' end for subsequent oligouridylation. At this point, my data suggests it is Lsm1-7 that likely binds the oligo(U) tail to regulate decapping and Xrn1, as well as the exosome activity, to the mRNA. How exactly are the 5'-3' decay machinery and exosome recruited to act on the same histone mRNA molecule? Yeast mutant for Lsm1 have stabilized mRNAs that have their 3' ends trimmed, suggesting that Lsm1-7 blocks the 3'-5' activity of the exosome (He and Parker, 2001). It is possible that Lsm1-7 is rapidly dissociated following activation of the 5' decapping enzymes (Dcp1/Dcp2) by the exosome and access to the 3' end unhindered at this point. It is also possible Lsm1-7 is required for recruitment of both decapping activity as well as the exosome since biochemical approaches have shown that Lsm1 and other components of the Lsm1-7 complex physically interact with subunits of the exosome (Lehner and Sanderson, 2004). SLBP does appear to be required for histone mRNA degradation since downregulation of SLBP protein by RNAi reduced the rate of histone H2A mRNA degradation compared to a control (Chapter 4). Since reduced expression of SLBP protein resulted in nuclear retention of processed histone mRNAs, I was not able to conclude any specific role that SLBP plays in histone mRNA degradation.

However, the SLBP:Upf1 interaction that occurs on the 3' end under conditions of histone mRNA degradation (Kaygun and Marzluff, 2005a) suggests SLBP plays an important role, likely by playing a central role in the formation of a histone mRNP that is primed for degradation under the appropriate cellular circumstances.

As the past 4 years have shown (Kaygun and Marzluff, 2005a, b; Mullen and Marzluff, 2008; Muller et al., 2007), we have made major strides towards understanding a detailed mechanism of how the half-life of mammalian replication-dependent histone mRNAs is regulated both when DNA synthesis is inhibited and upon the completion of DNA replication. Through my dissertation work I have uncovered a novel mechanism that regulates the rapid degradation of histone mRNA and involves oligouridylation followed by bidirectional degradation of the mRNA. In time, the pursuit by fellow colleagues and other scientists will likely reveal how the different components function to rapidly degrade histone mRNA.

Table 6. List of the Cid family of enzymes present in *S. pombe*. (C. e.) *C. elegans*, (S. c.) *S. cerevisiae*,

Noncanonical PAP/TUTase	Presumed orthologues	Localization	Function/Activity	Reference
Cid1	Cid1 (*C.e.*), TUT-7, Hs2	Cytoplasmic	Checkpoint response to replication block, TUTase	Rissland et al., 2007
Cid11	Unknown	Nuclear and cytoplasmic	Unknown	Matsuyama et al., 2006
Cid12	RDE-3 (*C.e.*)	Nuclear and cytoplasmic	RNAi-dependent transcriptional silencing, PAP, TUTase?	Motamedi et al., 2004
Cid13	Unknown	Nuclear and cytoplasmic	Maintains dNTP pools via ribonucleotide reductase mRNA,	Saitoh et al., 2002
Cid14	*S.c*. Trf4, Trf5	Nuclear and cytoplasmic	Exosome mediated degradation of RNAs, heterochromatic gene silencing, PAP	Buhler et al., 2007; Win et al., 2006
Cid16	hmtPAP	Cytoplasmic, mitochondrial?	unknown	Matsuyama et al., 2006; Stevenson and Norbury, 2006

Table 7. List of poly(A) polymerase-associated domain (PAPD)-containing proteins present in the human genome. The proteins listed are characterized terminal uridylyltransferases (TUTase), poly(A) polymerases (PAP), or currently uncharacterized.

TUTase	Other Names	Localization	Activity	Reference
TUTase-1	PAPD1, mtPAP, Q9NVV4	Mitochondrial, cytoplasmic	Mitochondrial PAP, putative histone TUTase	Nagaike et al., 2005; Tomecki et al., 2004, Mullen and Marzluff, 2008
TUTase-2	PAPD4, GLD2, Q6PIY7	Cytoplasmic	Cytoplasmic PAP	Kwak et al., 2004
TUTase-3	PAPD5, Q8NDF8, TRF4-2	Cytoplasmic and nuclear, predominantly cytoplasmic	Putative histone TUTase	Mullen and Marzluff, 2008
TUTase-4	Hs3, Q5TAX3	Unknown	TUTase	Kwak and Wickens, 2007
TUTase-5	Pol sigma, TRF4-1,	Unknown	Unknown	
U6 TUTase	PAPD2, Hs5, starPAP	Nucleolar, nuclear	TUTase for U6 snRNA, PAP for stress response	Trippe et al., 2006; Mellman et al., 2008
TUTase 7	PAPD6, Hs2, ZCCHC6, Cid1,	Cytoplasmic	TUTase	Rissland et al., 2007; Kwak and Wickens, 2007

Figure 34. Phylogenetic tree comparing the PAPD-containing proteins present in the genomes of humans, budding yeast, and fission yeast. Pairwise amino acid sequence alignments were performed using ClustalW software and a rooted phylogenetic tree constructed using distance matrix algorithms. The canonical human poly(A) polymerase α (PAPα) was used as the outgroup. (Sp), *S. pombe;* (Sc), *S. cerevisiae*.

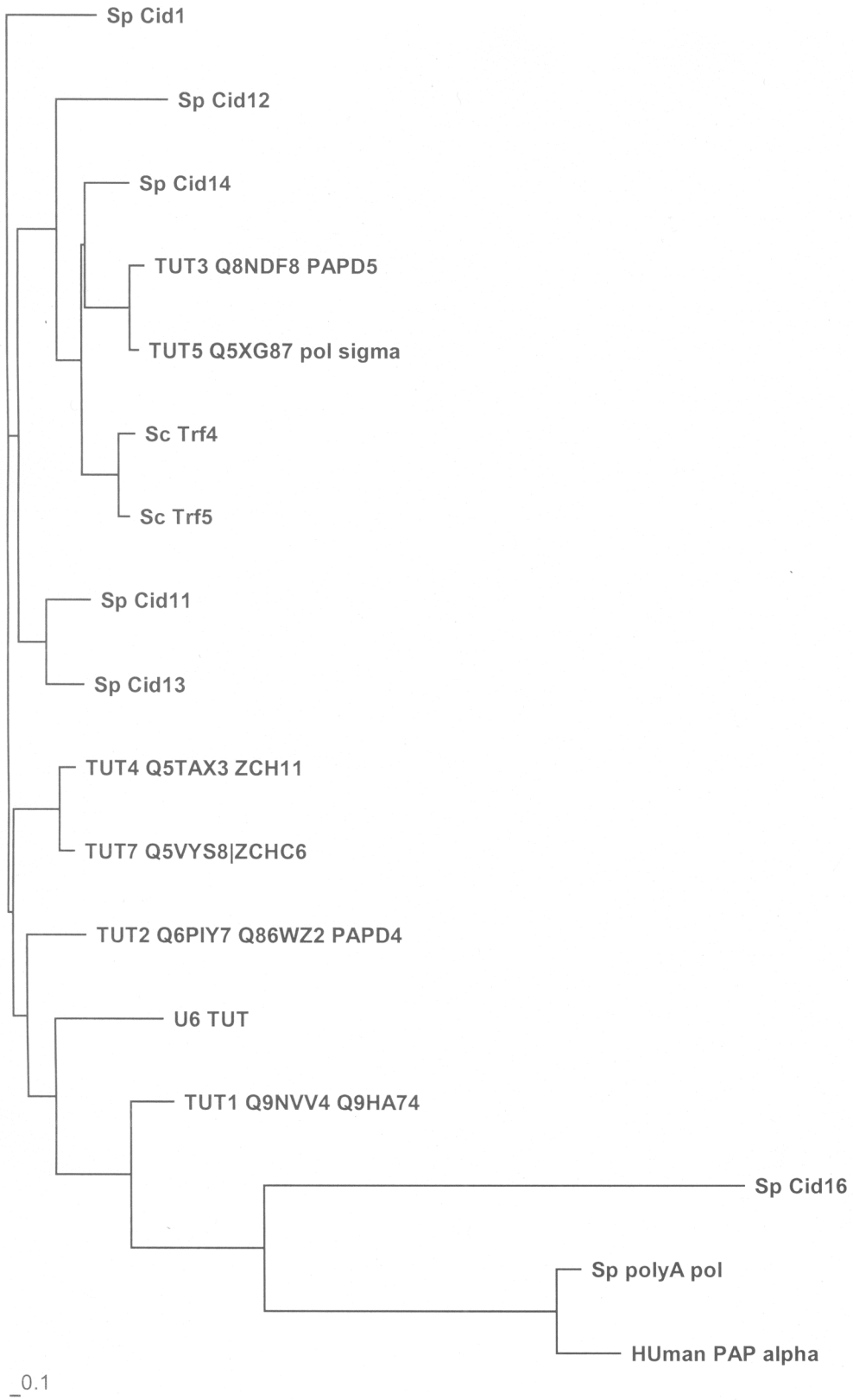
Sp Cid1
Sp Cid12
Sp Cid14
TUT3 Q8NDF8 PAPD5
TUT5 Q5XG87 pol sigma
Sc Trf4
Sc Trf5
Sp Cid11
Sp Cid13
TUT4 Q5TAX3 ZCH11
TUT7 Q5VYS8|ZCHC6
TUT2 Q6PIY7 Q86WZ2 PAPD4
U6 TUT
TUT1 Q9NVV4 Q9HA74
Sp Cid16
Sp polyA pol
HUman PAP alpha
_0.1

REFERENCES

Adler, B.K., and Hajduk, S.L. (1997). Guide RNA requirement for editing-site-specific endonucleolytic cleavage of preedited mRNA by mitochondrial ribonucleoprotein particles in Trypanosoma brucei. Mol Cell Biol *17*, 5377-5385.

Akimitsu, N. (2008). Messenger RNA surveillance systems monitoring proper translation termination. J Biochem *143*, 1-8.

Allmang, C., Kufel, J., Chanfreau, G., Mitchell, P., Petfalski, E., and Tollervey, D. (1999). Functions of the exosome in rRNA, snoRNA and snRNA synthesis. EMBO J *18*, 5399-5410.

Amrani, N., Ganesan, R., Kervestin, S., Mangus, D.A., Ghosh, S., and Jacobson, A. (2004). A faux 3'-UTR promotes aberrant termination and triggers nonsense-mediated mRNA decay. Nature *432*, 112-118.

Andrews, N.C., and Baltimore, D. (1986). Purification of a terminal uridylyltransferase that acts as host factor in the in vitro poliovirus replicase reaction. Proc Natl Acad Sci U S A *83*, 221-225.

Aphasizhev, R., Aphasizheva, I., and Simpson, L. (2003). A tale of two TUTases. Proc Natl Acad Sci U S A *100*, 10617-10622.

Azzouz, T.N., Gruber, A., and Schumperli, D. (2005a). U7 snRNP-specific Lsm11 protein: dual binding contacts with the 100 kDa zinc finger processing factor (ZFP100) and a ZFP100-independent function in histone RNA 3' end processing. Nucleic Acids Res *33*, 2106-2117.

Azzouz, T.N., Pillai, R.S., Dapp, C., Chari, A., Meister, G., Kambach, C., Fischer, U., and Schumperli, D. (2005b). Toward an assembly line for U7 snRNPs: interactions of U7-specific Lsm proteins with PRMT5 and SMN complexes. J Biol Chem *280*, 34435-34440.

Badis, G., Saveanu, C., Fromont-Racine, M., and Jacquier, A. (2004). Targeted mRNA degradation by deadenylation-independent decapping. Mol Cell *15*, 5-15.

Bagga, S., Bracht, J., Hunter, S., Massirer, K., Holtz, J., Eachus, R., and Pasquinelli, A.E. (2005). Regulation by let-7 and lin-4 miRNAs results in target mRNA degradation. Cell *122*, 553-563.

Belgrader, P., Cheng, J., Zhou, X., Stephenson, L.S., and Maquat, L.E. (1994). Mammalian nonsense codons can be cis effectors of nuclear mRNA half-life. Mol Cell Biol *14*, 8219-8228.

Berger, S.L., and Cooper, H.L. (1975). Very short-lived and stable mRNAs from resting human lymphocytes. Proc Natl Acad Sci U S A *72*, 3873-3877.

Bernstein, E., Caudy, A.A., Hammond, S.M., and Hannon, G.J. (2001). Role for a bidentate ribonuclease in the initiation step of RNA interference. Nature *409*, 363-366.

Blum, E., Carpousis, A.J., and Higgins, C.F. (1999). Polyadenylation promotes degradation of 3'-structured RNA by the Escherichia coli mRNA degradosome in vitro. J Biol Chem *274*, 4009-4016.

Bouveret, E., Rigaut, G., Shevchenko, A., Wilm, M., and Seraphin, B. (2000). A Sm-like protein complex that participates in mRNA degradation. EMBO J *19*, 1661-1671.

Brown, C.E., Tarun, S.Z., Jr., Boeck, R., and Sachs, A.B. (1996). PAN3 encodes a subunit of the Pab1p-dependent poly(A) nuclease in Saccharomyces cerevisiae. Mol Cell Biol *16*, 5744-5753.

Brumbaugh, K.M., Otterness, D.M., Geisen, C., Oliveira, V., Brognard, J., Li, X., Lejeune, F., Tibbetts, R.S., Maquat, L.E., and Abraham, R.T. (2004). The mRNA surveillance protein hSMG-1 functions in genotoxic stress response pathways in mammalian cells. Mol Cell *14*, 585-598.

Buhler, M., Haas, W., Gygi, S.P., and Moazed, D. (2007). RNAi-dependent and -independent RNA turnover mechanisms contribute to heterochromatic gene silencing. Cell *129*, 707-721.

Buhler, M., Verdel, A., and Moazed, D. (2006). Tethering RITS to a nascent transcript initiates RNAi- and heterochromatin-dependent gene silencing. Cell *125*, 873-886.

Burdon, R.H., and Smellie, R.M. (1961). The incorporation of uridine 5'-triphosphate into ribonucleic acid by enzyme fractions from Ehrlich ascites carcinoma cells. Biochim Biophys Acta *51*, 153-162.

Cabrera, C.V., Lee, J.J., Ellison, J.W., Britten, R.J., and Davidson, E.H. (1984). Regulation of cytoplasmic mRNA prevalence in sea urchin embryos. Rates of appearance and turnover for specific sequences. J Mol Biol *174*, 85-111.

Cakmakci, N.G., Lerner, R.S., Wagner, E.J., Zheng, L., and Marzluff, W.F. (2008). SLIP1, a factor required for activation of histone mRNA translation by the stem-loop binding protein. Mol Cell Biol *28*, 1182-1194.

Cao, D., and Parker, R. (2001). Computational modeling of eukaryotic mRNA turnover. RNA *7*, 1192-1212.

Cao, D., and Parker, R. (2003). Computational modeling and experimental analysis of nonsense-mediated decay in yeast. Cell *113*, 533-545.

Caponigro, G., and Parker, R. (1996). Mechanisms and control of mRNA turnover in Saccharomyces cerevisiae. Microbiol Rev *60*, 233-249.

Casolari, J.M., Brown, C.R., Komili, S., West, J., Hieronymus, H., and Silver, P.A. (2004). Genome-wide localization of the nuclear transport machinery couples transcriptional status and nuclear organization. Cell *117*, 427-439.

Cazalla, D., Sanford, J.R., and Caceres, J.F. (2005). A rapid and efficient protocol to purify biologically active recombinant proteins from mammalian cells. Protein Expr Purif *42*, 54-58.

Cheadle, C., Fan, J., Cho-Chung, Y.S., Werner, T., Ray, J., Do, L., Gorospe, M., and Becker, K.G. (2005). Control of gene expression during T cell activation: alternate regulation of mRNA transcription and mRNA stability. BMC Genomics *6*, 75.

Chomczynski, P., and Sacchi, N. (1987). Single-step method of RNA isolation by acid guanidinium thiocyanate-phenol-chloroform extraction. Anal Biochem *162*, 156-159.

Chomczynski, P., and Sacchi, N. (2006). The single-step method of RNA isolation by acid guanidinium thiocyanate-phenol-chloroform extraction: twenty-something years on. Nat Protoc *1*, 581-585.

Chowdhury, A., Mukhopadhyay, J., and Tharun, S. (2007). The decapping activator Lsm1p-7p-Pat1p complex has the intrinsic ability to distinguish between oligoadenylated and polyadenylated RNAs. RNA *13*, 998-1016.

Coller, J., and Parker, R. (2005). General translational repression by activators of mRNA decapping. Cell *122*, 875-886.

Coller, J.M., Tucker, M., Sheth, U., Valencia-Sanchez, M.A., and Parker, R. (2001). The DEAD box helicase, Dhh1p, functions in mRNA decapping and interacts with both the decapping and deadenylase complexes. RNA *7*, 1717-1727.

Costanzi, C., and Pehrson, J.R. (1998). Histone macroH2A1 is concentrated in the inactive X chromosome of female mammals. Nature *393*, 599-601.

Couttet, P., Fromont-Racine, M., Steel, D., Pictet, R., and Grange, T. (1997). Messenger RNA deadenylylation precedes decapping in mammalian cells. Proc Natl Acad Sci U S A *94*, 5628-5633.

Dasgupta, A., Zabel, P., and Baltimore, D. (1980). Dependence of the activity of the poliovirus replicase on the host cell protein. Cell *19*, 423-429.

Decker, C.J., and Parker, R. (1994). Mechanisms of mRNA degradation in eukaryotes. Trends Biochem Sci *19*, 336-340.

Dez, C., Houseley, J., and Tollervey, D. (2006). Surveillance of nuclear-restricted pre-ribosomes within a subnucleolar region of Saccharomyces cerevisiae. EMBO J *25*, 1534-1546.

Doherty, S.C., McKeown, S.R., McKelvey-Martin, V., Downes, C.S., Atala, A., Yoo, J.J., Simpson, D.A., and Kaufmann, W.K. (2003). Cell cycle checkpoint function in bladder cancer. J Natl Cancer Inst *95*, 1859-1868.

Doma, M.K., and Parker, R. (2006). Endonucleolytic cleavage of eukaryotic mRNAs with stalls in translation elongation. Nature *440*, 561-564.

Dominski, Z., Erkmann, J.A., Greenland, J.A., and Marzluff, W.F. (2001). Mutations in the RNA binding domain of stem-loop binding protein define separable requirements for RNA binding and for histone pre-mRNA processing. Mol Cell Biol *21*, 2008-2017.

Dominski, Z., Erkmann, J.A., Yang, X., Sanchez, R., and Marzluff, W.F. (2002). A novel zinc finger protein is associated with U7 snRNP and interacts with the stem-loop binding protein in the histone pre-mRNP to stimulate 3'-end processing. Genes Dev *16*, 58-71.

Dominski, Z., Sumerel, J., Hanson, R.J., and Marzluff, W.F. (1995). The polyribosomal protein bound to the 3' end of histone mRNA can function in histone pre-mRNA processing. RNA *1*, 915-923.

Dominski, Z., Yang, X.C., Kaygun, H., Dadlez, M., and Marzluff, W.F. (2003). A 3' exonuclease that specifically interacts with the 3' end of histone mRNA. Mol Cell *12*, 295-305.

Dominski, Z., Yang, X.C., and Marzluff, W.F. (2005a). The polyadenylation factor CPSF-73 is involved in histone-pre-mRNA processing. Cell *123*, 37-48.

Dominski, Z., Yang, X.C., Purdy, M., and Marzluff, W.F. (2005b). Differences and similarities between Drosophila and mammalian 3' end processing of histone pre-mRNAs. RNA *11*, 1835-1847.

Dominski, Z., Zheng, L.X., Sanchez, R., and Marzluff, W.F. (1999). Stem-loop binding protein facilitates 3'-end formation by stabilizing U7 snRNP binding to histone pre-mRNA. Mol Cell Biol *19*, 3561-3570.

Erkmann, J.A., Sanchez, R., Treichel, N., Marzluff, W.F., and Kutay, U. (2005a). Nuclear export of metazoan replication-dependent histone mRNAs is dependent on RNA length and is mediated by TAP. RNA *11*, 45-58.

Erkmann, J.A., Wagner, E.J., Dong, J., Zhang, Y., Kutay, U., and Marzluff, W.F. (2005b). Nuclear import of the stem-loop binding protein and localization during the cell cycle. Mol Biol Cell *16*, 2960-2971.

Eystathioy, T., Jakymiw, A., Chan, E.K., Seraphin, B., Cougot, N., and Fritzler, M.J. (2003). The GW182 protein colocalizes with mRNA degradation associated proteins hDcp1 and hLSm4 in cytoplasmic GW bodies. RNA *9*, 1171-1173.

Fan, J., Yang, X., Wang, W., Wood, W.H., 3rd, Becker, K.G., and Gorospe, M. (2002). Global analysis of stress-regulated mRNA turnover by using cDNA arrays. Proc Natl Acad Sci U S A *99*, 10611-10616.

Fenger-Gron, M., Fillman, C., Norrild, B., and Lykke-Andersen, J. (2005). Multiple processing body factors and the ARE binding protein TTP activate mRNA decapping. Mol Cell *20*, 905-915.

Friend, K., Lovejoy, A.F., and Steitz, J.A. (2007). U2 snRNP binds intronless histone pre-mRNAs to facilitate U7-snRNP-dependent 3' end formation. Mol Cell *28*, 240-252.

Frischmeyer, P.A., van Hoof, A., O'Donnell, K., Guerrerio, A.L., Parker, R., and Dietz, H.C. (2002). An mRNA surveillance mechanism that eliminates transcripts lacking termination codons. Science *295*, 2258-2261.

Fromont-Racine, M., Bertrand, E., Pictet, R., and Grange, T. (1993). A highly sensitive method for mapping the 5' termini of mRNAs. Nucleic Acids Res *21*, 1683-1684.

Funakoshi, Y., Doi, Y., Hosoda, N., Uchida, N., Osawa, M., Shimada, I., Tsujimoto, M., Suzuki, T., Katada, T., and Hoshino, S. (2007). Mechanism of mRNA deadenylation: evidence for a molecular interplay between translation termination factor eRF3 and mRNA deadenylases. Genes Dev *21*, 3135-3148.

Gallwitz, D. (1975). Kinetics of inactivation of histone mRNA in the cytoplasm after inhibition of DNA replication in synchronised HeLa cells. Nature *257*, 247-248.

Garneau, N.L., Wilusz, J., and Wilusz, C.J. (2007). The highways and byways of mRNA decay. Nat Rev Mol Cell Biol *8*, 113-126.

Gatfield, D., and Izaurralde, E. (2004). Nonsense-mediated messenger RNA decay is initiated by endonucleolytic cleavage in Drosophila. Nature *429*, 575-578.

Gautier, T., Abbott, D.W., Molla, A., Verdel, A., Ausio, J., and Dimitrov, S. (2004). Histone variant H2ABbd confers lower stability to the nucleosome. EMBO Rep *5*, 715-720.

Ge, H., Si, Y., and Wolffe, A.P. (1998). A novel transcriptional coactivator, p52, functionally interacts with the essential splicing factor ASF/SF2. Mol Cell *2*, 751-759.

Giorgi, C., Yeo, G.W., Stone, M.E., Katz, D.B., Burge, C., Turrigiano, G., and Moore, M.J. (2007). The EJC factor eIF4AIII modulates synaptic strength and neuronal protein expression. Cell *130*, 179-191.

Godfrey, A.C., Kupsco, J.M., Burch, B.D., Zimmerman, R.M., Dominski, Z., Marzluff, W.F., and Duronio, R.J. (2006). U7 snRNA mutations in Drosophila block histone pre-mRNA processing and disrupt oogenesis. RNA *12*, 396-409.

Goldstrohm, A.C., Greenleaf, A.L., and Garcia-Blanco, M.A. (2001). Co-transcriptional splicing of pre-messenger RNAs: considerations for the mechanism of alternative splicing. Gene *277*, 31-47.

Goldstrohm, A.C., Hook, B.A., Seay, D.J., and Wickens, M. (2006). PUF proteins bind Pop2p to regulate messenger RNAs. Nat Struct Mol Biol *13*, 533-539.

Gonsalvez, G.B., Tian, L., Ospina, J.K., Boisvert, F.M., Lamond, A.I., and Matera, A.G. (2007). Two distinct arginine methyltransferases are required for biogenesis of Sm-class ribonucleoproteins. J Cell Biol *178*, 733-740.

Gonzales, M.L., Mellman, D.L., and Anderson, R.A. (2008). Star-PAP is associated with and phosphorylated by the protein kinase CKIalpha which is also required for expression of select star-PAP target messenger RNA. J Biol Chem.

Gorgoni, B., Andrews, S., Schaller, A., Schumperli, D., Gray, N.K., and Muller, B. (2005). The stem-loop binding protein stimulates histone translation at an early step in the initiation pathway. RNA *11*, 1030-1042.

Graham, A.C., Kiss, D.L., and Andrulis, E.D. (2006). Differential distribution of exosome subunits at the nuclear lamina and in cytoplasmic foci. Mol Biol Cell *17*, 1399-1409.

Graveley, B.R. (2000). Sorting out the complexity of SR protein functions. RNA *6*, 1197-1211.

Graves, R.A., and Marzluff, W.F. (1984). Rapid reversible changes in the rate of histone gene transcription and histone mRNA levels in mouse myeloma cells. Mol Cell Biol *4*, 351-357.

Graves, R.A., Pandey, N.B., Chodchoy, N., and Marzluff, W.F. (1987). Translation is required for regulation of histone mRNA degradation. Cell *48*, 615-626.

Grimson, A., O'Connor, S., Newman, C.L., and Anderson, P. (2004). SMG-1 is a phosphatidylinositol kinase-related protein kinase required for nonsense-mediated mRNA Decay in Caenorhabditis elegans. Mol Cell Biol *24*, 7483-7490.

Gritsun, T.S., and Gould, E.A. (2007). Origin and evolution of 3'UTR of flaviviruses: long direct repeats as a basis for the formation of secondary structures and their significance for virus transmission. Adv Virus Res *69*, 203-248.

Groth, A., Rocha, W., Verreault, A., and Almouzni, G. (2007). Chromatin challenges during DNA replication and repair. Cell *128*, 721-733.

Gunjan, A., Paik, J., and Verreault, A. (2005). Regulation of histone synthesis and nucleosome assembly. Biochimie *87*, 625-635.

Gunjan, A., and Verreault, A. (2003). A Rad53 kinase-dependent surveillance mechanism that regulates histone protein levels in S. cerevisiae. Cell *115*, 537-549.

Hammond, S.M. (2005). Dicing and slicing: the core machinery of the RNA interference pathway. FEBS Lett *579*, 5822-5829.

Hammond, S.M., Boettcher, S., Caudy, A.A., Kobayashi, R., and Hannon, G.J. (2001). Argonaute2, a link between genetic and biochemical analyses of RNAi. Science *293*, 1146-1150.

Handwerger, K.E., and Gall, J.G. (2006). Subnuclear organelles: new insights into form and function. Trends Cell Biol *16*, 19-26.

Harris, M.E., Bohni, R., Schneiderman, M.H., Ramamurthy, L., Schumperli, D., and Marzluff, W.F. (1991). Regulation of histone mRNA in the unperturbed cell

cycle: evidence suggesting control at two posttranscriptional steps. Mol Cell Biol *11*, 2416-2424.

He, F., Li, X., Spatrick, P., Casillo, R., Dong, S., and Jacobson, A. (2003). Genome-wide analysis of mRNAs regulated by the nonsense-mediated and 5' to 3' mRNA decay pathways in yeast. Mol Cell *12*, 1439-1452.

He, F., Peltz, S.W., Donahue, J.L., Rosbash, M., and Jacobson, A. (1993). Stabilization and ribosome association of unspliced pre-mRNAs in a yeast upf1- mutant. Proc Natl Acad Sci U S A *90*, 7034-7038.

He, W., and Parker, R. (2001). The yeast cytoplasmic LsmI/Pat1p complex protects mRNA 3' termini from partial degradation. Genetics *158*, 1445-1455.

Heintz, N., Sive, H.L., and Roeder, R.G. (1983). Regulation of human histone gene expression: kinetics of accumulation and changes in the rate of synthesis and in the half-lives of individual histone mRNAs during the HeLa cell cycle. Mol Cell Biol *3*, 539-550.

Hentze, M.W., Caughman, S.W., Rouault, T.A., Barriocanal, J.G., Dancis, A., Harford, J.B., and Klausner, R.D. (1987). Identification of the iron-responsive element for the translational regulation of human ferritin mRNA. Science *238*, 1570-1573.

Hieronymus, H., Yu, M.C., and Silver, P.A. (2004). Genome-wide mRNA surveillance is coupled to mRNA export. Genes Dev *18*, 2652-2662.

Hoek, M., and Stillman, B. (2003). Chromatin assembly factor 1 is essential and couples chromatin assembly to DNA replication in vivo. Proc Natl Acad Sci U S A *100*, 12183-12188.

Houalla, R., Devaux, F., Fatica, A., Kufel, J., Barrass, D., Torchet, C., and Tollervey, D. (2006). Microarray detection of novel nuclear RNA substrates for the exosome. Yeast *23*, 439-454.

Houseley, J., Kotovic, K., El Hage, A., and Tollervey, D. (2007). Trf4 targets ncRNAs from telomeric and rDNA spacer regions and functions in rDNA copy number control. EMBO J *26*, 4996-5006.

Houseley, J., LaCava, J., and Tollervey, D. (2006). RNA-quality control by the exosome. Nat Rev Mol Cell Biol *7*, 529-539.

Houseley, J., and Tollervey, D. (2006). Yeast Trf5p is a nuclear poly(A) polymerase. EMBO Rep *7*, 205-211.

Huang, Y., and Steitz, J.A. (2001). Splicing factors SRp20 and 9G8 promote the nucleocytoplasmic export of mRNA. Mol Cell *7*, 899-905.

Ibrahim, F., Rohr, J., Jeong, W.J., Hesson, J., and Cerutti, H. (2006). Untemplated oligoadenylation promotes degradation of RISC-cleaved transcripts. Science *314*, 1893.

Ivanov, P.V., Gehring, N.H., Kunz, J.B., Hentze, M.W., and Kulozik, A.E. (2008). Interactions between UPF1, eRFs, PABP and the exon junction complex suggest an integrated model for mammalian NMD pathways. EMBO J.

Kashima, I., Yamashita, A., Izumi, N., Kataoka, N., Morishita, R., Hoshino, S., Ohno, M., Dreyfuss, G., and Ohno, S. (2006). Binding of a novel SMG-1-Upf1-eRF1-eRF3 complex (SURF) to the exon junction complex triggers Upf1 phosphorylation and nonsense-mediated mRNA decay. Genes Dev *20*, 355-367.

Kastan, M.B., and Bartek, J. (2004). Cell-cycle checkpoints and cancer. Nature *432*, 316-323.

Kaygun, H., and Marzluff, W.F. (2005a). Regulated degradation of replication-dependent histone mRNAs requires both ATR and Upf1. Nat Struct Mol Biol *12*, 794-800.

Kaygun, H., and Marzluff, W.F. (2005b). Translation termination is involved in histone mRNA degradation when DNA replication is inhibited. Mol Cell Biol *25*, 6879-6888.

Keeling, K.M., Salas-Marco, J., Osherovich, L.Z., and Bedwell, D.M. (2006). Tpa1p i s part of an mRNP complex that influences translation termination, mRNA deadenylation, and mRNA turnover in Saccharomyces cerevisiae. Mol Cell Biol *26*, 5237-5248.

Klausner, R.D., Rouault, T.A., and Harford, J.B. (1993). Regulating the fate of mRNA: the control of cellular iron metabolism. Cell *72*, 19-28.

Klemperer, H.G. (1963). The incorporation of uridine 5'-phosphate into ribonucleic acid by an enzyme preparation from rat liver. Biochim Biophys Acta *72*, 403-415.

Kolev, N.G., and Steitz, J.A. (2005). Symplekin and multiple other polyadenylation factors participate in 3'-end maturation of histone mRNAs. Genes Dev *19*, 2583-2592.

Kshirsagar, M., and Parker, R. (2004). Identification of Edc3p as an enhancer of mRNA decapping in Saccharomyces cerevisiae. Genetics *166*, 729-739.

Kufel, J., Allmang, C., Verdone, L., Beggs, J.D., and Tollervey, D. (2002). Lsm proteins are required for normal processing of pre-tRNAs and their efficient association with La-homologous protein Lhp1p. Mol Cell Biol *22*, 5248-5256.

Kupsco, J.M., Wu, M.J., Marzluff, W.F., Thapar, R., and Duronio, R.J. (2006). Genetic and biochemical characterization of Drosophila Snipper: A promiscuous member of the metazoan 3'hExo/ERI-1 family of 3' to 5' exonucleases. RNA *12*, 2103-2117.

Kushner, S.R. (2004). mRNA decay in prokaryotes and eukaryotes: different approaches to a similar problem. IUBMB Life *56*, 585-594.

Kwak, J.E., Wang, L., Ballantyne, S., Kimble, J., and Wickens, M. (2004). Mammalian GLD-2 homologs are poly(A) polymerases. Proc Natl Acad Sci U S A *101*, 4407-4412.

Kwak, J.E., and Wickens, M. (2007). A family of poly(U) polymerases. RNA *13*, 860-867.

LaCava, J., Houseley, J., Saveanu, C., Petfalski, E., Thompson, E., Jacquier, A., and Tollervey, D. (2005). RNA degradation by the exosome is promoted by a nuclear polyadenylation complex. Cell *121*, 713-724.

Lai, M.C., Lin, R.I., and Tarn, W.Y. (2001). Transportin-SR2 mediates nuclear import of phosphorylated SR proteins. Proc Natl Acad Sci U S A *98*, 10154-10159.

Lanzotti, D.J., Kaygun, H., Yang, X., Duronio, R.J., and Marzluff, W.F. (2002). Developmental control of histone mRNA and dSLBP synthesis during Drosophila embryogenesis and the role of dSLBP in histone mRNA 3' end processing in vivo. Mol Cell Biol *22*, 2267-2282.

Le Hir, H., Moore, M.J., and Maquat, L.E. (2000). Pre-mRNA splicing alters mRNP composition: evidence for stable association of proteins at exon-exon junctions. Genes Dev *14*, 1098-1108.

Leeds, P., Peltz, S.W., Jacobson, A., and Culbertson, M.R. (1991). The product of the yeast UPF1 gene is required for rapid turnover of mRNAs containing a premature translational termination codon. Genes Dev *5*, 2303-2314.

Lehner, B., and Sanderson, C.M. (2004). A protein interaction framework for human mRNA degradation. Genome Res *14*, 1315-1323.

Lehner, B., Semple, J.I., Brown, S.E., Counsell, D., Campbell, R.D., and Sanderson, C.M. (2004). Analysis of a high-throughput yeast two-hybrid system and its use to predict the function of intracellular proteins encoded within the human MHC class III region. Genomics *83*, 153-167.

Lei, E.P., Krebber, H., and Silver, P.A. (2001). Messenger RNAs are recruited for nuclear export during transcription. Genes Dev *15*, 1771-1782.

Lejeune, F., Li, X., and Maquat, L.E. (2003). Nonsense-mediated mRNA decay in mammalian cells involves decapping, deadenylating, and exonucleolytic activities. Mol Cell *12*, 675-687.

Lerner, R.S., and Nicchitta, C.V. (2006). mRNA translation is compartmentalized to the endoplasmic reticulum following physiological inhibition of cap-dependent translation. RNA *12*, 775-789.

Lerner, R.S., Seiser, R.M., Zheng, T., Lager, P.J., Reedy, M.C., Keene, J.D., and Nicchitta, C.V. (2003). Partitioning and translation of mRNAs encoding soluble proteins on membrane-bound ribosomes. RNA *9*, 1123-1137.

Li, B., Carey, M., and Workman, J.L. (2007). The role of chromatin during transcription. Cell *128*, 707-719.

Lin, Q., Inselman, A., Han, X., Xu, H., Zhang, W., Handel, M.A., and Skoultchi, A.I. (2004). Reductions in linker histone levels are tolerated in developing spermatocytes but cause changes in specific gene expression. J Biol Chem *279*, 23525-23535.

Liu, H., Rodgers, N.D., Jiao, X., and Kiledjian, M. (2002). The scavenger mRNA decapping enzyme DcpS is a member of the HIT family of pyrophosphatases. EMBO J *21*, 4699-4708.

Liu, Q., Greimann, J.C., and Lima, C.D. (2006). Reconstitution, activities, and structure of the eukaryotic RNA exosome. Cell *127*, 1223-1237.

Long, R.M., and McNally, M.T. (2003). mRNA decay: x (XRN1) marks the spot. Mol Cell *11*, 1126-1128.

Lund, E., and Dahlberg, J.E. (1992). Cyclic 2',3'-phosphates and nontemplated nucleotides at the 3' end of spliceosomal U6 small nuclear RNA's. Science *255*, 327-330.

Lykke-Andersen, J., Shu, M.D., and Steitz, J.A. (2000). Human Upf proteins target an mRNA for nonsense-mediated decay when bound downstream of a termination codon. Cell *103*, 1121-1131.

Ma, T., Van Tine, B.A., Wei, Y., Garrett, M.D., Nelson, D., Adams, P.D., Wang, J., Qin, J., Chow, L.T., and Harper, J.W. (2000). Cell cycle-regulated phosphorylation of p220(NPAT) by cyclin E/Cdk2 in Cajal bodies promotes histone gene transcription. Genes Dev *14*, 2298-2313.

Macbeth, M.R., Schubert, H.L., Vandemark, A.P., Lingam, A.T., Hill, C.P., and Bass, B.L. (2005). Inositol hexakisphosphate is bound in the ADAR2 core and required for RNA editing. Science *309*, 1534-1539.

Madison-Antenucci, S., Grams, J., and Hajduk, S.L. (2002). Editing machines: the complexities of trypanosome RNA editing. Cell *108*, 435-438.

Malik, H.S., and Henikoff, S. (2003). Phylogenomics of the nucleosome. Nat Struct Biol *10*, 882-891.

Maniatis, T., and Reed, R. (2002). An extensive network of coupling among gene expression machines. Nature *416*, 499-506.

Maquat, L.E. (2004). Nonsense-mediated mRNA decay: splicing, translation and mRNP dynamics. Nat Rev Mol Cell Biol *5*, 89-99.

Maquat, L.E., and Carmichael, G.G. (2001). Quality control of mRNA function. Cell *104*, 173-176.

Maquat, L.E., and Li, X. (2001). Mammalian heat shock p70 and histone H4 transcripts, which derive from naturally intronless genes, are immune to nonsense-mediated decay. RNA *7*, 445-456.

Martin, F., Schaller, A., Eglite, S., Schumperli, D., and Muller, B. (1997). The gene for histone RNA hairpin binding protein is located on human chromosome 4 and encodes a novel type of RNA binding protein. EMBO J *16*, 769-778.

Marzluff, W.F. (2005). Metazoan replication-dependent histone mRNAs: a distinct set of RNA polymerase II transcripts. Curr Opin Cell Biol *17*, 274-280.

Marzluff, W.F., and Duronio, R.J. (2002). Histone mRNA expression: multiple levels of cell cycle regulation and important developmental consequences. Curr Opin Cell Biol *14*, 692-699.

Marzluff, W.F., Gongidi, P., Woods, K.R., Jin, J., and Maltais, L.J. (2002). The human and mouse replication-dependent histone genes. Genomics *80*, 487-498.

Matsuyama, A., Arai, R., Yashiroda, Y., Shirai, A., Kamata, A., Sekido, S., Kobayashi, Y., Hashimoto, A., Hamamoto, M., Hiraoka, Y.*, et al.* (2006). ORFeome cloning and global analysis of protein localization in the fission yeast Schizosaccharomyces pombe. Nat Biotechnol *24*, 841-847.

Meeks-Wagner, D., and Hartwell, L.H. (1986). Normal stoichiometry of histone dimer sets is necessary for high fidelity of mitotic chromosome transmission. Cell *44*, 43-52.

Mellman, D.L., Gonzales, M.L., Song, C., Barlow, C.A., Wang, P., Kendziorski, C., and Anderson, R.A. (2008). A PtdIns4,5P2-regulated nuclear poly(A) polymerase controls expression of select mRNAs. Nature *451*, 1013-1017.

Mitchell, P., Petfalski, E., Shevchenko, A., Mann, M., and Tollervey, D. (1997). The exosome: a conserved eukaryotic RNA processing complex containing multiple 3'-->5' exoribonucleases. Cell *91*, 457-466.

Mohanty, B.K., and Kushner, S.R. (2000). Polynucleotide phosphorylase, RNase II and RNase E play different roles in the in vivo modulation of polyadenylation in Escherichia coli. Mol Microbiol *36*, 982-994.

Moore, M.J. (2005). From birth to death: the complex lives of eukaryotic mRNAs. Science *309*, 1514-1518.

Morris, T.D., Weber, L.A., Hickey, E., Stein, G.S., and Stein, J.L. (1991). Changes in the stability of a human H3 histone mRNA during the HeLa cell cycle. Mol Cell Biol *11*, 544-553.

Morrissey, J.P., Deardorff, J.A., Hebron, C., and Sachs, A.B. (1999). Decapping of stabilized, polyadenylated mRNA in yeast pab1 mutants. Yeast *15*, 687-702.

Motamedi, M.R., Verdel, A., Colmenares, S.U., Gerber, S.A., Gygi, S.P., and Moazed, D. (2004). Two RNAi complexes, RITS and RDRC, physically interact and localize to noncoding centromeric RNAs. Cell *119*, 789-802.

Mowry, K.L., Oh, R., and Steitz, J.A. (1989). Each of the conserved sequence elements flanking the cleavage site of mammalian histone pre-mRNAs has a distinct role in the 3'-end processing reaction. Mol Cell Biol *9*, 3105-3108.

Mowry, K.L., and Steitz, J.A. (1987). Identification of the human U7 snRNP as one of several factors involved in the 3' end maturation of histone premessenger RNA's. Science *238*, 1682-1687.

Muhlrad, D., and Parker, R. (2005). The yeast EDC1 mRNA undergoes deadenylation-independent decapping stimulated by Not2p, Not4p, and Not5p. EMBO J *24*, 1033-1045.

Mukherjee, D., Gao, M., O'Connor, J.P., Raijmakers, R., Pruijn, G., Lutz, C.S., and Wilusz, J. (2002). The mammalian exosome mediates the efficient degradation of mRNAs that contain AU-rich elements. EMBO J *21*, 165-174.

Mullen, T.E., and Marzluff, W.F. (2008). Degradation of histone mRNA requires oligouridylation followed by decapping and simultaneous degradation of the mRNA both 5' to 3' and 3' to 5'. Genes Dev *22*, 50-65.

Muller, B., Blackburn, J., Feijoo, C., Zhao, X., and Smythe, C. (2007). DNA-activated protein kinase functions in a newly observed S phase checkpoint that links histone mRNA abundance with DNA replication. J Cell Biol *179*, 1385-1398.

Murray, E.L., and Schoenberg, D.R. (2007). A+U-rich instability elements differentially activate 5'-3' and 3'-5' mRNA decay. Mol Cell Biol *27*, 2791-2799.

Nagaike, T., Suzuki, T., Katoh, T., and Ueda, T. (2005). Human mitochondrial mRNAs are stabilized with polyadenylation regulated by mitochondria-specific poly(A) polymerase and polynucleotide phosphorylase. J Biol Chem *280*, 19721-19727.

Nakamura, A., Amikura, R., Hanyu, K., and Kobayashi, S. (2001). Me31B silences translation of oocyte-localizing RNAs through the formation of cytoplasmic RNP complex during Drosophila oogenesis. Development *128*, 3233-3242.

Narita, T., Yung, T.M., Yamamoto, J., Tsuboi, Y., Tanabe, H., Tanaka, K., Yamaguchi, Y., and Handa, H. (2007). NELF interacts with CBC and participates in 3' end processing of replication-dependent histone mRNAs. Mol Cell *26*, 349-365.

Orban, T.I., and Izaurralde, E. (2005). Decay of mRNAs targeted by RISC requires XRN1, the Ski complex, and the exosome. RNA *11*, 459-469.

Pandey, N.B., and Marzluff, W.F. (1987). The stem-loop structure at the 3' end of histone mRNA is necessary and sufficient for regulation of histone mRNA stability. Mol Cell Biol *7*, 4557-4559.

Parker, R., and Song, H. (2004). The enzymes and control of eukaryotic mRNA turnover. Nat Struct Mol Biol *11*, 121-127.

Perry, R.P., and Kelley, D.E. (1973). Messenger RNA turnover in mouse L cells. J Mol Biol *79*, 681-696.

Pettitt, J., Crombie, C., Schumperli, D., and Muller, B. (2002). The Caenorhabditis elegans histone hairpin-binding protein is required for core histone gene expression and is essential for embryonic and postembryonic cell division. J Cell Sci *115*, 857-866.

Pillai, R.S., Bhattacharyya, S.N., Artus, C.G., Zoller, T., Cougot, N., Basyuk, E., Bertrand, E., and Filipowicz, W. (2005). Inhibition of translational initiation by Let-7 MicroRNA in human cells. Science *309*, 1573-1576.

Pillai, R.S., Will, C.L., Luhrmann, R., Schumperli, D., and Muller, B. (2001). Purified U7 snRNPs lack the Sm proteins D1 and D2 but contain Lsm10, a new 14 kDa Sm D1-like protein. EMBO J *20*, 5470-5479.

Pleiss, J.A., Derrick, M.L., and Uhlenbeck, O.C. (1998). T7 RNA polymerase produces 5' end heterogeneity during in vitro transcription from certain templates. RNA *4*, 1313-1317.

Pulak, R., and Anderson, P. (1993). mRNA surveillance by the Caenorhabditis elegans smg genes. Genes Dev *7*, 1885-1897.

Read, R.L., Martinho, R.G., Wang, S.W., Carr, A.M., and Norbury, C.J. (2002). Cytoplasmic poly(A) polymerases mediate cellular responses to S phase arrest. Proc Natl Acad Sci U S A *99*, 12079-12084.

Rinke, J., and Steitz, J.A. (1985). Association of the lupus antigen La with a subset of U6 snRNA molecules. Nucleic Acids Res *13*, 2617-2629.

Rissland, O.S., Mikulasova, A., and Norbury, C.J. (2007). Efficient RNA polyuridylation by noncanonical poly(A) polymerases. Mol Cell Biol *27*, 3612-3624.

Rogakou, E.P., Pilch, D.R., Orr, A.H., Ivanova, V.S., and Bonner, W.M. (1998). DNA double-stranded breaks induce histone H2AX phosphorylation on serine 139. J Biol Chem *273*, 5858-5868.

Ross, J., and Kobs, G. (1986). H4 histone messenger RNA decay in cell-free extracts initiates at or near the 3' terminus and proceeds 3' to 5'. J Mol Biol *188*, 579-593.

Ross, J., Peltz, S.W., Kobs, G., and Brewer, G. (1986). Histone mRNA degradation in vivo: the first detectable step occurs at or near the 3' terminus. Mol Cell Biol *6*, 4362-4371.

Saitoh, S., Chabes, A., McDonald, W.H., Thelander, L., Yates, J.R., and Russell, P. (2002). Cid13 is a cytoplasmic poly(A) polymerase that regulates ribonucleotide reductase mRNA. Cell *109*, 563-573.

Sancar, A., Lindsey-Boltz, L.A., Unsal-Kacmaz, K., and Linn, S. (2004). Molecular mechanisms of mammalian DNA repair and the DNA damage checkpoints. Annu Rev Biochem *73*, 39-85.

Sanchez, R., and Marzluff, W.F. (2002). The stem-loop binding protein is required for efficient translation of histone mRNA in vivo and in vitro. Mol Cell Biol *22*, 7093-7104.

Sanchez, R., and Marzluff, W.F. (2004). The oligo(A) tail on histone mRNA plays an active role in translational silencing of histone mRNA during Xenopus oogenesis. Mol Cell Biol *24*, 2513-2525.

Sariban, E., Wu, R.S., Erickson, L.C., and Bonner, W.M. (1985). Interrelationships of protein and DNA syntheses during replication of mammalian cells. Mol Cell Biol *5*, 1279-1286.

Scharl, E.C., and Steitz, J.A. (1994). The site of 3' end formation of histone messenger RNA is a fixed distance from the downstream element recognized by the U7 snRNP. EMBO J *13*, 2432-2440.

Schell, T., Kocher, T., Wilm, M., Seraphin, B., Kulozik, A.E., and Hentze, M.W. (2003). Complexes between the nonsense-mediated mRNA decay pathway factor human upf1 (up-frameshift protein 1) and essential nonsense-mediated mRNA decay factors in HeLa cells. Biochem J *373*, 775-783.

Schneider, C., Anderson, J.T., and Tollervey, D. (2007). The exosome subunit Rrp44 plays a direct role in RNA substrate recognition. Mol Cell *27*, 324-331.

Schratt, G.M., Tuebing, F., Nigh, E.A., Kane, C.G., Sabatini, M.E., Kiebler, M., and Greenberg, M.E. (2006). A brain-specific microRNA regulates dendritic spine development. Nature *439*, 283-289.

Schumacher, M.A., Pearson, R.F., Moller, T., Valentin-Hansen, P., and Brennan, R.G. (2002). Structures of the pleiotropic translational regulator Hfq and an Hfq-RNA complex: a bacterial Sm-like protein. EMBO J *21*, 3546-3556.

Shaw, G., and Kamen, R. (1986). A conserved AU sequence from the 3' untranslated region of GM-CSF mRNA mediates selective mRNA degradation. Cell *46*, 659-667.

Shaw, J.M., Feagin, J.E., Stuart, K., and Simpson, L. (1988). Editing of kinetoplastid mitochondrial mRNAs by uridine addition and deletion generates conserved amino acid sequences and AUG initiation codons. Cell *53*, 401-411.

Shen, B., and Goodman, H.M. (2004). Uridine addition after microRNA-directed cleavage. Science *306*, 997.

Sheth, U., and Parker, R. (2003). Decapping and decay of messenger RNA occur in cytoplasmic processing bodies. Science *300*, 805-808.

Singer, R.H., and Penman, S. (1973). Messenger RNA in HeLa cells: kinetics of formation and decay. J Mol Biol *78*, 321-334.

Slomovic, S., Laufer, D., Geiger, D., and Schuster, G. (2005). Polyadenylation and degradation of human mitochondrial RNA: the prokaryotic past leaves its mark. Mol Cell Biol *25*, 6427-6435.

Song, M.G., and Kiledjian, M. (2007). 3' Terminal oligo U-tract-mediated stimulation of decapping. RNA *13*, 2356-2365.

Steger, D.J., and Workman, J.L. (1999). Transcriptional analysis of purified histone acetyltransferase complexes. Methods *19*, 410-416.

Stevens, A., Wang, Y., Bremer, K., Zhang, J., Hoepfner, R., Antoniou, M., Schoenberg, D.R., and Maquat, L.E. (2002). Beta -Globin mRNA decay in erythroid cells: UG site-preferred endonucleolytic cleavage that is augmented

by a premature termination codon. Proc Natl Acad Sci U S A *99*, 12741-12746.

Stevenson, A.L., and Norbury, C.J. (2006). The Cid1 family of non-canonical poly(A) polymerases. Yeast *23*, 991-1000.

Stoecklin, G., Mayo, T., and Anderson, P. (2006). ARE-mRNA degradation requires the 5'-3' decay pathway. EMBO Rep *7*, 72-77.

Stuart, K. (1991). RNA editing in trypanosomatid mitochondria. Annu Rev Microbiol *45*, 327-344.

Sullivan, E., Santiago, C., Parker, E.D., Dominski, Z., Yang, X., Lanzotti, D.J., Ingledue, T.C., Marzluff, W.F., and Duronio, R.J. (2001). Drosophila stem loop binding protein coordinates accumulation of mature histone mRNA with cell cycle progression. Genes Dev *15*, 173-187.

Sutton, M.A., and Schuman, E.M. (2006). Dendritic protein synthesis, synaptic plasticity, and memory. Cell *127*, 49-58.

Tagami, H., Ray-Gallet, D., Almouzni, G., and Nakatani, Y. (2004). Histone H3.1 and H3.3 complexes mediate nucleosome assembly pathways dependent or independent of DNA synthesis. Cell *116*, 51-61.

Takagaki, Y., and Manley, J.L. (2000). Complex protein interactions within the human polyadenylation machinery identify a novel component. Mol Cell Biol *20*, 1515-1525.

Terns, M.P., Lund, E., and Dahlberg, J.E. (1992). 3'-end-dependent formation of U6 small nuclear ribonucleoprotein particles in Xenopus laevis oocyte nuclei. Mol Cell Biol *12*, 3032-3040.

Tharun, S., He, W., Mayes, A.E., Lennertz, P., Beggs, J.D., and Parker, R. (2000). Yeast Sm-like proteins function in mRNA decapping and decay. Nature *404*, 515-518.

Tharun, S., Muhlrad, D., Chowdhury, A., and Parker, R. (2005). Mutations in the Saccharomyces cerevisiae LSM1 gene that affect mRNA decapping and 3' end protection. Genetics *170*, 33-46.

Tharun, S., and Parker, R. (2001). Targeting an mRNA for decapping: displacement of translation factors and association of the Lsm1p-7p complex on deadenylated yeast mRNAs. Mol Cell *8*, 1075-1083.

Tomecki, R., Dmochowska, A., Gewartowski, K., Dziembowski, A., and Stepien, P.P. (2004). Identification of a novel human nuclear-encoded mitochondrial poly(A) polymerase. Nucleic Acids Res *32*, 6001-6014.

Trippe, R., Guschina, E., Hossbach, M., Urlaub, H., Luhrmann, R., and Benecke, B.J. (2006). Identification, cloning, and functional analysis of the human U6 snRNA-specific terminal uridylyl transferase. RNA *12*, 1494-1504.

Trippe, R., Richly, H., and Benecke, B.J. (2003). Biochemical characterization of a U6 small nuclear RNA-specific terminal uridylyltransferase. Eur J Biochem *270*, 971-980.

Trippe, R., Sandrock, B., and Benecke, B.J. (1998). A highly specific terminal uridylyl transferase modifies the 3'-end of U6 small nuclear RNA. Nucleic Acids Res *26*, 3119-3126.

Tsukada, Y., Fang, J., Erdjument-Bromage, H., Warren, M.E., Borchers, C.H., Tempst, P., and Zhang, Y. (2006). Histone demethylation by a family of JmjC domain-containing proteins. Nature *439*, 811-816.

Tsukada, Y., and Zhang, Y. (2006). Purification of histone demethylases from HeLa cells. Methods *40*, 318-326.

Tucker, M., and Parker, R. (2000). Mechanisms and control of mRNA decapping in Saccharomyces cerevisiae. Annu Rev Biochem *69*, 571-595.

Valentin-Hansen, P., Eriksen, M., and Udesen, C. (2004). The bacterial Sm-like protein Hfq: a key player in RNA transactions. Mol Microbiol *51*, 1525-1533.

van Hoof, A., and Parker, R. (1999). The exosome: a proteasome for RNA? Cell *99*, 347-350.

Vanacova, S., Wolf, J., Martin, G., Blank, D., Dettwiler, S., Friedlein, A., Langen, H., Keith, G., and Keller, W. (2005). A new yeast poly(A) polymerase complex involved in RNA quality control. PLoS Biol *3*, e189.

Vasudevan, S., and Steitz, J.A. (2007). AU-rich-element-mediated upregulation of translation by FXR1 and Argonaute 2. Cell *128*, 1105-1118.

Vasudevan, S., Tong, Y., and Steitz, J.A. (2007). Switching from repression to activation: microRNAs can up-regulate translation. Science *318*, 1931-1934.

Verreault, A., Kaufman, P.D., Kobayashi, R., and Stillman, B. (1996). Nucleosome assembly by a complex of CAF-1 and acetylated histones H3/H4. Cell *87*, 95-104.

Wagner, E.J., Berkow, A., and Marzluff, W.F. (2005). Expression of an RNAi-resistant SLBP restores proper S-phase progression. Biochem Soc Trans *33*, 471-473.

Wagner, E.J., Burch, B.D., Godfrey, A.C., Salzler, H.R., Duronio, R.J., and Marzluff, W.F. (2007). A genome-wide RNA interference screen reveals that variant histones are necessary for replication-dependent histone pre-mRNA processing. Mol Cell *28*, 692-699.

Wagner, E.J., and Garcia-Blanco, M.A. (2002). RNAi-mediated PTB depletion leads to enhanced exon definition. Mol Cell *10*, 943-949.

Wagner, E.J., and Marzluff, W.F. (2006). ZFP100, a component of the active U7 snRNP limiting for histone pre-mRNA processing, is required for entry into S phase. Mol Cell Biol *26*, 6702-6712.

Wagner, E.J., Ospina, J.K., Hu, Y., Dundr, M., Matera, A.G., and Marzluff, W.F. (2006). Conserved zinc fingers mediate multiple functions of ZFP100, a U7snRNP associated protein. RNA *12*, 1206-1218.

Wang, S.W., Norbury, C., Harris, A.L., and Toda, T. (1999). Caffeine can override the S-M checkpoint in fission yeast. J Cell Sci *112 (Pt 6)*, 927-937.

Wang, Z., Jiao, X., Carr-Schmid, A., and Kiledjian, M. (2002). The hDcp2 protein is a mammalian mRNA decapping enzyme. Proc Natl Acad Sci U S A *99*, 12663-12668.

Wang, Z.F., Krasikov, T., Frey, M.R., Wang, J., Matera, A.G., and Marzluff, W.F. (1996a). Characterization of the mouse histone gene cluster on chromosome

13: 45 histone genes in three patches spread over 1Mb. Genome Res *6*, 688-701.

Wang, Z.F., Tisovec, R., Debry, R.W., Frey, M.R., Matera, A.G., and Marzluff, W.F. (1996b). Characterization of the 55-kb mouse histone gene cluster on chromosome 3. Genome Res *6*, 702-714.

Wang, Z.F., Whitfield, M.L., Ingledue, T.C., 3rd, Dominski, Z., and Marzluff, W.F. (1996c). The protein that binds the 3' end of histone mRNA: a novel RNA-binding protein required for histone pre-mRNA processing. Genes Dev *10*, 3028-3040.

Whitfield, M.L., Kaygun, H., Erkmann, J.A., Townley-Tilson, W.H., Dominski, Z., and Marzluff, W.F. (2004). SLBP is associated with histone mRNA on polyribosomes as a component of the histone mRNP. Nucleic Acids Res *32*, 4833-4842.

Whitfield, M.L., Zheng, L.X., Baldwin, A., Ohta, T., Hurt, M.M., and Marzluff, W.F. (2000). Stem-loop binding protein, the protein that binds the 3' end of histone mRNA, is cell cycle regulated by both translational and posttranslational mechanisms. Mol Cell Biol *20*, 4188-4198.

Wilusz, C.J., and Wilusz, J. (2005). Eukaryotic Lsm proteins: lessons from bacteria. Nat Struct Mol Biol *12*, 1031-1036.

Wilusz, C.J., and Wilusz, J. (2008). New ways to meet your (3') end oligouridylation as a step on the path to destruction. Genes Dev *22*, 1-7.

Yamashita, A., Chang, T.C., Yamashita, Y., Zhu, W., Zhong, Z., Chen, C.Y., and Shyu, A.B. (2005). Concerted action of poly(A) nucleases and decapping enzyme in mammalian mRNA turnover. Nat Struct Mol Biol *12*, 1054-1063.

Yang, F., and Schoenberg, D.R. (2004). Endonuclease-mediated mRNA decay involves the selective targeting of PMR1 to polyribosome-bound substrate mRNA. Mol Cell *14*, 435-445.

Yang, X.C., Purdy, M., Marzluff, W.F., and Dominski, Z. (2006). Characterization of 3'hExo, a 3' exonuclease specifically interacting with the 3' end of histone mRNA. J Biol Chem *281*, 30447-30454.

Yang, Z., Jakymiw, A., Wood, M.R., Eystathioy, T., Rubin, R.L., Fritzler, M.J., and Chan, E.K. (2004). GW182 is critical for the stability of GW bodies expressed during the cell cycle and cell proliferation. J Cell Sci *117*, 5567-5578.

Ye, X., Franco, A.A., Santos, H., Nelson, D.M., Kaufman, P.D., and Adams, P.D. (2003a). Defective S phase chromatin assembly causes DNA damage, activation of the S phase checkpoint, and S phase arrest. Mol Cell *11*, 341-351.

Ye, X., Wei, Y., Nalepa, G., and Harper, J.W. (2003b). The cyclin E/Cdk2 substrate p220(NPAT) is required for S-phase entry, histone gene expression, and Cajal body maintenance in human somatic cells. Mol Cell Biol *23*, 8586-8600.

Zamore, P.D., and Haley, B. (2005). Ribo-gnome: the big world of small RNAs. Science *309*, 1519-1524.

Zhao, X., McKillop-Smith, S., and Muller, B. (2004). The human histone gene expression regulator HBP/SLBP is required for histone and DNA synthesis, cell cycle progression and cell proliferation in mitotic cells. J Cell Sci *117*, 6043-6051.

Zheng, L., Dominski, Z., Yang, X.C., Elms, P., Raska, C.S., Borchers, C.H., and Marzluff, W.F. (2003). Phosphorylation of stem-loop binding protein (SLBP) on two threonines triggers degradation of SLBP, the sole cell cycle-regulated factor required for regulation of histone mRNA processing, at the end of S phase. Mol Cell Biol *23*, 1590-1601.